FACULTY OF SCIENCE
UNIVERSITY OF COPENHAGEN

Master Thesis (M.Sc)

Charlotte Ditlevsen

Electrical Conductivity Measurements (ECM) of Greenland ice cores

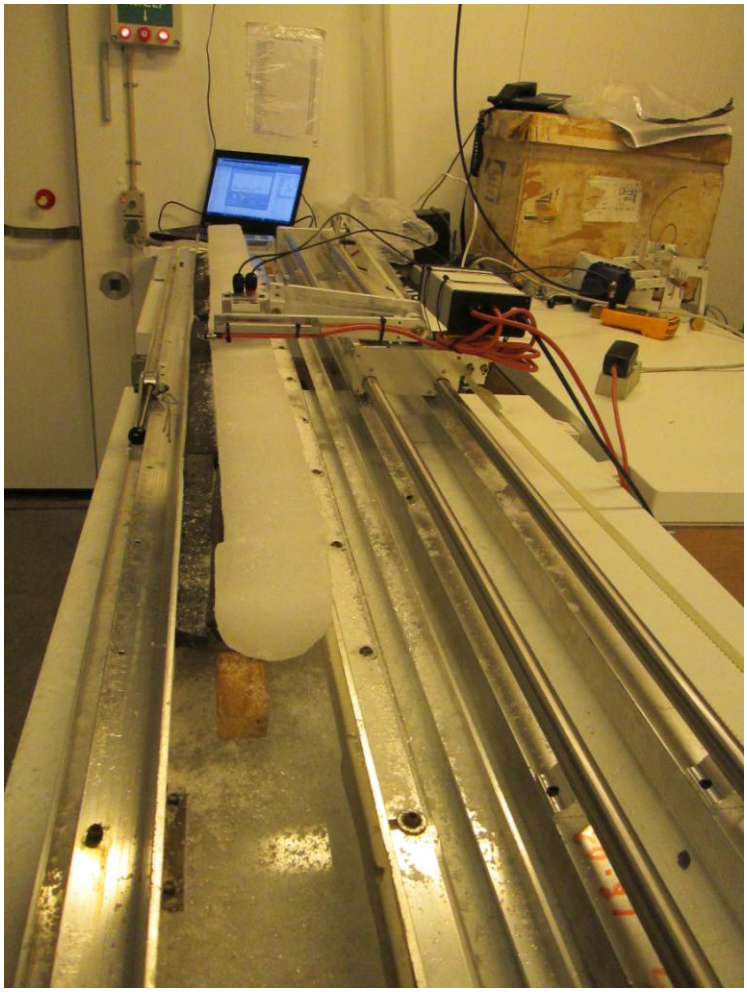

Academic advisors: Anders Svensson and Christoph Korte

Submitted: 01/11/14

CENTRE FOR ICE AND CLIMATE

University: University of Copenhagen

Institute: Niels Bohr Institute

Department: Centre for Ice and Climate

Author: Charlotte Ditlevsen

E-mail: charlotteditlevsen@hotmail.com

Title: Electrical Conductivity Measurements (ECM) of Greenland ice cores

Subject description: Electrical Conductivity Measurements (ECM) of ice cores is an established non-destructive technique to identify volcanic acidity spikes in ice cores. A new and improved ECM setup is now available at Ice and Climate, NBI. In this project the new setup will be calibrated and applied to identify well-known historical

volcanic signals in Greenland ice cores.

Academic advisor: Anders Svensson and Christoph Korte

Submitted: 1. November 2014

Grade:

Abstract

The study presented in this thesis is the new calibration found by the relationship between acidity and conductivity based on electric conductivity measurements (ECM) on three Greenland ice cores. The new sulphate distribution based on the values calculated from the new calibration, are also in focus. Five volcanic eruptions were specifically selected to be measured. In NGRIP all five of them were measured, only three in GRIP and Dye-3 due to insufficient amount of ice preserved. The eruptions measured are Krakatoa (1883), Tambora (1815), Laki (1783), Unknown (1257) and Unknown (9305) B.C. All eruptions are well known which makes it possible to compare the new data with previously measured and published data. The measurements were performed on a new ECM setup where a new calibration was produced by finding the relationship between sulphate and the newly measured ECM current. The sulphate values were old measurements done on ion-chromatography (IC) in 5 cm intervals.

The study shows that three parameters control the reproducibility of the measurements: the overall core quality, temperature and polarization. Six out of the eleven measurements on the five eruptions were done on firn, which turned out to be less stable measurements and possibly somewhat destructive regarding the calibration. The new calibration gave a linear relationship between sulphate and current, which is different from any published calibrations. The reason for this is assumed to be due to complications associated with some of the measurements used and/or the change in direct use of sulphate instead of H^+, which have been used for all other calibrations. The sulphate distribution was found by the calibration function and the deposition values of each eruption in all cores. The values showed that there was a favouring of distribution in central Greenland at the GRIP core followed by NGRIP and last Dye-3. However this is questioned by the over all quality of the measurements done on Dye-3 and the comparison between the values produced here and others.

Resumé

De præsenteret resultater i dette speciale er baseret på elektrisk konduktivitets målinger (ECM), der viser kalibreringsforholdet mellem sulfat og konduktivitet i tre Grønlandske iskerner. Et andet fokus punkt er distribueringen af sulfat baseret på værdier fra den nye kalibrering. Fem vulkanske udbrud er specifikt udvalgt med henblik på målingerne. Alle fem udbrud blev målt i NGRIP kernen, mens der i GRIP og Dye-3 kun kunne måles på tre på grund af for lidt resterende is at måle på. De målte udbrud kommer fra Krakatoa (1883), Tambora (1815), Laki (1783), Ukendt (1257) og Ukendt 9305 (f.Kr.). Alle udbruddene er velkendte, hvilket gør det muligt at sammenligne det nye data med allerede eksisterende data. Målingerne er foretaget på et nyt ECM instrument, hvorfra en ny kalibrering funktion er fundet gennem plotning af forholdet mellem sulfat og de nye ECM data. Alt sulfat data kommer fra gamle diskrete IC målinger af 5 cm gennemsnits intervaller. Resultaterne viser at tre hovedparametre kontrollerer målingernes reproducerbarehed: iskernens kvalitet, temperatur og polarisering i isen. Seks ud af elleve målinger er fortaget på firn, hvilket har vist sig at give ustabile målinger og dårlig reproducerbarhed, hvilket kan have haft indflydelse på den nye kalibrering.

Den nye kalibrering viser et lineært forhold mellem sulfat og konduktivitet, hvilket er anderledes fra alle andre udgivet ECM kalibreringer. Der anses to mulige årssager for dette; der er problemer med de målinger, der er benyttet og foretaget, og/eller forholdet mellem sulfat og H^+ er anderledes end forventet. H^+ har været brugt til alle andre kalibreringer. Distribueringen er fundet ved brug af den nye kalibrering og de derfra udregnede sulfat aflejringer. Værdierne viser en meteorologisk favorisering af central Grønland (GRIP) efterfulgt af det nordlige- (NGRIP) og sidst det sydlige Grønland (Dye-3). Distribueringsværdierne fra Dye-3 bliver betragtet varsomt, da flere usikkerheder er linket til målingerne, og sammenligningen mellem data præcenteret her og andre værdier argumenterer imod denne distribuering.

Acknowledgements

First would I like to give a big thanks to Centre for Ice and Climate for letting me be part of an institution with so many inspiring people part of it.

A very special thank you is given to Anders Svensson for his excellent supervisor work and unlimited inspiration. Paul Vallelonga and Lars Berg Larsen are thanked very much for their help with finding and retrieving the ice cores with me, for without them everything would have taken much longer time. Jørgen Peder Steffensen helped with interpretations of the CIC database which clarified several strange observations in some of the data. I would also like to thank Simon Geoffrey Sheldon and all the rest of the people who helped building the new ECM setup for without them this thesis could never have been written.

A special thank you also goes out to Christoph Korte for accepting me as his master student and allowing me to write my thesis as it is presented here.

An additional thank you goes Rolf Justesen Pedersen, Line Rosendahl Meldgaard Pedersen and Line Juhler Smith for helping with mathematical complications as well as a general structure throughout the project. Britta Ohlsen and Yvonne Xina Ditlevsen should also be mentioned for their excellent grammatical comprehension and corrections of such.

Last but not least should the people who have been part of this process be acknowledged for their support and endless help with whatever I need helped with. All of you also helped making this a very special experience and for that I am thankful.

Charlotte Ditlevsen
Centre for Ice and Climate, Niels Bohr Institute
University of Copenhagen
November 2014

Table of content

Table of content 1
List of figures 4
List of Tables 5
List of Equations 5
Preface 6
Purpose 7
Structure of thesis 9
1. A basic introduction to ice core studies 10
1.1 Ice core studies 10
1.2 Ice formation 14
1.3 Ice flow 15
1.4 Brittle zone 16
1.5 Background information on ice cores used in this thesis 16
1.6 Ice core processing 16
1.7 The Ion-Chromatography (IC) method 17
1.8 The Continuous Flow Analysis (CFA) method 17
1.9 Impurities in ice 17
1.10 Using volcanic eruptions as time markers in ice cores 18
1.11 Volcanisms influence on climate 18
2. Introduction of topics related to the ECM 20
2.1 Introducing the volcanoes 20
Unknown, 9305 B.C. 20
Unknown, 1257 A.D. 20
Laki, Iceland, A.D. 1783 20
Tambora, Indonesia, A.D. 1815 21
Krakatoa, Indonesia, A.D. 1883 21
2.2 Transportation of sulphur 22
2.3 Density - Firn vs. Ice 24
2.4 Conductivity – Temperature and polarization effect 26
3. Method 27
3.1 The modified ECM setup 28
3.2 ECM- and depth-scale conversion programs 29
3.3 Ice core measurement procedure 30

3.4 Temperature measurements 33
3.5 Stationary measurements 33
3.6 Comparison to the old instrument 33
3.7 Sample description 35
4. DATA 37
4.1 Calculations 37
5. Results 44
5.1 New and old ECM figures for all eruptions 44
5.1.1 NGRIP ECM measurements 44
5.1.1.1 ECM on NGRIP 48
5.1.2 GRIP ECM measurements 51
5.1.2.1 ECM on GRIP 53
5.1.3 Dye-3 ECM measurements 55
5.1.3.1 ECM on Dye-3 57
5.2 New and old ECM and IC sulphur figures, averaged over 5 cm 58
5.2.1 NGRIP 59
5.2.2 GRIP 64
5.3 Temperature experiment 66
5.4 Stationary measurements 67
5.4.1 NGRIP 109 67
5.4.2 NGRIP 110 68
5.4.3. NGRIP 293 69
5.5 The calibration curve 71
5.6 Sulfate deposition in Greenland 71
5.7 Major findings of this thesis 72
5.7.1 The reproducibility on ECM measurements 72
5.7.2 Temperature experiment 72
5.7.3 Stationary measurements 73
5.7.4 The calibration 73
5.7.5 Sulphate distribution on Greenland 73
6. Discussion 74
6.1 Some general uncertainties related to the signal reproducibility 74
6.1.1 Surface of the ice 74
6.1.2 Ice thickness 74
6.1.3 Voltage 74

6.1.4 Temperature 75
6.1.5 Electrodes 75
6.2 Interpretation of major findings 75
6.2.1 ECM on NGRIP 75
6.2.2 ECM on GRIP 76
6.2.3 ECM on Dye-3 77
6.2.4 Temperature experiment 78
6.2.5 Stationary measurements 79
6.2.6 The Calibration 81
6.2.6.1 Some uncertainties involved with the ECM and IC sulphate 81
6.2.6.2 Conductivity is also caused by H^+ from other impurities than H_2SO_4 82
6.2.6.3 Insufficient amount of measurements 82
6.2.7 Sulphate deposition and distribution 83
6.3 Explanation of what the major findings could mean 84
6.3.2 Temperature 84
6.3.3 Stationary measurements 84
6.3.4 The calibration 84
6.3.5 Sulphate distribution 84
6.4 Comparing the results to published literature 85
6.4.1 New ECM compared to old ECM and sulphate 85
6.4.2 Calibration 85
6.4.3 Sulphate per area 86
6.5 The limitations of this study 89
6.5.1 Too few measurements on ice 89
6.5.2 Bad ice core quality 89
6.5.3 Temperature dependence 89
6.5.4 Comparison of calibration 90
6.6 The generalisability of the results 90
6.7 A couple of unanswered questions 90
6.8 Proposals for further research on the subject 90
6.9 General considerations on ECM 91
7. Conclusion 92
8. References 93

List of figures

Figure 1 8
Figure 2 11
Figure 3 12
Figure 4 14
Figure 5 15
Figure 6 17
Figure 7 19
Figure 8. 22
Figure 9 23
Figure 10 25
Figure 11. 28
Figure 12 29
Figure 13. 30
Figure 14. 31
Figure 15a) & 15b) 32
Figure 16 33
Figure 17 38
Figure 18 41
Figure 19 42
Figure 20. 44
Figure 21. 45
Figure 22 46
Figure 23. 47
Figure 24. 48
Figure 25. 51
Figure 26 52
Figure 27 53
Figure 28. 55
Figure 29. 56
Figure 30. 57
Figure 31 59
Figure 32 60
Figure 33. 61
Figure 34. 62
Figure 35. 63
Figure 36 64
Figure 37. 65
Figure 38. 66
Figure 39 67
Figure 40 68
Figure 41. 69
Figure 42. 70
Figure 43 71
Figure 44. 78
Figure 45 80
Figure 46 80
Figure 47 81
Figure 48. 82
Figure 49. 83

List of Tables

Table 1 8
Table 2. 36
Table 3 39
Table 4 43
Table 5 66
Table 6. 71
Table 7 87

List of Equations

Equation 1 6
Equation 2 12
Equation 3 24
Equation 4 37
Equation 5 38
Equation 6 40
Equation 7 40
Equation 8 40
Equation 9 40
Equation 10 40
Equation 11 41
Equation 12 41
Equation 13 41

Preface

Greenland ice cores have been studied since the 1960's where Willi Dansgaard did his first isotopic measurements (Dansgaard, 2004). During the 1950's he found a connection between the ration of O^{16}/O^{18} and temperature in H_2O molecules. This started the study of ice cores and has over time evolved into a worldwide field of climate research (Dansgaard, 2004).

When snow falls on e.g. Greenland it is deposited on top of the previously fallen annual precipitation resulting in a stratification of the snow with the youngest closest to the surface. Because of changes in season, hence a change in weather, most annual layers in the top of the ice sheet is easily distinguishable, which makes counting of them possible and thereby estimating the age of the ice. When drilling an ice core it is essential that the stratification is complete meaning that no layers are missing from the core. Because of this annul layering of snow the ice cores represent a climate archive revealing some of the past climate conditions as well as connections such as the oxygen isotope ratio. This climate archive reveals fascinating stories of past conditions allowing researchers to reconstruct the past and the attempt to predict the future.

One of the most significant and abrupt natural climate changes occurs after large volcanic eruptions. Some volcanism has been so extreme that it has changed temperatures for years at a time (Thordarson and Self 2003). In the time of the human, such extreme events have been well documented through descriptions of first notion and duration. These are often found along a description of how it affected the everyday living. It is not always known that it was volcanism on the other side of the world that changed the lives of the people documenting the event, but with modern interpretations of the weather/climate description and paleo-forensic it appears to be the effect of extreme volcanism.

During a volcanic eruption sulphate is ejected into the atmosphere, which amongst other creates aerosols that induces a significant cooling due to the back scattering of radiation from the sun. When entering the atmosphere the sulphate is spread as far as the winds can take it, which in some cases includes the Greenlandic ice sheet, where it is deposited as part of the annual precipitation. This results in some layers containing sulphate, which then indicates volcanic activity. Sections of sulphate can be found in ice cores by measuring the conductivity, since ice without impurities do not conduct well on its own. The method of measuring current through ice is called Electrical Conductivity Measurements (ECM) (Hammer, 1980). Hammer, C. 1980 produced a calibration, which also enabled him to calculate the amount of sulphate deposited in the ice based on EC-measurements (Hammer, 1980). The calibration produced by Hammer in 1980 is as follows

$$H^+ = 0.045 * i^{1.73} (micro.equiv./kg)$$ (Equation 1)

34 years later a new setup is introduced with certain improvements to the design hoping to stabilize future measurements and to give a general improvement of data. A description of the improved setup is found in section 3.1. Some key features of the new setup are the removal of possible change of weight as well as the measuring rate during a measurement. Much data of this sort is used for improvement of climate models.

Reductions of uncertainties related to EC measurements will inevitably improve the models, which will then improve the understanding of paleoclimate and possibly the climate of the future.

Purpose

This thesis will focus on measuring the electric conductivity (EC) of five volcanic eruptions in three different ice cores; NGRIP, GRIP and Dye-3 with the purpose of producing a new calibration for ECM in response to sulphate and the new setup. The measurements have been done with a setup at Centre for Ice and Climate, part of the Niels Bohr Institute, University of Copenhagen. The new setup is expected to show more reliable data on several parameters than the old and a new more reliable relation between acidity and current should therefore be expected. Five eruptions in each core were originally supposed to be measured, but due to bad conditions, or not enough material left of the core containing the eruption, measurements were performed on the following; five from NGRIP (the 9305 B.C. eruption was measured on NGRIP2 which was drilled next to NGRIP and is throughout the rest of the thesis referred to as part of the NGRIP ice core), three from GRIP and three from Dye-3. The five eruptions are seen in table 1. Besides producing a new calibration relationship, distribution of sulphate and the total deposition (kg/km^2) of such will be calculated to examine the meteorological conditions of depositing on Greenland for the future use of modellers.

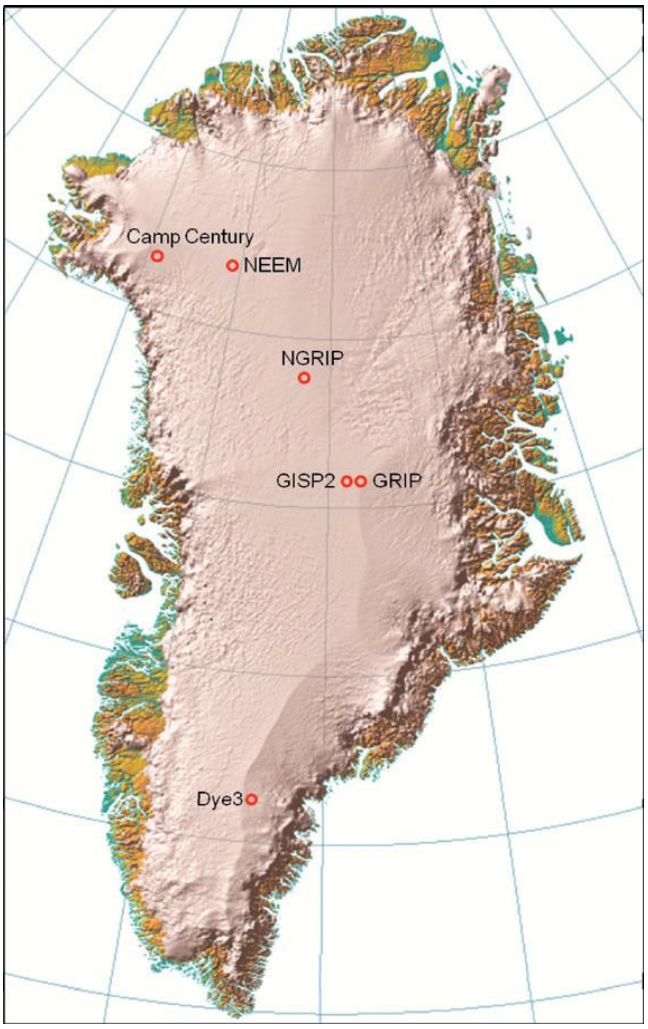

Figure 1 shows the geographical position of selected ice core drilling sites (Hvidberg *et al.,* 2013)

	Geographical origin	Time AD (or BC dates)	Bag numbers	Depth (m)
NGRIP2	Unknown	9305 B.C.	2674-2676	1470.15-1471.8
NGRIP	Unknown	1257	293-295	160.6-162.35
	Grímsvøtn (Laki), Iceland	1783	109-111	59.4-61.05
	Tambora, Indonesia	1815	95-97	51.7-53.35
	Krakatoa, Indonesia	1883	64-66	34.65-36.3
GRIP	Unknown	9305 B.C.	2907-2909	1598.3-1599.95
	Tambora, Indonesia	1815	107-109	58.3-59.95
	Krakatoa, Indonesia	1883	72-74	39.05-40.7
DYE3	Unknown	9305 B.C.	3235-3237	1778.7-1780.35
	Unknown	1257	672-674	269.05-370.7
	Krakatoa, Indonesia	1883	135-137	73.7-75.35

Table 1 shows the different volcanic eruptions measured and their dates in the four ice cores. (CIC database 2014)

With a new calibration between sulphate and current and a the new values of sulphate deposited as well as the distribution this thesis supply an understanding of the new ECM setup as well as data for modellers to use with, hopefully, less uncertainties.

Structure of thesis

The thesis is structured in 7 main sections listed below:

1. A basic introduction to ice core studies
Introduction to Greenland ice core studies where some basic definitions are given.

2. Introduction of topics related to the ECM done in this thesis
Some repetitions are to be expected but with the purpose of emphasize the process of the effect described.

3. Method
The method section is introducing the new setup and its improvements as well as a measure procedure and a sample description.

4. Data
The data part goes thorough the calculations used in this thesis and assumptions made in any case.

5. Results
Results will provide figures on all measurements as well as the calibration and the table containing the sulphate distribution. It will also point out the major findings of this thesis.

6. Discussion
The discussion gives an interpretation and explanation of the major findings and provides prospects on future ECM measuring.

7. Conclusion

All sections have sub-paragraphs; these are shortly described at the beginning of each main section.

1. A basic introduction to ice core studies

The following sections contain some basic introductions and simple descriptions of processes related to ice core studies. First some background on the origin of ice core studies and what they are used for. Followed by two sections on how ice is formed and how it flows. Then the brittle zone is quickly introduced to put focus on possible complications involved with measurements of certain sections of ice on ice cores. Then the ice core processing is introduced followed by two descriptions of methods used to measure chemistry in the ice and finally three sections on which impurities typically found in the ice, how some of these are used as time markers and how volcanism generally affects the climate.

1.1 Ice core studies

(Greenland ice cores)

Greenland lies between latitudes 59° and 83° N and longitudes 11° and 74° W. The average annual temperatures in the central part of Greenland are between -31°C and -20°C (Hvidberg *et al.,* 2013). The Greenland ice sheet is covering approximately 1.755.600 km^2, which corresponds to around 80% of the surface in Greenland and is the biggest ice sheet in the northern hemisphere. The ice sheet is around 2400 km long (north-south) and is 1100 km at its biggest width. The thickness is generally more than 2 km and at the thickest point more than 3 km. Due to the ice sheet central positioning of Greenland the bedrock has been lowered by the isostatic pressure and is about the same as sea level. However because of the surrounding mountains the ice sheet and ocean water is separated. The accumulation rate of the ice sheet varies with latitude as a result of change in temperature. In the central part of Greenland the rate is so high that there is good preservation of annual snow layers for ice core studies. Based on Greenland ice cores, Bales et al. 2009, produced a map of annual accumulation (g cm^2/a), (figure 2) which shows the variation over Greenland.

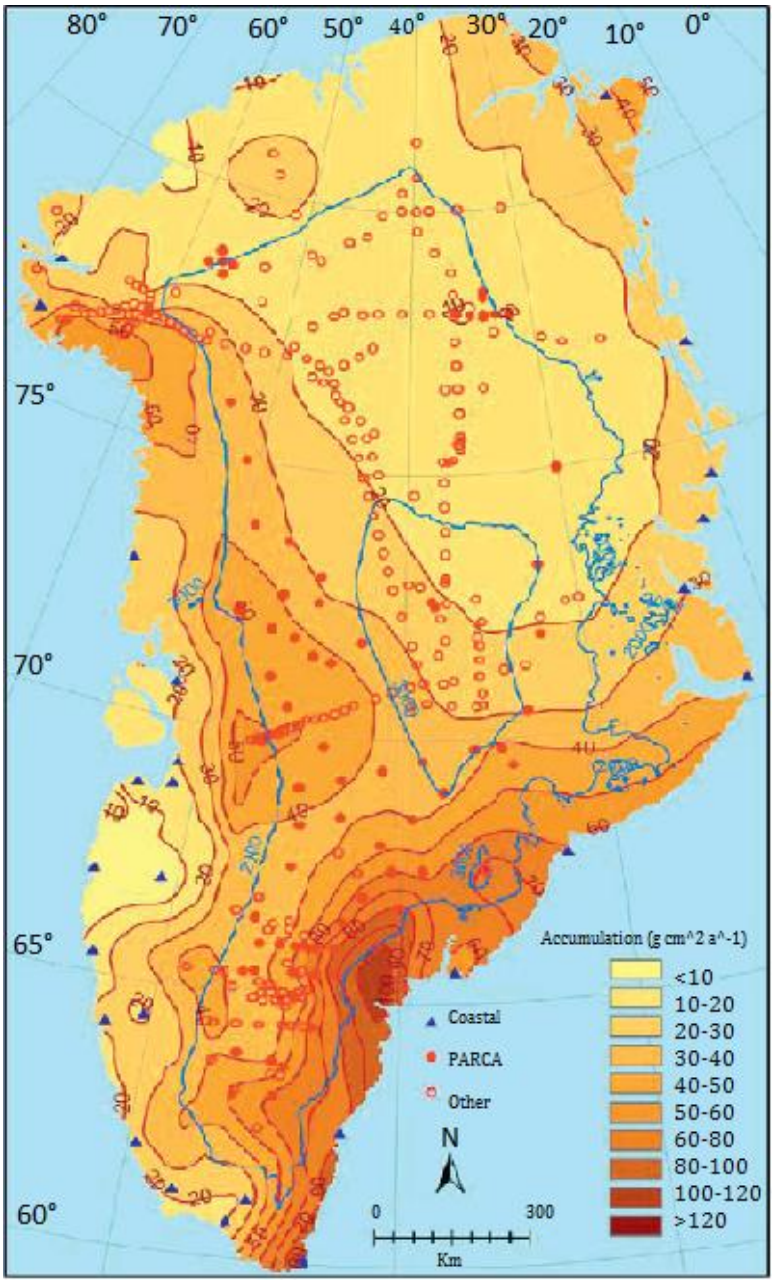

Figure 2 shows the accumulation rate across Greenland (Hvidberg *et al.*, 2013)

In 1952 Willi Dansgaard linked the isotopic signal/ratio of water molecules (heavy oxygen isotopes) to the temperature at the location where the precipitation was formed. From measurements on isotopes of precipitation in Denmark his results showed that there were a lot more heavy isotopes (Deuterium and Oxygen 18) present in his first samples than those that followed (Dansgaard, 1964). From this he noticed that a fractionation process occurred during the evaporation and precipitation of the isotopes. He found this through the presence of more heavy isotopes in the early stages of a specific rain event compared to the later.

The ocean is considered the "true" value with a relationship of O^{16} and O^{18} being δ = 0‰. The δO^{18}-value is the ratio of stable isotopes ^{18}O:^{16}O as such:

$$\delta^{18}O = \left(\frac{\left(\frac{^{18}O}{^{16}O}\right)_{Sample}}{\left(\frac{^{18}O}{^{16}O}\right)_{S\,\mathrm{tan}\,dard}} - 1 \right) * 1000\,‰ \quad \text{(Equation 2)}$$

As evaporation happens the water vapour is considered depleted from O^{18}, compared to the water of which it evaporated, and is indicated by a delta value of -10‰ as seen on figure 3 below. The water vapour ending up as part of a cloud is then transported and from each precipitation event it loses more and more H_2O^{18} and the δ-value decreases with each event. If the cloud does not take up any new water vapour along its travels then the δ-value of the precipitation decreases by approximately 0.7‰ per °C cooling (Dansgaard, 2004). This enables the calculation of the surface temperature at the time of evaporation and can be determined from the use of water isotopes in e.g. ice cores. Several parameters are included in the calculations of the temperature but since isotopes are not in focus throughout this thesis it will not be mentioned any further.

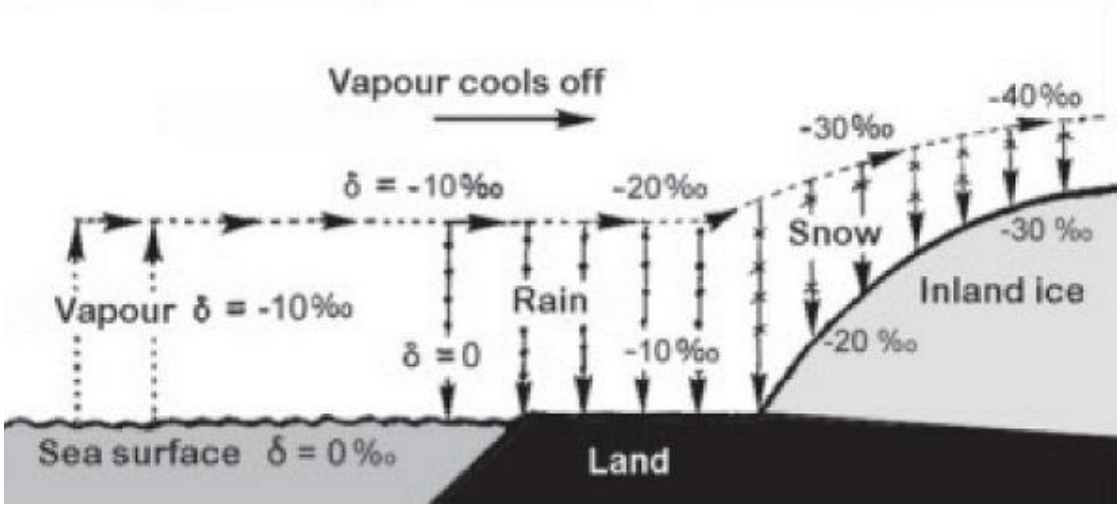

Figure 3 shows the idea of isotope fractionation along a random travelling path (Dansgaard, 2004)

During 1958-59 the U. S. Army established a "subsurface military research facility" in Greenland some 220 km east of Thule called Camp Century. During the 1960's Willi Dansgaard got to measure the isotopic values in the American Camp Century ice core which had reached a total depth of 1390 m before hitting bedrock. This enabled him to reconstruct the temperatures of the last ice ages for the first time (Dansgaard, 2004)

During the last decades several drillings, both shallow as well as a few deep ones, have been done in Greenland providing more data and information on climate changes dating back more than 130,000 years. (CIC database, 2014)

Today it is not only the proxy temperature found from hydrogen and oxygen isotopes that are in focus. Gasses and such impurities within the ice are examined to look at the past atmospheric composition e.g. Carbon dioxide (CO_2) and Methane (CH_4). Impurities in the ice reveal seasonal changes, volcanism as well as other factors causing sudden changes in climate. The physical behaviour/movement of the ice is studied through the ice crystal structure and biological remains e.g. DNA found in the bottom ice is used to recreate past ecosystems and in some cases used for dating.

Dating of the ice is essential to the use of data gained from the section of interest. In most of the upper layers it is possible to count the *cloudy bands* generally layers that show the annual change due to impurities and/or melting and through that find a time scale. Further down the layers are affected by thinning so much that it is no longer possible to differentiate between them, in those regions computer modelling is used to produce a depth/age scale. The modelling is only as reliable as the assumptions made therefore certain time markers, such as volcanism or ^{10}Be-concentrations, are used to benchmark known events through time (Kinnison et al., 1994). These benchmarks/reference horizon/points are also used to synchronize different ice cores due to change in accumulation rate throughout Greenland. Synchronization also happens between other climate archives such as sediment, lacustrine and marine cores. The corresponding horizon in e.g. the ice core is given an age which is then implemented in the age/depth modelling program and a more correct model can be produced. In some newer cases, concerning volcanism, the events have been very well documented by humans all around the world giving an exact time and place for the eruption which makes it possible to correlate between the dated material and the observations - thereby possibly making the dating method more reliable. As mentioned, other climate archives not originating from Greenland or even the northern hemisphere, such as other kind of cores, trees and caves, are used to correlate and synchronize data globally.

Sometimes extreme climate events seem to have occurred when examining data in e.g. an ice core but if they are not shown in any other climate archive then chances are that it was only a local event. Such mistakes would complicate the attempt to learn from the conditions of paleoclimate resulting in wrong predictions of future climate scenarios. For this amongst of other reasons data should always be backed up by other sorts of proxy data/ climate archives. One parameter that is often used for synchronization and age/depth modelling is, as mentioned previously, volcanism. During a volcanic eruption lots of sulphur dioxide (SO_2) is emitted into the air entering streams in the troposphere and is transported throughout the atmosphere. As soon as the sulphur dioxide enters the atmosphere it oxidizes with the water molecules/droplets and gets diluted by water vapour (H_2O) becoming sulphuric acid (H_2SO_4). This is then transported and as part of the precipitation and is deposited as part of the annual layering on e.g. Greenland. This process results in higher acidity in some layers of the ice, which can be measured by ECM and located in the ice cores (Hammer, 1980). There are two ways of measuring the conductivity of an ice core; one being on solid ice the other is measuring on a melted sample. This thesis will examine conductivity on solid ice.

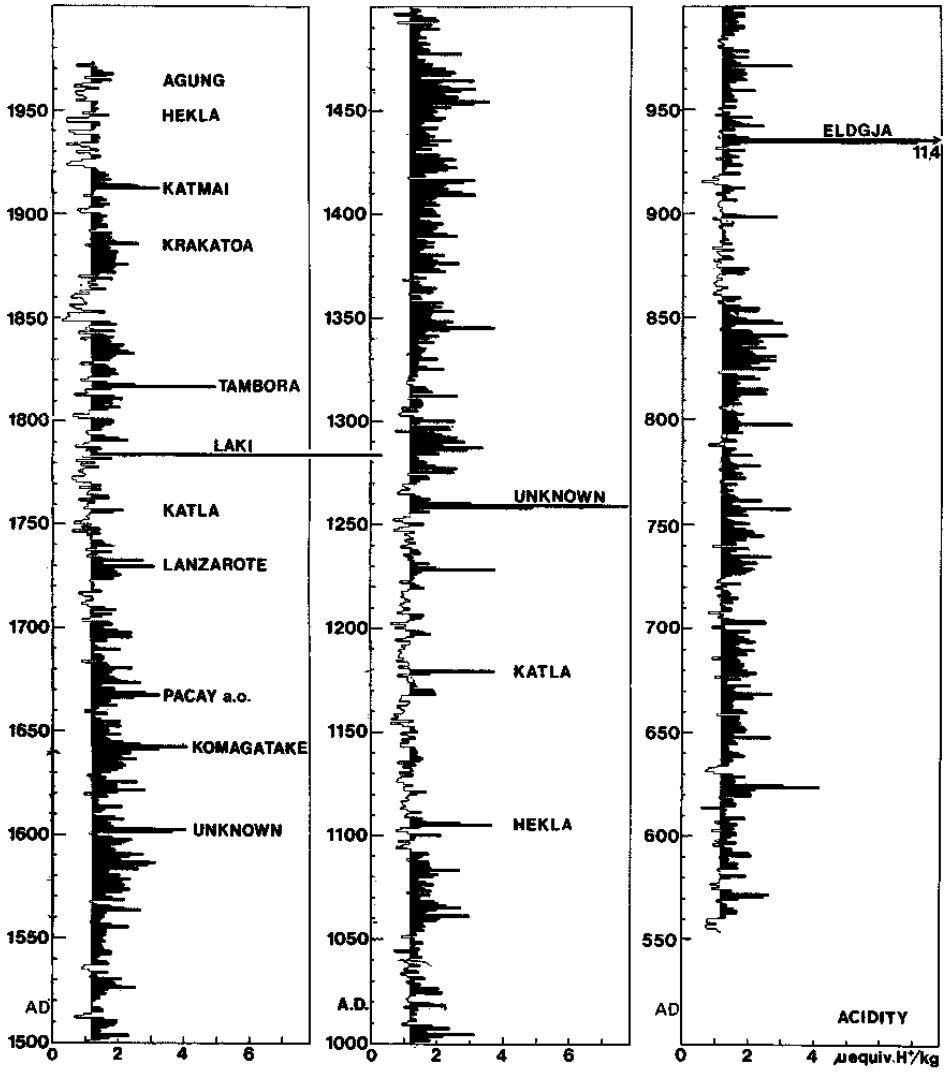

Figure 4 shows the ECM record produced by Hammer (Hammer, 1980)

ECM is a DC measurement of conductivity through ice. It is performed on an even surface of an ice core by dragging two electrodes along the ice with an electric potential difference between then. This method registers acidity and creates a signal in correspondence to the amount present in the ice.

This section gave an introduction to the study of ice cores from Greenland and why it is of interest to climate research. The next sections are focusing more on aspects of consideration regarding ice core drilling and processing.

1.2 Ice formation

Storing of information about past climate changes in ice cores are closely related to the transformation of snow to ice. When snow falls on a surface it becomes a fine low-density layer with plenty of air in between the still whole ice crystals. The ice crystals are broken down by wind, which results in a higher densification of the layer but still a relatively high air content. With new annual precipitation the layers gradually become more compact but an exchange between the atmospheric air and the air originally captured in the layer is still possible. With time a further densification of the snow layer occur as a result of continuously annual

adding of snow. This process is called pressure-sintering (Cuffey and Paterson, 2010). During this the ice crystals change shape, size and ultimately mass - all due to sublimation and become what is defined as firn. Firn is the state between snow and ice where air still enter and escapes the snow pack. With time the density increases due to the densification mentioned above and *pore close off* has occurs - the density is around 550 kg/m^3 at this stage. This also means that there is no further exchange of air between the atmosphere and the layer. The layer reaches a state of ice at a density of around 820 kg/m^3. Moving further in time and densification the air bobbles will become even more compact due to the hydrostatic pressure of the ice and can eventually reach the maximum density of around 930 kg/m^3 (Cuffey and Paterson, 2010). As the air pressure increases with depth the air bubbles are pushed into the ice matrix as clathrate hydrates which means that they are trapped in the centre of the ice crystals. A more detailed explanation of densification is described in section 2.3.

1.3 Ice flow

Information on ice flow in the desired location of investigation is essential since this could have a possible effect on the depth/age chronology through the ice core. Snow deposited above the Equilibrium-Line Altitude (ELA) typically survives the summer temperature. This means the information of the snow deposited will not be too influenced by evaporation and melting. As the snow is transformed to ice by compression the layers expand horizontally creating a flow towards the ice margins where it eventually is removed by melting (Hvidberg *et al.,* 2013). The most stable area of an ice sheet, in terms of stable annual ice representation, is at or near the ice divide because the horizontal velocity field is close to zero (see figure 5). The ice divide is the place on the ice sheet where opposing flow directions are separated hence the low velocity. Another important factor to the stability of ice representation is topography. Topography contributes to the physical behaviour of the flow therefore it is studied considerably before the drilling of an ice core (Hvidberg *et al.,* 2013). The ice flow is also related to the precipitation where high precipitation results in thicker annual layers which also results in the old ice layers being thinned out faster. Thus the resolution, when investigating, will be low and hiatuses are possible. With low precipitation one risks once more a bad resolution of measurements because too little ice is available. When drilling an ice core all mentioned above factors are taken into account.

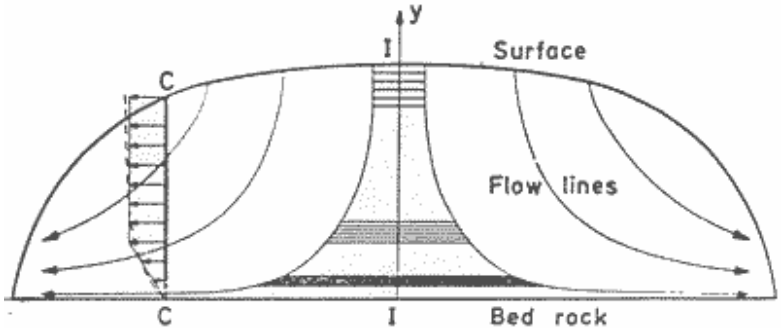

Figure 5 shows the simplified flow pattern of an ice sheet with thinning of the layers with depth due to flow and densification. The y-axis marks the position of ideal drilling position across the ice sheet (2014c, CIC publications)

1.4 Brittle zone

Moving down the ice sheet a zone known as the Brittle Zone occurs. This is a transition zone where the air bubbles are so compressed that they become clathrate hydrates. The air bubbles in the ice in those zones are 50-100 times the atmospheric surface pressure (Uchida *et al.,* 1994). During an uplift of the deep ice from e.g. -35°C or lower to around -20°C and a change in pressure from 100 to below 1 atmospheric pressure the ice experiences internal stress, which results in ice cracks and even shattering of core pieces. To prevent the ice from being useless the ice is put to rest where it has time to expand slowly until the internal stress is gone or so low that this part of the core is ready to be processed. The brittle zone for Dye-3 is from 600 m to 1100 m (Uchida *et al.,* 1994) and for NGRIP and GRIP the zone is around 800 m to 1200 m depth (Vinther *et al.,* 2006). The measuring of ECM signal on ice from the brittle zone could be influenced by this cracking factor but is not reported on here since none of the eruptions are within the zone boundaries.

1.5 Background information on ice cores used in this thesis

The Dye-3 core was part of the Greenland Ice Sheet Project and was drilled in south Greenland (65.18°N and 43.8°W) (see figure 1 in Preface) from 1979 to 1981. It was collaborative work by Denmark, USA and Switzerland and was the first scientifically based ice core drilling. The length of the full core is 2037 m. The mean air temperature around the area of the Dye-3 ice core is -20°C, the accumulation of m ice per year is 0.56 and elevation is 2480 m above sea level (asl) (Uchida *et al.,* 1994). Dye-3 was not chosen by any of the scientists for its significant position. It was, on the other hand, decided that it was the least difficult position to reach and therefore the cheapest (Dansgaard, 2004)

The GReenland Ice core Project (GRIP) was an ice core drilled in the central part of Greenland (72.58°N and 37.6°W), elevation 3230m asl, accumulation of m ice per year is 0.23 and a mean air temperature of -32°C (Uchida *et al.,* 1994). This site was chosen possible because it is at the highest elevation and therefore has the most ice and possibly information in high resolution on Greenland. It was drilled from 1988 until 1992 when they reached bedrock at a 3027 m of depth. This project was in association with and funded by multiple European countries and the European Union (Dansgaard, 2004)

North GReenland Ice core Project (NGRIP and NGRIP2) was drilled in the northern part of Greenland (75.1°N and 42.3°W) from 1996 to 2004. The elevation of the site is 2917 m asl. The mean air temperature is -32°C and the accumulation of m ice per year is 0.19 (Uchida *et al.,* 1994). The total drilling depth is 3090 m before hitting bedrock. Participating institutions in Denmark, Germany, Japan, Sweden, Switzerland, France, Belgium, Iceland and the USA funded this project (2014a)

1.6 Ice core processing

After an ice core is retrieved from the drill it is cut, bagged and transported to a research facility for storing and examination. All cores measured on (NGRIP, GRIP and Dye-3) were cut in pieces of approximately 55 cm. The brittle ice is typically kept in storage for a few years to de-stress the ice and give the drill liquid time to evaporate, but anything else is ready to be used for measurements. The cutting of the ice core piece (cylinder form) is typically done in five pieces (see figure 6 below) where each part of the upper half is used for measurements.

- Piece number 1 is used for looking at the physical properties (ice crystal structure, size and alignment/direction) of the ice.
- Number 2 is used for gas measurements.
- Number 3 is used for Continuous Flow Analysis (CFA) measurements.
- Number 4 is for the study of stable isotopes and finally piece.
- Number 5 is used for measuring Electric Conductivity Measurements (ECM) and then stored for possible later investigations. (2014b)

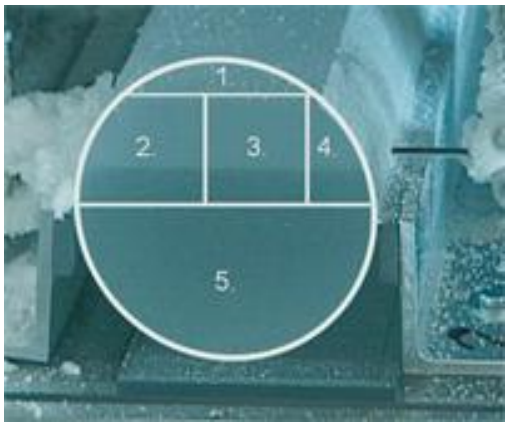

Figure 6 shows the cutting of an ice core. It also shows the piece numbers for understanding purposes of ice core processing (2014, CIC database)

1.7 The Ion-Chromatography (IC) method

The IC method finds different chemical impurities in the ice. The ice is cut into 5 cm intervals that is melted, mixed into one quantity, and measured. With 5 cm ice samples the yearly resolution in the deep parts of the ice cores disappears due to the great layer thinning. For the upper levels of the ice this method is very reliable.

1.8 The Continuous Flow Analysis (CFA) method

Compared to the IC method this is a continuous measurement of the ice core resulting in a high resolution of 1 mm. The ice core is slowly melted on a melt head, in a vertical position, with the water being transported to detectors and mixed with different reagents along the path of measuring. It is still being discussed if the CFA method is as stable and consistent as the IC method. (Bigler *et al.,* 2011)

1.9 Impurities in ice

The impurities which are found in the ice are very relevant to climate research. These impurities are typically particles like dust and chemical signals, which typically indicate a climatic proxy occurrence or specific tendencies of the past. The whole process behind how impurities reach the ice sheet is of great

importance to climate research. Amongst them are the very dominating meteorological conditions and ocean current systems. In ice of the Greenlandic ice sheet the most prominent ionic impurities are

- Sea salt ions such as Na and Cl^- . (Wolff *et al.,* 1996)
- Acids found across volcanic eruption peaks where the main acid is sulphuric. There is also a background of mainly nitric and sulphuric acids. (Wolff *et al.,* 1997)
- Ammonium and organic anions have been found in high concentrations in the Greenland ice sheet but only occasionally. (ibid.)
- Ice from around the last ice age in Greenland also shows terrestrial dust and ions derived from it. (ibid.)

In focus throughout this thesis is sulphate.

1.10 Using volcanic eruptions as time markers in ice cores

Volcanoes are not just used as indicators of climate variability but also as time markers throughout the ice cores.

The volcanoes provide age information which enables the possibility of establishing a boundary chronology between known marks. Highly explosive eruption generally injects a high amount of sulphur all the way into the stratosphere which creates a relation between the distribution of the emitted material and the origin of the eruption. The widespread distribution of the sulphate aerosols gives rise to well-documented dates that makes it possible to give the horizons of sulphuric acid an absolute age in the ice cores. Absolute dating of a volcanic layer is also possible when looking at sedimentary, marine, lacustrine cores. With some volcanic eruptions being so apparent in many ice cores, they are often used to synchronize different proxy climate archives. For instance the Laki eruption from Iceland 1783 is detected in Greenland, Svalbard and the Alps (Sigl *el al.,* 2013).

1.11 Volcanisms influence on climate

Volcanism is one of the natural climate forces that can cause temporarily changes and variations in temperature. Through the history of Earth volcanism have occurred on a “regular” basis due to the dynamic plate tectonic system. Some geological periods have been more affected by volcanism than others, which are reflected in the geology, species of vegetation as well as animals found from those times. A large eruption such as the Laki eruption in 1783 changed the temperature in the northern hemisphere for several years after the eruption had ended. Temperatures were generally lower, summers were sparse in sun and winters were even colder than usual (Sigl *el al.,* 2013). This is all an effect of the volcanic gas, aerosol droplets and the ash that are ejected into the stratosphere. These aerosols naturally increase the reflection of radiation from the sun back to space resulting in a cooling of the surface and because of back scattering of solar radiation a lower troposphere (Sigl *el al.,* 2013) (see figure 7 below). Typically a large eruption can change the temperature several degrees Celsius for a period of 2-3 years after the event (ibid.). The ash it-self is relatively quickly removed from the stratosphere by wash out - most is removed within days or weeks - but the volcanic gases, such as sulphur dioxide, have the ability to cause global cooling. When sulphur dioxide is converted into sulphuric acid and then condensates in the stratosphere it forms aerosols of sulphate that causes the cooling.

These effects of violent volcanism are well documented throughout recent times because they left numerous years of cooling which is thought to have changed the world by reduction in human populations, change of and or removal of vegetation as well as a possible alternate development of human culture. (Sigl *el al.,* 2013) The climatic change that is caused by volcanism changes parameters which can then be studied and possibly lead to better predictions on future climate behaviour.

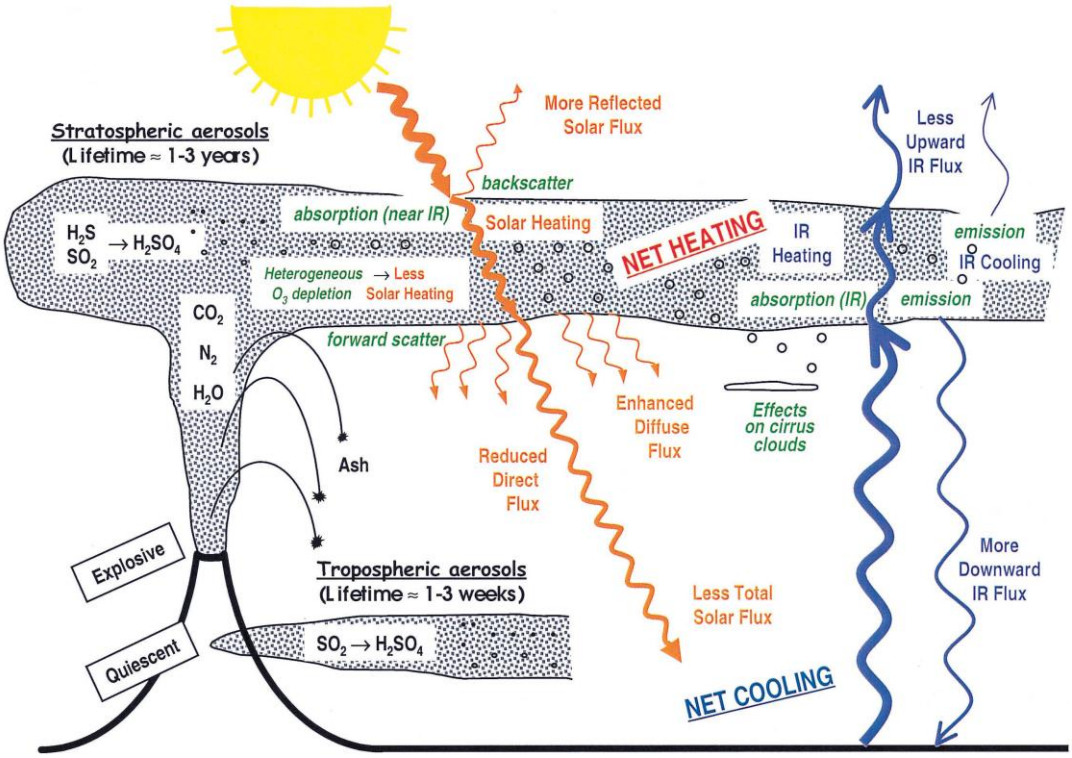

Figure 7 - The illustration above is showing the effect on the atmosphere by a small-scale eruption (quiescent) and a strong volcanic eruption (explosive) (Robock, 2000)

2. Introduction of topics related to the ECM

These sections will consist of topics more directly related to the measurements presented in this thesis. Basic background information on the different volcanoes and their eruptions are listed below followed by a description of transportation of sulphate from eruptions. Next there is a more detailed description of density followed by a section on conductivity serving the purpose of introducing the reader to the concepts influencing the measurements.

2.1 Introducing the volcanoes

Introducing the five volcanoes that are being measured in the ice cores (NGRIP, GRIP and Dye-3) to give some basic background information on the eruptions used.

Unknown, 9305 B.C.

The oldest eruption of the five also the least investigated. There are no known location and no direct literature on this eruption.

Unknown, 1257 A.D.

The eruption from 1257 is believed to be from the Samalas volcano, Rinjani Volcanoc Complex, Indonesia (Lavigne et al. 2013) but it is still being investigated and therefore this eruption will be referred to as 1257. Based on ice cores archives of sulphate and tephra depositions this appears to be the largest eruption in the last 7000 years. Tree-rings, archaeological and historical records tell of climate changes in the northern hemisphere around 1258 A.D. it is highlighted that the summers were cold and very rainy and that there were flooding and poor harvests.

The total estimate of stratospheric sulphate load is around eight- and two times higher than those of Krakatoa and Tambora (Lavigne et al. 2013). From the interhemispheric transport of tephra and sulphate it is suggested that this was a low latitude eruption of an eruption plume in heights of 34-52 km and with a DRE (dense –rock equivalent) of 2.8 km^3 (Lavigne et al. 2013).

Laki, Iceland, A.D. 1783

The Laki volcano erupted in 1783 covering a large part of the northern hemisphere with a sulphuric aerosol cloud (Thordarson and Self 2003). Observation of the haze is well documented in anything from weather logs and scientific publications to personal diaries (Thordarson and Self 2003). The eruption lasted around 8 months (from 8th of June 1783 to 7th of February 1784) (Fiacco *et al.,* 1994). The eruption history is described detailed by Thordarson and Self 2003 and will only be described shortly here; The first five months ten eruption episodes occurred with a 0.5-4 day(s) explosive phase followed by a longer phase of lava emission. The first 12 days ~40% of the total erupted volume of tephra and lava was released. This period is considered very vigorous and did not show a significant decline in activity before 1.5 month had

gone by (Thordarson and Self 2003). Over the next three months time span between each eruption became longer and the last 3.5 month a typical eruption is categorized by quiet emission of gas and lava. It is estimated that the explosive eruption columns were >13 km in the early months (Thordarson and Self, 2003) leading into the westerly jet stream. The DRE value is estimated to 15.1 by Fiacco, *et al.* in 1994.

The eruption had a massive environmental impact in Europe where it did considerable damage to vegetation and through that peoples living. There was a general sulphuric odour, acidic precipitation and haze in Europe affecting everything (Thordarson and Self 2003).

Tambora, Indonesia, A.D. 1815

The 10-11th of April 1815 the Tambora volcano erupted on Sumbawa Island, Indonesia (8.25°S, 117.96°E) (Self *et al.,* 1984). There have been made several estimations on eruption size and distribution pattern of volcanic gasses, acids, salts, tephra etc. because this eruption is considered one of the greatest of history. Estimates of volume of tephra erupted are between >300 km^3– 30 km^3 (Self *et al.,* 1984). 90000 people died at this eruption due to direct damage, destruction, tsunami, famine and disease in the central part of Indonesia (ibid). This massive ejection of volcanic gasses and material into the atmosphere changed the climate of the Northern Hemisphere for two or more years resulting in generally colder temperatures.

Tambora is 2860m high and is a >1000 km^3 big shield volcano formed of alkalic mafic to undersaturated intermediate lavas. The geochemistry of the 1815 eruption is the most evolved found on Tambora which leads people to think that volcano is undergoing a transition period in not only magmatic composition but also style of activity going from effusive to explosive. (Self *et al.,* 1984). Before the 1815 eruption Tambora had a total height of 4300 m but that eruption removed a summit cone set of approximately 1400m from the top of the volcano. The DRE value is estimated to >33 Km^3 (Lavigne *el al.,* 2013). Through eyewitnesses and other historical descriptions of the eruption, the different stages of the eruption has been estimated and described in other assessment reports amongst others the article *Volcanological study of the great Tambora eruption of 1815* by Self et al. 1984 (Rampino *et al.,* 2003)

Krakatoa, Indonesia, A.D. 1883

Krakatoa is well known for its loudness during the eruption on August 26th and 27th 1883. The eruption column is estimated to a height of 40 km (Rampino and Self, 1982). There was a decrease in temperature, primarily in the northern hemisphere, of 0.3°C to 0.4°C one to two years following the eruption (Rampino and Self, 1982). This eruption caused a globally visible evidence of sea-waves and air-waves (Yokoyama, 1980). The DRE was estimated to 12.1 km^3 (Lavigne *el al.,* 2013) and is considered the smallest eruptions of the five investigated in this thesis.

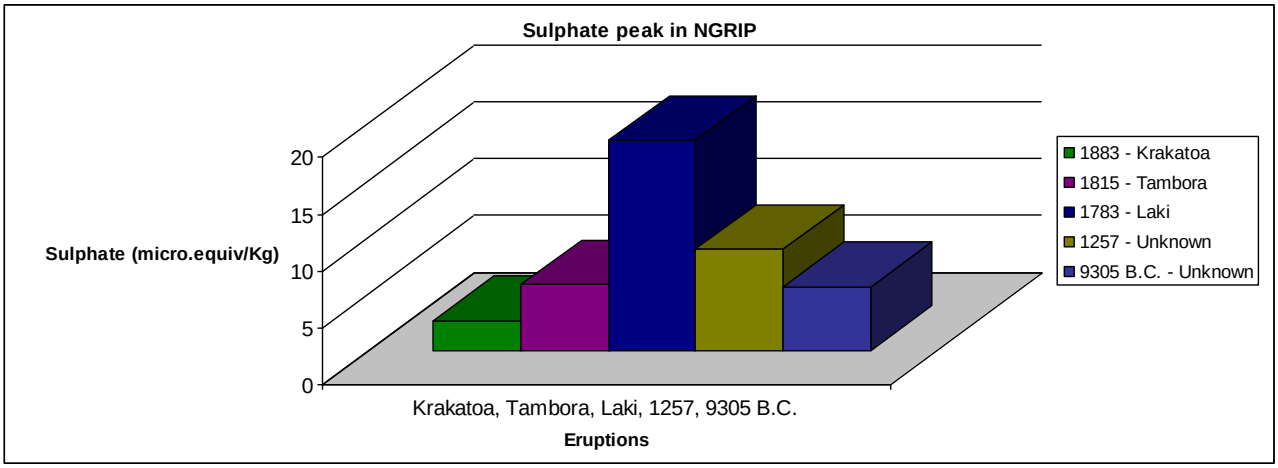

Figure 8 shows the relative peak size of each eruption in the NGRIP ice core.

2.2 Transportation of sulphur

During a major volcanic eruption extreme amounts of acid and salts of acids, such as sulphur dioxide (SO_2), hydrochloric acid (HCl), sulphuric acid (H_2SO_4), hexafluorosilicic acid (H_2SiF_6) and hydrogen fluoride (HF), are ejected into the atmosphere. Some of it is neutralized in the troposphere forming a vast amount of different salts e.g. ammonium salts which are of great interest when studying volcanic activity in ice. This is because the ammonia found in the troposphere is the only reacting compound able to neutralize volcanic acids in the middle and upper troposphere on a significant level. All this is mostly indicated by the background values of e.g. calcium (Ca), potassium (K), sodium (Na) and magnesium (Mg) (Hammer, 1980). The neutralization process is expected to be higher when the eruption material is transported to Greenland in the troposphere (medium eruptions at a high-latitude origin) contra transportation through the stratosphere (extreme eruption scale on the Northern Hemisphere) (Hammer, 1980).

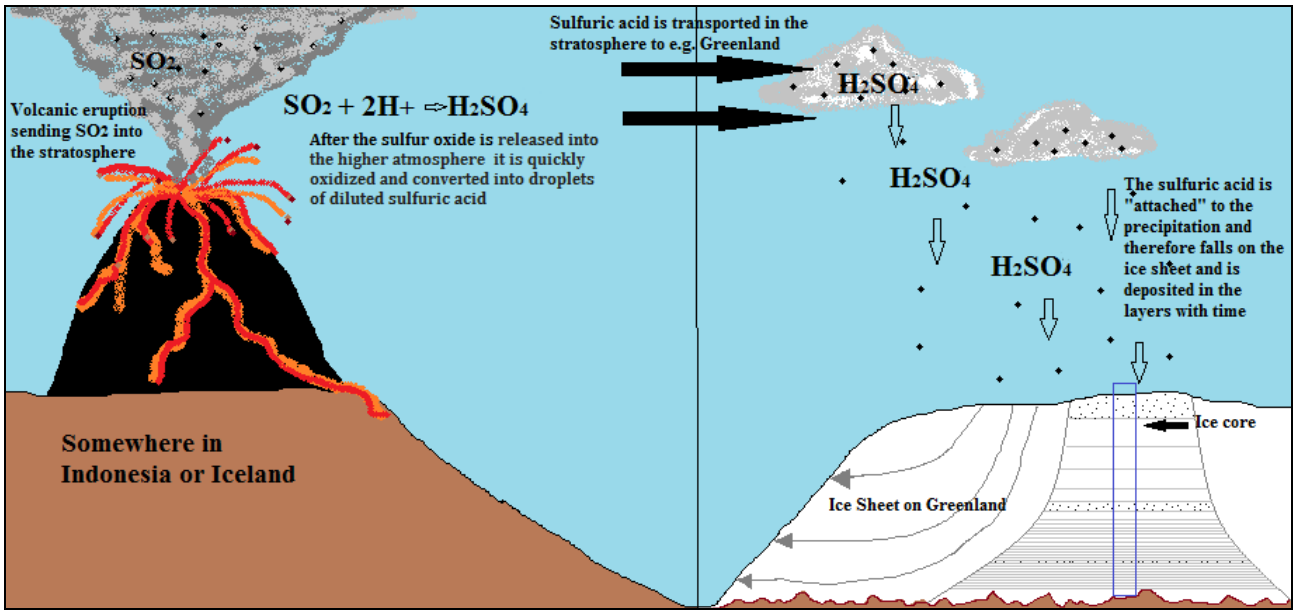

Figure 9 illustrates simplified sulphate transportation

Sulphuric acid (H_2SO_4) is consequently the most important content, when it comes to ECM, since it creates the signal through the inducted current and through the signal size, the free H^+ ions can be calculated and elaborate on eruption size and possible origin. When SO_4^{2-} is oxidized in the atmosphere, through water, it is turned into H_2SO_4. Subsequently through the meteorological conditions all volcanic aerosols are washed out by precipitation in the troposphere and the sulphuric acid ends up being deposited as e.g. snowfall on the Greenland ice sheet (Hammer, 1980). As mentioned earlier, most of the volcanism found in Greenland ice cores origin from the Northern Hemisphere (north of 20° S) (Hammer and Dansgaard, 1980). There are some eruptions that originated from the southern hemisphere, where the eruption size has been extreme enough to enter the stratosphere where it can stay for much longer (up to three years) compared to the troposphere and then reach further distances (Hammer, 1980). Some of the acid from the eruptions is neutralized in the troposphere where it forms different salts where ammonium salts are the most important of such as mentioned above figure 9. In cases of high degree neutralization and weak to medium eruption scales the result could be the disappearance/missing of signal in the ice cores (Hammer, 1980).

The behaviour of sulphate (and other) particles in the atmosphere are based on extensive measurements done by the Atomic Energy Commission (AEC), Department of Defence and National Oceanographic and Atmospheric Administration. These measurements were of radioactive products as a result of nuclear test bombings (Kinnison *et al.,* 1994). The products from the large above-ground nuclear bomb test in 1952-1958 and 1961-1962 were measured in all heights, using balloons, up to 35 km. The air was tested for Carbon 14 (C^{14}) and other radioactive elements such as strontium 90. Because Strontium 90 is produced only by fission reactions and C^{14} is produced as a result of a nuclear of atmospheric nitrogen with neutrons, which are produced by fission and fusion they work as tracers through the atmosphere. By tracking the changes over time and space, a distribution pattern was produced which is used in e.g. the search for finding possible transportation routes and thereby the origin of some volcanic eruptions going back in time. (Kinnison *et al.,* 1994)

2.3 Density - Firn vs. Ice

(Transformation from snow to firn to ice)

Snow is defined as the unchanged stage of the substance as it is falling (Cuffey and Paterson, 2010). Firn is not easily defined but for the sake of understanding it will be defined as layered snow that remains to have a density less than 830 kg/m^3 after one season or more (Cuffey and Paterson, 2010, p. 11). The clear definition is that firn becomes ice when interconnecting passages are closed off (also known as pore close-off) and this process occurs at a density of around 830 kg/m^3. Further increase in density can still happen as the compression of the individual air bubbles in the ice can become smaller leading to a maximum density of 923 kg/m^3 for glacier ice at temperatures lower than close to 0°C (Cuffey and Paterson, 2010, p. 12). The densification rate is dependent on the temperature and accumulation rate of the specific location of interest which means, that large variations in the depth-density relationship are expected all over Greenland.

There is a connection between the temperature, accumulation rate and density, and that an empirical density-depth relation was published by Schytt in 1956. This relation is noted as follows:

$$\rho(z) = \rho_i - \left[\rho_i - \rho_s\right]^{\left(\frac{-z}{z_\rho}\right)} \quad \text{(Equation 3)}$$

Here ρ is the density at depth z, ρ_i is the density of ice being 917 kg/m^3 and ρs is the density of the surface snow. z_ρ is a constant for each site and corresponds to a characteristic depth of the firn. The use of this empirical formula implicitly assumes that the site is a "steady-state density profile" meaning that the density at a given place does not change with time. This requires that the temperature, accumulation rate and the amount of melting remain constant (Cuffey and Paterson, 2010, p. 19).

When measuring ECM on ice cores you are measuring the electrical current going through the ice core with an electric potential difference of 1250 V. By dragging two electrodes along the ice core current is created (see section 2.4). The strength of the signal is varying with acidity changes in the ice but also the condition of the ice core measured. Focusing only on the quality of the ice cores in terms of reproducibility, density is a dominating factor.

Looking at a density profile it shows that with depth, density increases. This is due to the adding of mass on top of previously deposited snow. The densification of snow occur over three stages:

First stage – critical density is the most rapid process where the most dominant mechanism is considered to be due to grain settling and packing. Newly fallen snow has a density of 50-70 kg/m^3 (Cuffey and Paterson, 2010).

The second stage – density increases slowly with depth resulting in the intercommunicating air passages becomes closed off to form individual bubbles reaching a density of 830 kg/m^3.

The third stage – This occurs below the pore close-off zone meaning that air no longer can be excluded. Further densification only takes place by compression of the air bubbles even further resulting in the incorporation of it in the ice crystal structure also known as clathrate hydrates. Now having a density around 917 Kg/m^3 the firn is defined as ice. The depth-density profile is considered to be controlled by the snow accumulation rate and the temperature in mid/south Greenland the firn-ice boundary is between 70-100 m (Herron and Langway 1980).

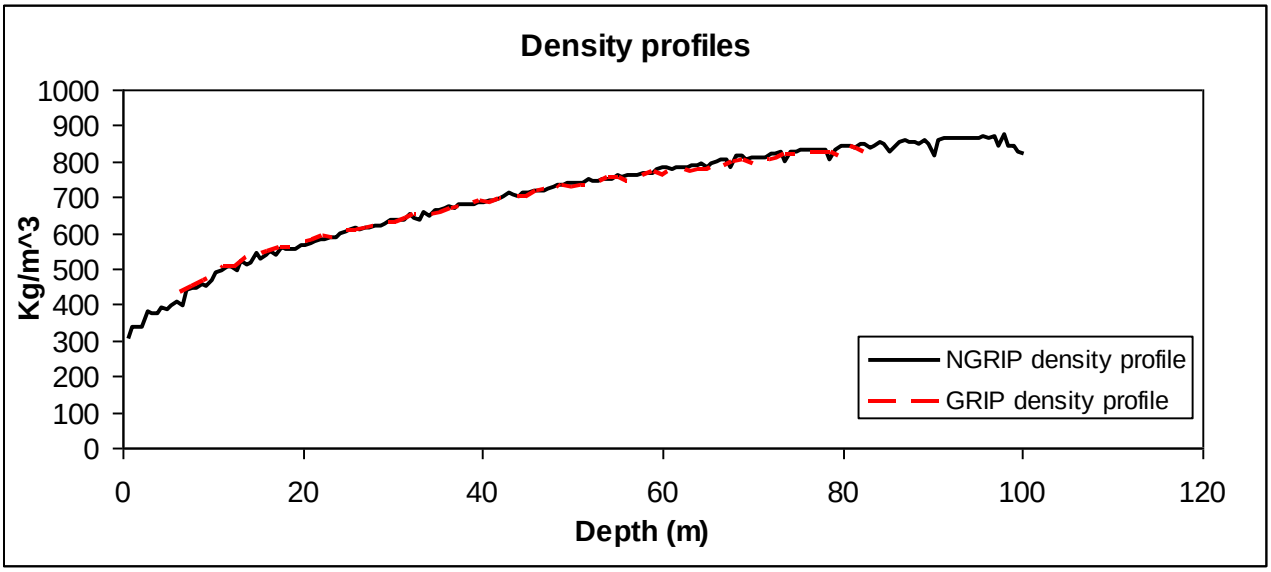

Figure 10 Density profile for NGRIP and GRIP (density profile of NGRIP2 is irrelevant due to the depth of bag 2674-2676)

Concerning EC measurements on ice cores; measuring on firn is much more difficult than on ice. This is due to the density of the ice core. Measuring EC on firn will complicate the measurement quality due to the low density leaving the mobility of the H^+ ions limited. See section 2.4 for assumptions on H^+ being the creator of current. This high porosity affects not only the mobility of ions within the core but also a technical part of the measurement. It could result in a momentarily "no contact" situation between one or both electrodes and the ice core, which would remove signal or at "best" would reduce the signal in case of unequal weight pressure.

Looking at the depths of interest in the four cores see table 1, it is clear that at least Krakatoa (1883), Tambora (1815) and Laki (1783) are at depths shallow enough to be influenced by the lack of maximum densification. In NGRIP and GRIP it seems to reach its maximum density around 100 m. GRIP possibly a bit sooner than NGRIP. Because Dye-3 is the most southern measurement position, it has the highest accumulation rate of the three positions. The maximum density is reached further up at around 80 m.

Part of this thesis is to calculate the total sulphate content in each annual deposition layer and look at the distribution between the cores. Thereby looking closer at the variation over time-depth where the calculation used includes the density of the ice hence its importance. It is important to use the density corresponding to the depth of interest and knowing that several of the measurements are performed at depths with a density lower than 917 kg/m^3 it should be kept in mind.

For the chemical aspect of quality of ECM signal see section 2.4 below where the conducting impurities are defined and some assumptions on the behaviour of the current mentioned.

2.4 Conductivity – Temperature and polarization effect

Ice can become a conductor when impurities are trapped in it. In polar ice the dominating acidic impurities are sulphuric acid (H_2SO_4), nitric acid (HNO_3) and to a minor degree, hydrochloric (HCl) and hydrofluoric acid (HF) (Clausen *et al.,* 1997). The conduction created in ice is ionic conduction and is assumed to be due to the motion of protons (H^+ ions) from the acids mentioned above (Taylor *et al.,* 1992). The ions are incorporated into the ice crystals which prevents movement of large ions but still allow motion of small ions such as single protons (Wolff *et al.,* 1996). Two theories on this proton motion are mentioned further down.

ECM is kind of a *direct current* (DC) measurement, which means that it is a constant one directional flow of electric charge (Wolff *et al.,* 1996). By considering ice as a kind of electrolyte, the conductivity can be defined through the chemical processes happening when creating a potential difference through the ice (Plummer *et al.,* 2012). If two electrodes are placed on the ice with a voltage a chemical reaction occurs where the cathode (the "positively charged" electrode) from where the conventional current departs the electrical device and begins to consume electrons from the anode (the "negatively charged" electrode). The conventional current is defined by the direction in which positive electronic charges move which is opposite of the movement of electrons, due to their negative charge. Concurrent to the cathode process is another reaction happening at the anode. The anode is producing electrons that eventually will be transferred to the cathode by H^+ motion. This results in a negatively charged mass (electrons) around the cathode and a positively charge mass (protons) around the anode (Neftel et al.).

When a complete separation of negative and positive ions occurs it is referred to as polarization, more specifically known as space-charge polarization (Moore *et al.,* 1984). When this happens the transport of electrons ceases to exist which equals no current resulting in no signal. The polarization rate depends on temperature and the density of the current. High density current and high temperature both speed up the process (Heinmets and Blum, 1962) See section 5.4 for results on polarization experiments.

Temperature is in general a factor that is of great significance to the signal amplitude but not the shape of the signal. With higher temperature the mobility of the ions increases because of the lowering in stability of the crystal structure. The bindings of the molecules in which the ionic defects occur also weakens with temperature making the defects happening a lot faster and thereby creating the current faster (Muto and Shimizu, 2013). See section 5.3 for results on the temperature experiment. Another important parameter controlling the mobility of the protons is the activation energy, which is the minimum energy, needed for the particles to react through collision. This is also closely related to temperature (Heinmets and Blum, 1962). This however, will not be discussed any further.

Another factor controlling the signal form as well as amplitude is density, due to the change in mobility of the ions with density; see section 2.3 for further explanation.

Decay in signal is expected from cores that have been stored over a long time (Schwander *et al.,* 1983). This is also referred to as the *Aging* effect and is likely due to diffusion of impurities entering/leaving the ice from/to the atmosphere or change in defects caused by the relaxation time (ibid.).

The DC method is perfect for EC measurements on ice, since neutral salts do not show any ECM current and sea salts show a signal, which is so small that it can be neglected even for concentrated samples of meteoric ice (Wolff *et al.,* 1996). However it is still being discussed if ECM currents respond differently to different acids of same quantity (in μequiv. per L) (Moore *et al.,* 1984) (ECM calibration curves)). Also it has been shown that there is no DC current when there are no acids present in the ice, which also shows that ionization of the ice is not significant in EC measurements (Moore *et al.,* 1984). A description of the conduction in polar ice has been attempted in two theories based on; 1st) the processes occurring within the ice lattice 2nd) on conduction in the grain boundaries. (Moore *et al.,* 1984)

- The first theory is called the Jaccard theory and describes that conductivity in ice, with impurities, is dominated by intracrystalline ionic H_3O^+ defects (DC conductivity primarily) and primarily Bjerrum L- and D-defects at high frequencies, as carriers (Wolff *et al.,* 1996). See section 6.2.5 for illustration of L- and D-defects. This means that the protons (H^+) changes position due to the defects and in that order responds with a movement toward the anode. This theory is limited by the size of the ion and therefore explains the dominance of H^+ in creating conductivity (Wolff *et al.,* 1996).

- The other theory is focusing on grain-boundary conduction which states that DC conductivity is taking place through connected liquid veins at triple junctions (Wolff *et al.,* 1996) of the molecules. This was the electrons are transported through the veins between the ice crystals. This theory will allow movement of larger ions, compared to the Jaccard theory, and could therefore help explain the signal found in times where no H_2SO_4 is supposed present in the ice.

3. Method

The next section describes the new ECM setup. This is followed by a short description on computer programs used and a detailed description on the procedure for normal EC measurements. Then the temperature experiment and the stationary measurements are introduced. Followed by a comparison of

the old setup and the new are listed, in terms of stabilization factors added to the new setup and last a sample description.

3.1 The modified ECM setup

Several improvements were done to the new setup in order to try and stabilize or minimize some of the factors influencing the reproducibility of the signal. A comparison of the two instruments will be described later in section 3.6.

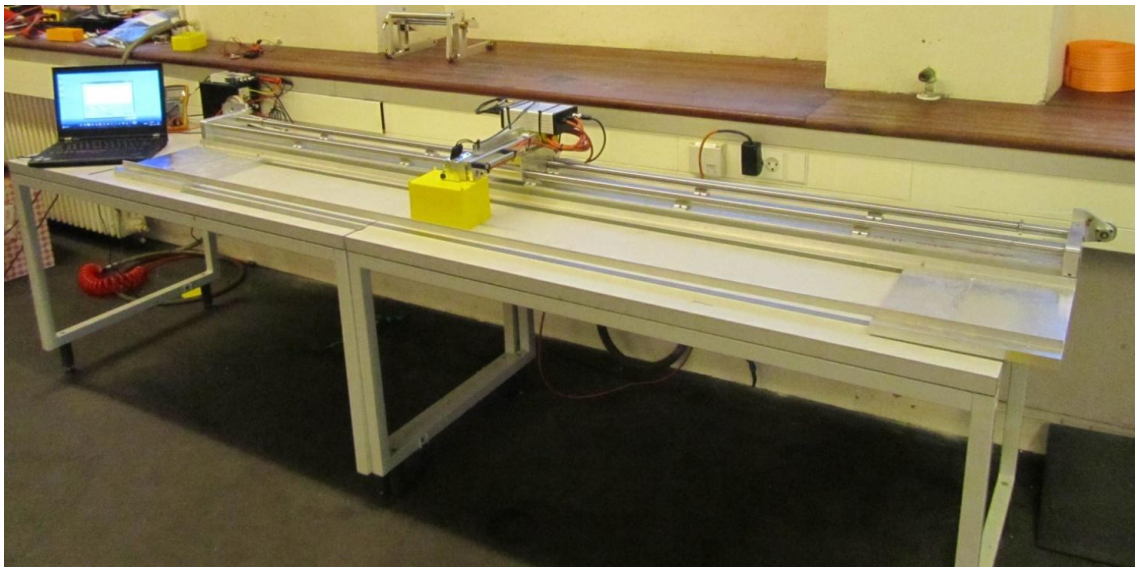

Figure 11 - The new setup is shown here with the computer on the left, the trails on which to place the ice core holders and the electrodes holder, and power supply, resting on the yellow box.

The setup consists of the following parts:

1. Laptop with ECM software
2. Laptop power supplies (PSU)
3. Heating mat (for the laptop)
4. ECM High Voltage and Pre-amp electronics
5. ECM High Voltage and Pre-amp electronics PSU
6. Coax BNC-BNC cables
7. X-axis 10 Volts PSU
8. 5 way power outlet
9. Microtome trammel
10. High resistance test box
11. Digital Voltmeter
12. Horizontal rails
13. Microtome trammel guide rails (only possible to use on bags of ice with the same diameter)
14. ECM base plates (top and Bottom)
15. Electrode holder and electrode arm assembly
16. X-axis toothed belts
17. Ice core holder
18. Ice core holders
19. Ice core holder opener/closer

The measurements of current are in unit micro Ampere. 1 Volt is equivalent to 1 micro Ampere and when the amplification is on (gain x10) then 1V is equivalent to 10 micro Amperes. The notation for amplified runs will throughout the thesis be shown as *Current (x10) (micro.A)*.

The electrodes are made of brass and are separated by 1.3 cm. The part in contact with the ice is 0.1 cm wide (see figure 12 below).

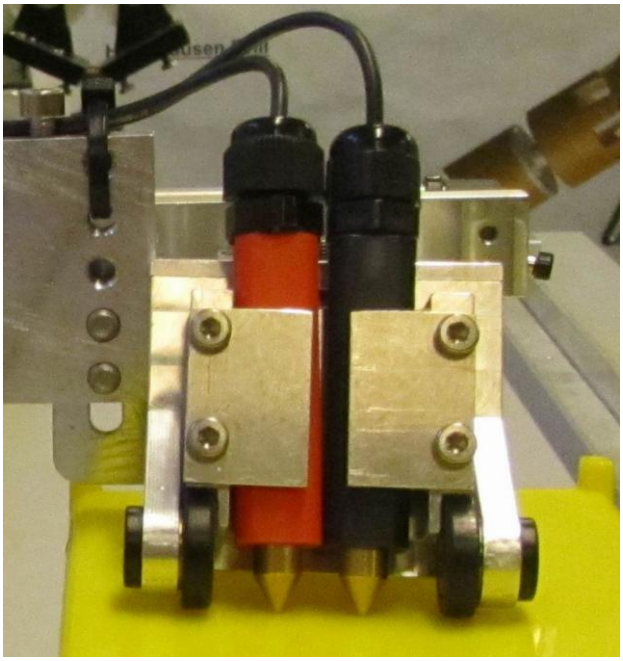

Figure 12 - The electrodes used in the new setup.

3.2 ECM- and depth-scale conversion programs

- ECM program

  The program is started by pressing the “Ecm 55cm” shortcut icon, a Matlab icon, on the laptop then entering *Ecm*. The “ECM 55cm” is for measurements of bags of 55 cm apiece.

- Depth-scale conversion program

  After getting the raw data of the ECM computer with the ECM program the file consists of two columns of data. The X-axis (first column) is showing data from 1-6000 where the Y-axis (second column) is showing the conductivity signal in micro.A also shown over 6000 data points giving a resolution of 0.0275 cm per measuring point. To get the correct depth scale, of the bags measured,

the raw data file is run through another MatLab program that converts the bag number into the corresponding depth.

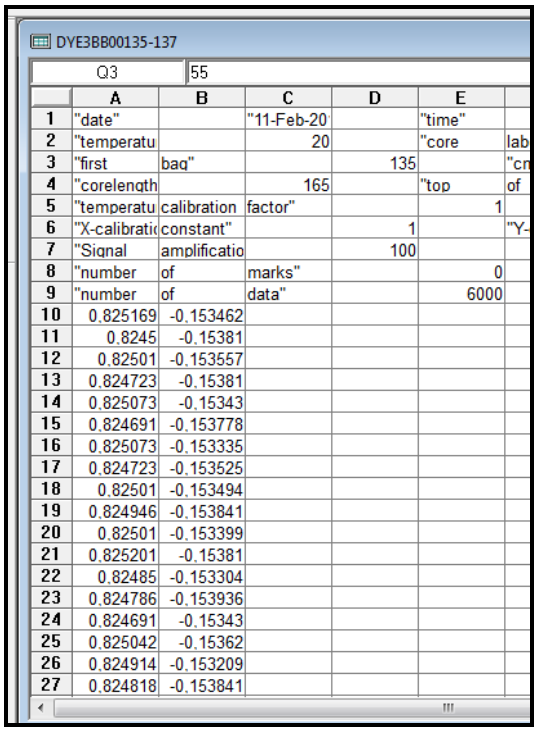

DYE3BB00135-137

Q3 | 55

	A	B	C	D	E	
1	"date"		"11-Feb-20		"time"	
2	"temperatu		20		"core	lab
3	"first	bag"		135		"cr
4	"corelength		165		"top	of
5	"temperatu	calibration	factor"		1	
6	"X-calibrati	constant"		1		"Y-
7	"Signal	amplificatio		100		
8	"number	of	marks"		0	
9	"number	of	data"		6000	
10	0.825169	-0.153462				
11	0.8245	-0.15381				
12	0.82501	-0.153557				
13	0.824723	-0.15381				
14	0.825073	-0.15343				
15	0.824691	-0.153778				
16	0.825073	-0.153335				
17	0.824723	-0.153525				
18	0.82501	-0.153494				
19	0.824946	-0.153841				
20	0.82501	-0.153399				
21	0.825201	-0.15381				
22	0.82485	-0.153304				
23	0.824786	-0.153936				
24	0.824691	-0.15343				
25	0.825042	-0.15362				
26	0.824914	-0.153209				
27	0.824818	-0.153841				

Figure 13 shows a screenshot of the raw file. Notice the values of the first column. The bags 135-137 from Dye-3 are at a depth 73.7-75.35 m when corrected.

3.3 Ice core measurement procedure

Assuming that the setup is ready to be used, this includes all electronics turned on and the stabilization of core temperature; the following preparations are done to the ice;

1. When taking out the first piece of core (lowest bag number) note down the direction on the core as indicated on the bag it was in. Then place the piece of core in the ice core holder with the upward direction pointing to left. This will be the most shallow bag number first indicating the motion of moving from high to low or from shallow to deep in the ice core. The second and third piece is placed after the first with the same instructions as above.

2. The ice core holder opener/closer is closed so that the ice is stabilized in the ice core holder. In case of a smaller core diameter the cores were stabilized with flamingo.

3. A reliable thermometer is placed between two of the cores and the temperature is measured over a couple of minutes (time enough for the thermometer to stabilize).

4. In the MatLab ECM program the temperature measured is found through resistance, e.g. resistance of 20.23 equals a temperature of -18.7°C (see the box named *Temperature* figure 13 above). This means that the user needs to find the resistance matching the temperature and entering that in the box. When already at the computer the user should enter an acquisition name (*Filename*) and here it also shows the type of file (e.g. 746.DO2). The bag numbers measured on are entered under *First bag name* and *Last bag name* for later depth calculations and the length of the cores in *cm's from this bag*.

5. After removing the thermometer from the ice the surface of all three pieces is cleaned by scraping off 1-2 mm with the microtome knife. It is important that the whole surface is cleaned and that the surface is as smooth as possible.

6. When the cleaning is finished and all information entered in the MatLab program the first measurement is ready to be done. Then - place the electrodes in the beginning of the first ice piece (here bag 746). NOTE if several runs are performed without cleaning the surface in between, crossing of different runs should be avoided. With a core diameter of approx. 10 cm three runs can be performed without crossing the previous tracks (see figure 16 further down) a fourth run was performed, in or crossing of the previously made trails, with a x10 amplification. When ready pres *Go* in the program. Once *Go* has been pressed a sound is played and a percentage counting starts. The timer indicates the pace of witch the user should drag the electrode arm along the pieces of ice. After 100% the measurement should be done if not then the last ice is not measured and the run is useless. Note the small black bottom on the electrode arm should be held in during the whole measurement (30 sec.).

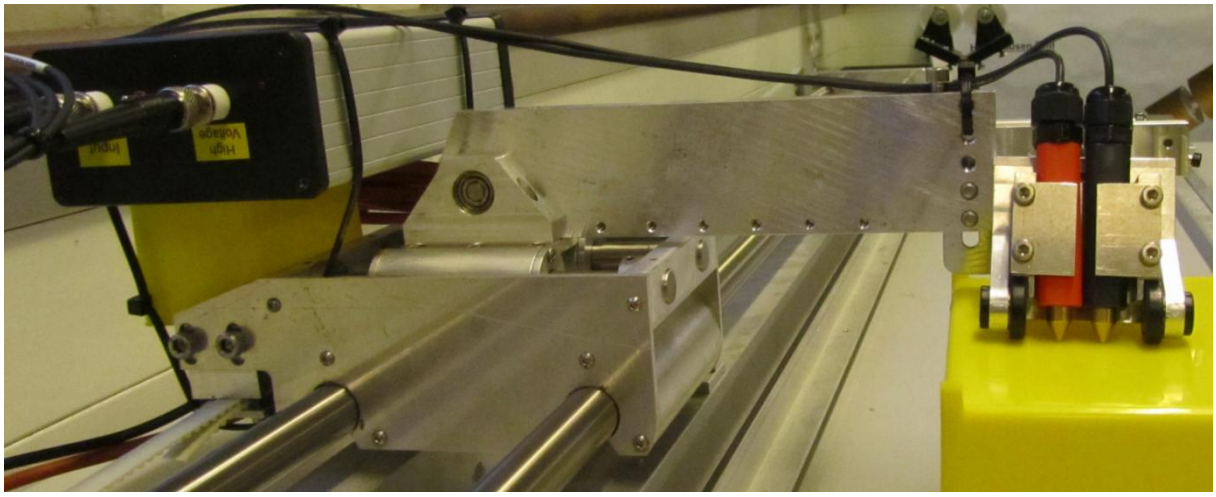

Figure 14 showing the powersupply, electrodes and their holding system.

7. After the first run place the electrodes on bag separation points and press *Abag* in the program. These marks are shown in the program and could explain an unexpected rise or drop in the signal. Should there be breaks in the ice pieces then place the electrodes by the breaks and press *Break* in the program. This shows another mark on the graph and could possibly once more explain unexpected signals.

8. Save the run by pressing *Zave*. By pressing *Remeasure* after the program is ready for the next run.

9. Place the electrodes once more on the first piece of ice but this time different from the first tracks. Redo the same procedure as before and save the run. By pressing *Remeasure* the filename changes from DO1 (run 1) to DO2 indicating that this is run 2.

10. After finishing the measurements open up for the ice core holder and return the ice to the corresponding bags. Note; remember to position the ice with the same direction indicated on the ice as the bag.

11. Should a new section of an ice core be measured then simply press *New Core*, enter the new information and follow the steps written above.

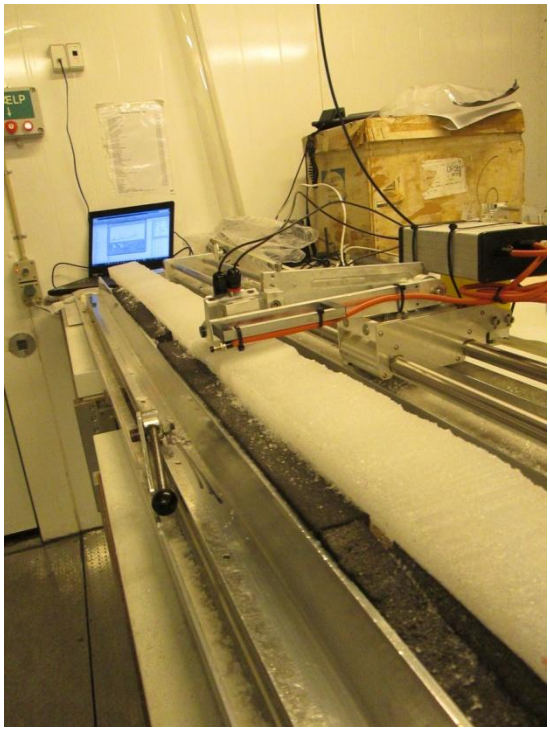

Figure 15a) shows the setup looking opposite of the dragging movement.

Figure 15b) shows how the electrodes are dragged by the handle along the ice.

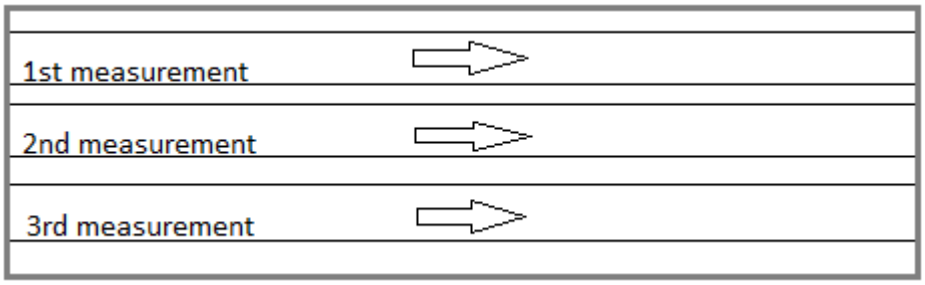

Figure 16 shows the typical electrode positioning/trail on an ice core surface during the three first measurements.

3.4 Temperature measurements

The temperature measurements were done on different days due to the temperature stabilization time. The -17°C measurement was done like any other, as described in measurement procedure. During the -25°C measurement the freezer laboratory's temperature was lowered to approximately -25°C to minimize the temperature change effect as much as possible. Other than that all preparations was the same as described earlier.

3.5 Stationary measurements

The preparation of the ice is the same as mentioned above in the measurement procedure though only one piece of ice was measured at a time.

During stationary measurements the electrodes were placed at the wanted depth and the whole measurement (all 30 seconds) was done at the same position. Three measurements were done on each core at three different positions.

3.6 Comparison to the old instrument

Compared to the old ECM system then the following improvements were done:

1. Improved repeatability on X-axis position.
2. Improved signal to noise ratio
3. Improved signal sensitivity
4. Improved safety
5. Reduced ice saturation effect
6. Reduced complexity and components influencing the signal
7. Longer ice core length measurements

1) The old electrodes were hold by a string and were pulled by hand. Because of the possible change of hand position, when walking along the core, a change in the x-axis measurement could occur. This could result in a 1-2 cm offset in the depth scale. With the new setup the electrodes are attached to a metal arm with no influence on the *depth measuring counter*.

2-3) The noise is reduced by 10% by the use of DAQ (Data Acquisition Q) LSB (Least Significant Bit) (the ability to record and store data) compared to the old 1 LSB system. This result in a drift that is less than 1/5 of an LSB over the sampling time - compares to drift of ~1 LSB. The reduction of noise is also a result of screening of sensitive signal paths and suppressing unwanted high frequency noise.

4) The old instrument had a large part of the electrodes exposed making it dangerous to handle the instrument should the user come in contact with the metal, which is a high voltage component (more than 1000 Volts).

5) Because of the new time counter installed as part of the ECM program there is a limitation change in measure time/rate. The constant measure rate decreases the chances of polarization of the ice.

6) Because the instrument no longer rely on the weight added by the user but has a constant weight that factor can be removed from the uncertainties in the measurements.

7) The tracks are simply made longer.

3.7 Sample description

The table below gives a description for all measured bags.

Ice core	Bag no.	Depth (m)	Length (m)	Width (cm) (positions; 0, 27.5, 55)	Breaks (m depth)	Notes
NGRIP2	2674	1470.15-1470.7	0.55	10, 10, 8.5		1.5*8 cm piece missing at the end of bag (2674)
	2675	1470.7-1471.25	0.55	10, 10, 10	1470.99 & 1471.01	
	2676	1471.25-1471.8	0.55	10, 9.5, 10		
NGRIP	293	160.6-161.15	0.55	8, 8.5, 8	160.67	
	294	161.15-161.8	0.55	8.5, 8.5, 8.5		
	295	161.8-162.35	0.55	6, 6, 6.5		
	109	59.4-59.95	0.57	10, 10, 10	59.62	
	110	59.95-60.5	0.55	6, 6, 6		
	111	60.5-61.05	0.55	6, 6, 6	60.8 & 60.875	
	95	51.7-52.25	0.55	10, 10, 10		
	96	52.25-52.8	0.55	10, 10, 10		
	97	52.8-53.35	0.545	9.5, 9.5, 10	53.03	Re-freezing
	64	34.65-35.2	0.58	10, 10, 10		
	65	35.2-35.75	0.52	10, 10, 10		Re-freezing
	66	35.75-36.3	0.55	10, 10, 10		Re-freezing
GRIP	2907	1598.3-1598.85	0.55	9, 9, 9	1598.67	
	2908	1598.85-1599.4	0.55	7.5, 7.5, 7.5		
	2909	1599.4-1599.95	0.55	7.5, 7.5, 7.5		
	107	58.3-58.85	0.55	8, 8, 8		Re-freezing
	108	58.85-59.4	0.55	8, 8, 8		Re-freezing
	109	59.4-59.95	0.55	8, 8, 8		Re-freezing
	72	39.05-39.6	0.55	8, 8, 8	39.285	Re-freezing
	73	39.6-40.15	0.55	8, 8, 8		Re-freezing
	74	40.15-40.7	0.55	8, 8, 8	40.625	Re-freezing
Dye-3	3235	1778.7-1779.25	0.56	6.5, 7, 7	1779.02	Re-freezing
	3236	1779.25-1779.8	0.55	6.5, 6.5, 6.5	1779.59	Re-freezing
	3237	1779.8-1780.35	0.56	6.5, 6.5, 6.5	1780.9	Re-freezing
	672	369.05-369.6	0.54	7, 7.5, 7.5	369.32	Re-freezing

	673	369.6-370.15	0.56	7, 7.5, 7		Re-freezing
	674	370.15-370.7	0.55	8, 8, 8		Re-freezing
	135	73.7-74.25	0.545	7.5, 7.5, 4		-3.5*11 cm piece missing at the end of this bag (135) also re-freezing.
	136	74.25-74.8	0.585	8, 8, 9		-Re-freezing. Melt layer at 74.51 m depth.
	137	74.8-75.35	0.55	8, 8, 8		-Re-freezing. Melt layer at 75.33 m depth.

Table 2 - Sample description of all bags.

4. DATA

The sections below show the calculations used to get the results in the next chapter, it describes how they are done and what assumptions are associated with them.

4.1 Calculations

From the raw ECM signal data and melt samples of sulphate, at a corresponding depth, the calibration formula was produced. The ECM (mirco.A) and sulphate (microequivalents SO_4^{2-} /Kg ice) values were all averaged over 5 cm intervals due to the discrete IC samples of the melted and measured sulphate. The value given in depth is the bottom of the sample interval meaning that if the value is given at depth 150 cm then the averaged interval is from 145 cm to 150 cm depth. Some sulphate values were only available in 55 cm average. This means that is a whole bag that is melted and the average value is given. In order to make the values comparable to the old measurements all new ECM values are multiplied by ten. The runs made with the amplification on cannot be used due to the saturation limit of the instrument. The points are chosen by their fit with the sulphate and not an average of all runs made on the section (see section 5.2). The run showing the highest signal is considered the most correct to use since signals with lower values would result in an underestimation of sulphate therefore these are used for the calibration. One point (pink point) in figure 17 below is not used in the calibration. This is due to the strange circumstances of its values. The IC sulphate is averaged over 5 cm but the value is much higher (3-4 times) than any other value in that entire core. Data will not be discarded based on a bad fit but in this case none of the other points that are around 4 micro.A in current signal show values anywhere this point, which is used to argument why it will not be used in the calibration.

With ECM and Sulphate plotted the best fit between then is a linear relationship. Compared to the old produced calibration curves, with focus on H^+ and not SO_4^{2-}, this is a completely different relationship (Hammer, 1980). This will is discussed in section 6.4. The best linear fit gives the equation:

$$Y = 2.0229x + 0.6297 \quad \text{(Equation 4)}$$

Also shown in figure 17 below

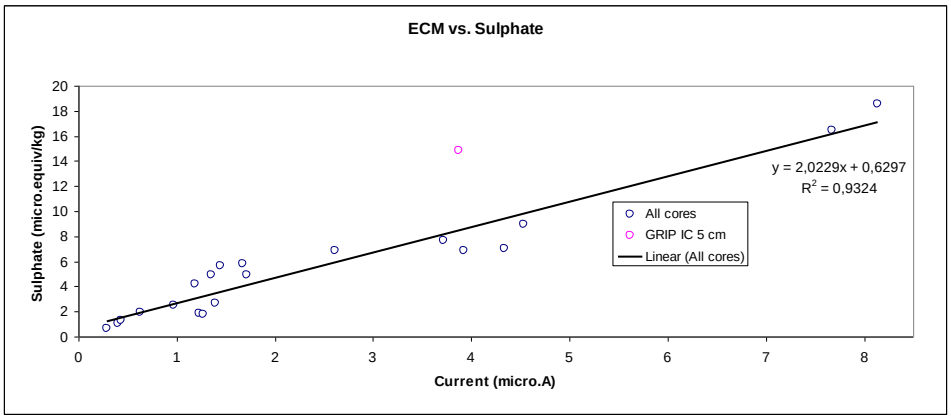

Figure 17 - The plot shows the calibration produced from the new ECM measurements and previously measured IC sulphate values.

This linear fit equation is the calibration that will be used for later calculations. The equation will be written as:

$$SO_4^{2-} = 2.0229i + 0.6297 \text{ (Equation 5)}$$

i is the conductivity (μA) and SO_4^{2-} (micro.equiv. SO_4^{2-} /Kg) is the sulphate content.

The fit line is not forced through the Origin (0, 0) since that would be equal to no conductivity without sulphate but since it is assumed that the conductivity is created by the free H^+ ions, that could come from other impurities, and not just the sulphate this is not done (Wolff *et al.,* 1996). Being that we assume that the free H^+ ions are the dominating current producing factor, the cutting of the positive y-axis by the linear regression curve would indicate that it is either because of the less good fitting of the data points to the fitted curve, or that there is a different relationship between SO_4^{2-} and H^+ and the conductivity than assumed see section 6.2. Table 3 below is showing the data used for the calibration and any specific notes to the data.

Core/Bags	**Depth**	**Current (x10)** (micro.A)	**Sulphate** (micro.equiv SO_4^{2-} /kg ice)	**Notes**
NGRIP2				
2674-2676	1470,7	1,4	5,6	Run no. 1 used
293-295	161,5	4,5	8,9	Run no. 2 used
	161,55	3,7	7,7	
	160,95	1,2	1,9	
	162,1	0,4	1,0	
	161,45	2,6	6,8	
	161,6	1,7	4,9	
109-111	60	1,3	1,8	Run no. 1 used
	60,05	3,9	6,8	
	60,1	7,7	16,5	
	60,15	8,1	18,5	
	60,2	4,3	7,0	
95-97	52,45	1,7	5,8	Run no. 1 used
	52,15	0,6	1,9	
	52,8	0,4	1,3	
	52,5	1,4	4,9	
64-66	35,65	1,4	2,7	Run no. 2 used
	35,7	1,0	2,5	
GRIP	1598,85	1,2	4,2	Run no. 2 used
2907-2909	1599,4	0,3	0,7	
GRIP				NOT USED for
2907-2909	1598,9	**3,9**	**14,8**	calibration

Table 3 shows the data values for current and sulphate used to produce the calibration. It also shows what run is used for the calculations.

To calculate the amount of sulphate per area that is found in the ice the following equations and assumptions were made. The unit of sulphate is given by micro.equiv. SO_4^{2-} /Kg ice.

1 equiv. corresponds to the amount of substance that reacts with 1 mol of H^+ (Skjoldborg *et al.,* 2013). Because it is assumed that all H^+ is attached to sulphate in form of sulphuric acid (H_2SO_4), from the volcanic eruption, there is a direct 2:1 relationship between the amount of H^+ and SO_4^{2-} ions for the reaction creating H_2SO_4:

$$2H^+ + SO_4^{2-} \rightarrow H_2SO_4$$ (Equation 7)

The molar masses for H^+ and SO_4^{2-} are M_{H+} = 1g/mole and $M_{SO_4^{2-}}$ = 96.06 g/mole respectively.

Microequivalents are corresponding to micromoles multiplied by the charge of the ion. To go from micro.equiv to micrograms the amount of SO_4^{2-} is divided by the charge of the ion (2) and then multiplied by the molecular weight of the ion (96.06 g/mole). So;

$$\frac{1\left(micro.equiv SO_4^{2-}\right)}{2} = 0.5\left(micro.moles SO_4^{2-}\right)$$ (Equation 8)

Followed by

$$0.5\left(micro.moles SO_4^{2-}\right) * 96.06\left(\frac{micro.grams}{micro.mole}\right) = 48.03\left(micro.grams SO_4^{2-}\right)$$ (Equation 9)

To calculate the sulphate deposition the concentration of sulphate ($C_{sulphate}$) is found first.

Going from micro.equiv.SO_4^{2-}/kg to ppb, and thereby getting the correct concentration, the SO_4^{2-} value is multiplied by 48.03 microgram/micro.equiv:

SO_4^{2-} (micro.equiv./kg) * 48.03 (microgram Sulphate/Kg_{ice}) = sulphate in ppb (Equation 10)

To get $Kg_{sulphate}/Kg_{ice}$ and thereby calculating $C_{sulphate}$ the value is divided by 10^9:

$$C_{sulphate} = SO_4^{2-}\left(\frac{micro.equiv.}{Kg_{ice}}\right) * \frac{48.03}{10^9}\left(\frac{Kg_{sulphate}}{Kg_{ice}}\right)$$ (Equation 11)

$C_{sulphate}$ is also defined as:

$$C_{sulphate} = \frac{m_{sulphate}}{m_{ice}},\ (m_{ice} = A * D * \rho_{icelayer})$$ (Equation 12)

A is the surface area, *D* is its depth interval and $\rho_{ice\ layer}$ (Kg_{ice}/m^3) is the density of the firn/ice layer measured on. Rearranging a little, sulphate per area is given by equation 13. See figure 18 below.

$$\frac{m_{sulphate}}{A} = \rho_{icelayer} * D * C_{sulphate}$$ (Equation 13)

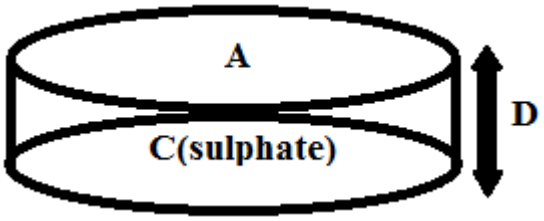

Figure 18 shows a piece of e.g. ice core and the quantities we are interested in calculating.

The amount of sulphate varies with time/depth therefore summation is needed:

$$\frac{m_{sulfat}}{A} \approx \rho_{icelayer} * 0.05m * \sum C_{sulphate}$$ (Equation 4)

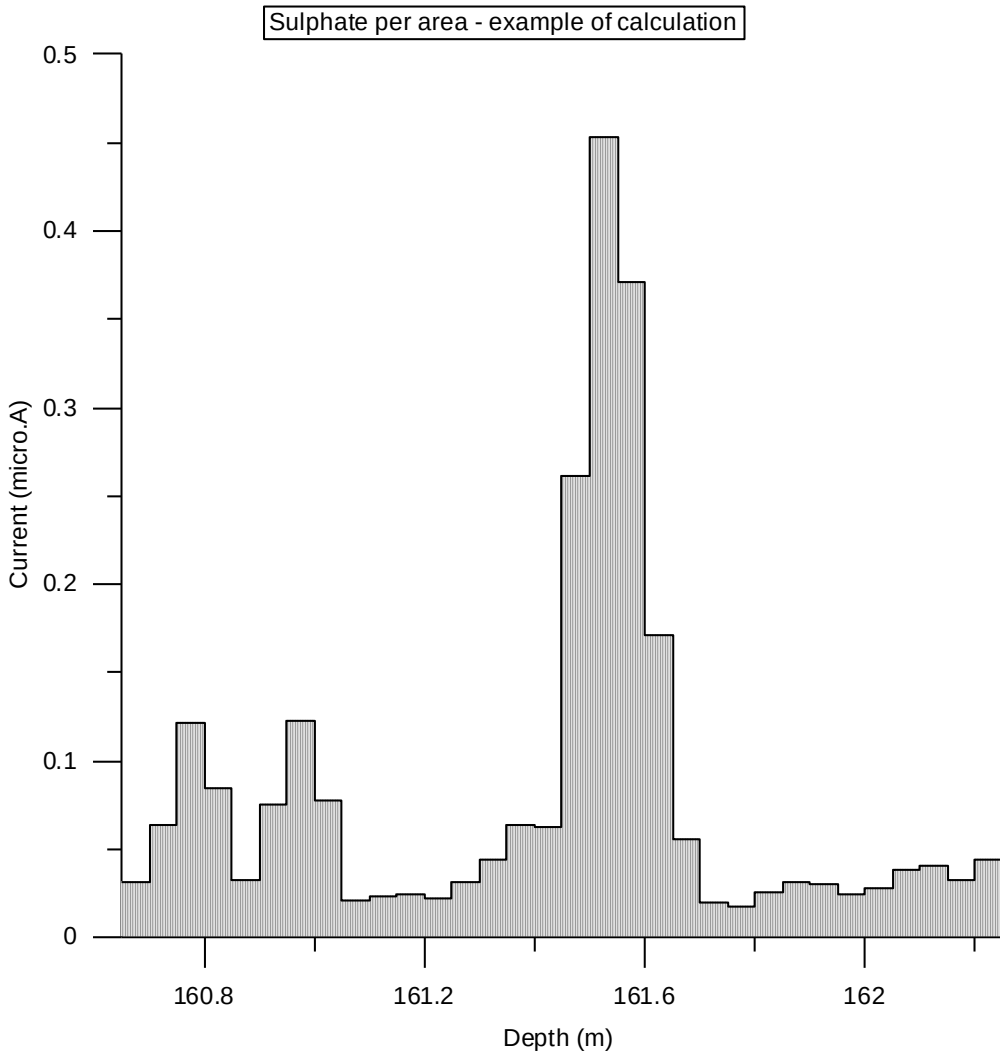

Figure 19 illustrates the basic principle and argument for the summation over the depth intervals

A calculation looks like this (see table 4 below);

First) A1 is inserted into the calibration formula, giving B1 (equation 5)

Secondly) B1 is multiplied by the 48.03 and divided by 10^9, giving $C_{sulphate}$ (equation 10)

Thirdly) $C_{sulphate}$ is then multiplied by E1 and F1 and finally multiplied by 10^6 for the units, giving Sulphate per area for calculation Number 1.

Fourthly) Because this only gives the sulphate per area for the 5cm chosen integration over the whole peak is necessary. This is done by adding all the calculations for each Number (equation 13). In this case it would be from Number 1 to 6 which would result in the total sulphate per are (108.7 kg/km^2) for the whole peak equation.

NGRIP 109-111								
Number-Depth		**A** ECM (x10) (Run 1)	**B** micro.equiv SO_4^{2-} /kg_{ice}	**C** ppb	**D** $C_{(sulphate)}$	**E** $\rho_{ice\ layer}$ (kg/m^3)	**F** Depth (m)	**G** Sulphate per area (kg/km^2)
1	60	1.3	3.2	153.3	1.53E-07	783.8	0.05	**108.7**
2	60,05	3.9	8.6	411,5	4.11E-07	783.8	0.05	
3	60,1	7.7	16.2	775.7	7.76E-07	783.8	0.05	
4	60,15	8.1	17.1	820.8	8.21E-07	783.8	0.05	
5	60,2	4.3	9.4	452.0	4.52E-07	783.8	0.05	
6	60,25	1.3	3.4	160.7	1.61E-07	783.8	0.05	

Table 4 shows one example of the average sulphate per area calculations.

The width of an eruption should be relatively stable in the EC measurements but in cases of variation the widest depth interval was chosen. This could give an overestimation of sulphate per area but within accepted uncertainties.

Calculations for the table 6 – Sulphate deposition and distribution.

Table 6 showing Sulphate per area in section xx is based on the average of sulphate per area of two to three runs (depending on the form and size of the signal). For instance signals that, appeared by eye are less than 2/3 within alignment of the first run, is not used. This was done to produce error bars to look at the reproducibility of the signal between the runs. It is assumed that an average sum is more useful for models because of the error bars produced and the possibility for accounting for variation in distribution patterns. This is compared to the calibration it self where the signal of the first run generally represents the sulphate content better than the following measurements (done on a used surface). Here are exceptions as referred to earlier in this section when the selection of points used for the calibration were based on the biggest signal, sometimes turned out to be that of the second run. An average of each run could have the effect of lowering the average sum, since only the biggest signal is used for the calibration, which is why the biggest error interval is also given to the averaged value (table 6).

Background values

The background values are not subtracted from the calibration curve calculations or the sulphate distribution. This is because the background values have been either too difficult to determine due to low signal measurements or considered negligible in measurements with strong signal. It is assumed that the background levels are H^+ coming from other impurities than sulphuric acid, which could affect the true value of sulphate per area if background levels were significant enough (Wolff *et al.,* 1996).

Temperature effect

The temperature effect is shown by figure 38 and table 5, which are based on the same calculations as those of table 6 explained above.

5. Results

The result section is separated into several paragraphs first all ECM figures for all cores are presented. These are shortly described in the section to follow. After this figures of 5 cm-averaged new/old ECM and IC sulphate values are shown. Then the temperature experiment and stationary measurements are presented. Last but not least, the presentation of the new calibration curve and the table of sulphate per area.

5.1 New and old ECM figures for all eruptions

All mentioned deposition depths are taken from the old EC measurements and are gathered from CIC's own database (2014, CIC database).

5.1.1 NGRIP ECM measurements

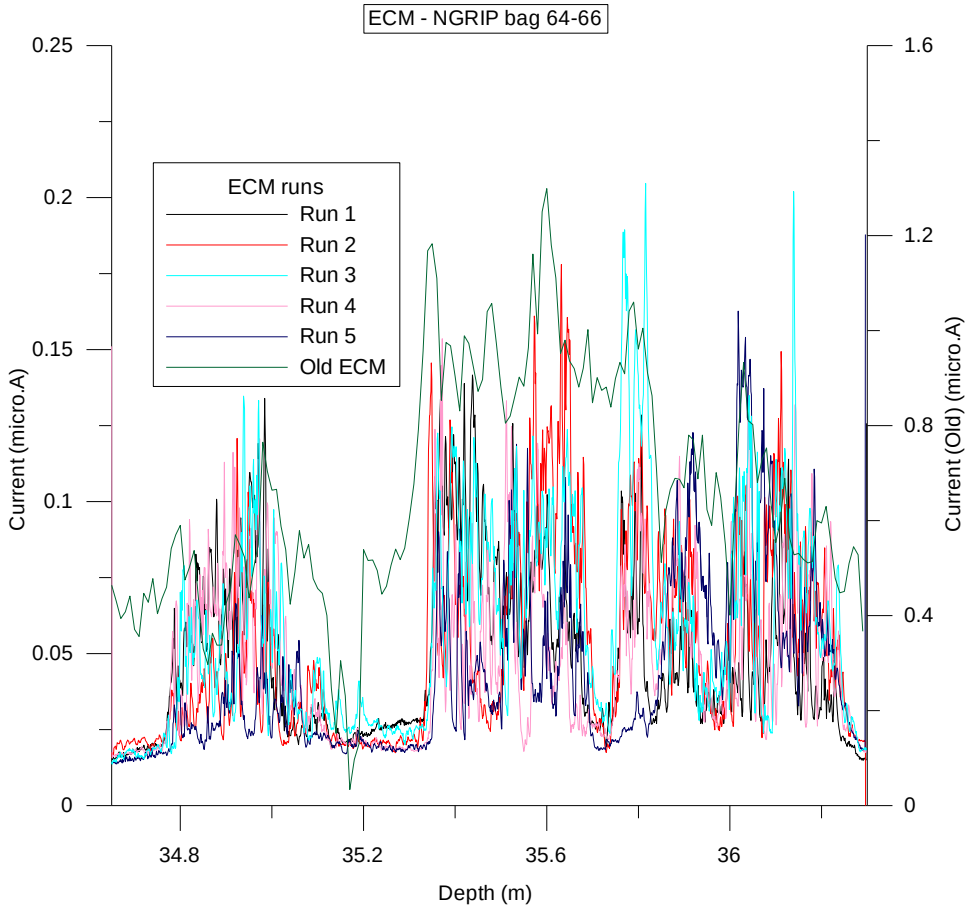

Figure 20 - Five ECM runs on the same bags are shown above. The measurements were done with an air temperature of -18.1°C and the ice was -18.6°C. Maximum deposition of this eruption is around the depth 35.35 m based on the old EC measurements. The figure also shows the old EC measurement shown in green. It should be remembered that the old ECM is calibrated after Hammers calibration (equation 1).

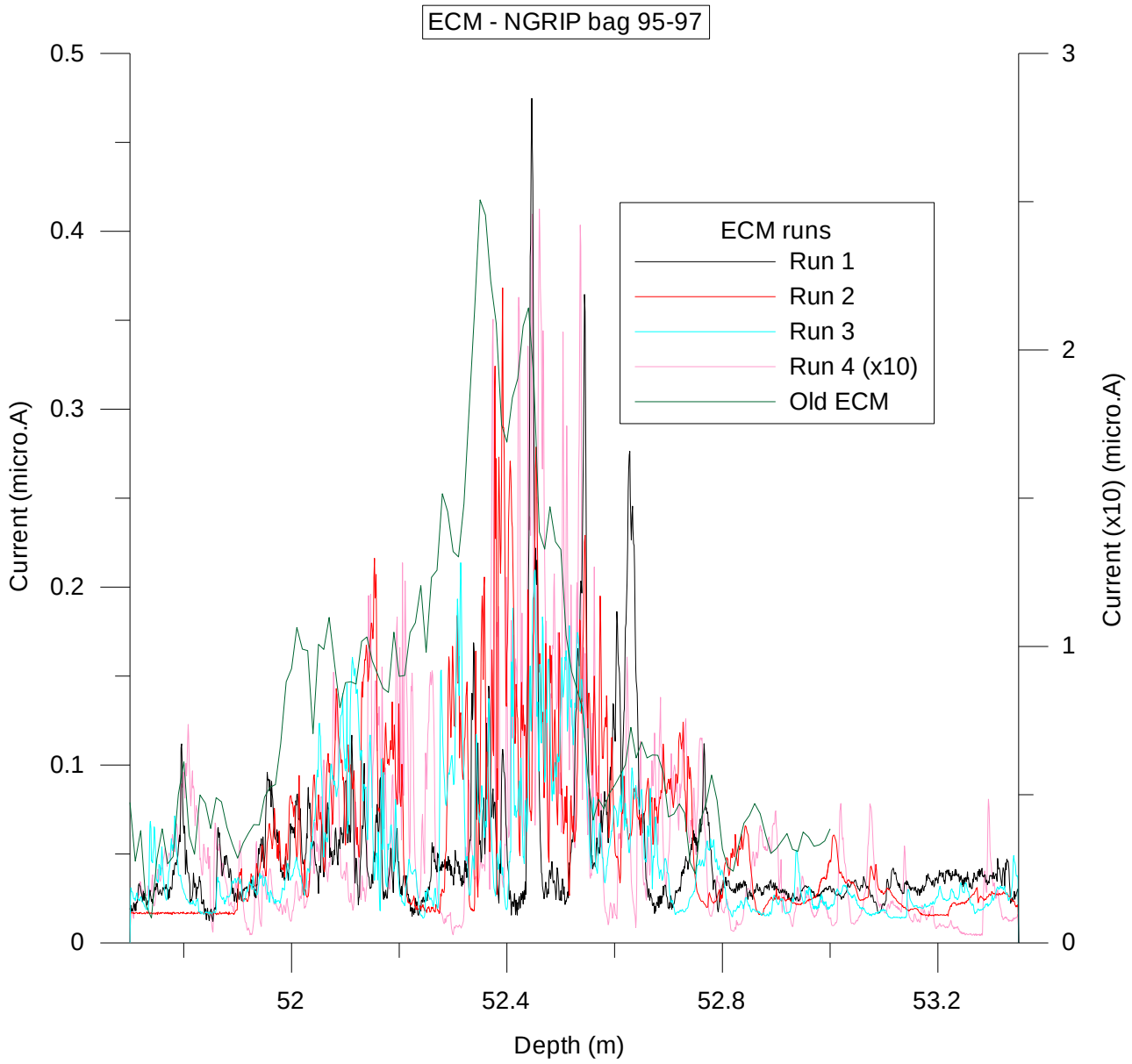

Figure 21 - Four runs are shown one being a times 10 amplification. The air temperature was -17.8°C and ice core temperature of -18.2°C during measurements. The old ECM is shown in green and follows the x10 y-axis on the right. The deposition depth of the Tambora eruption is around 52.38 m.

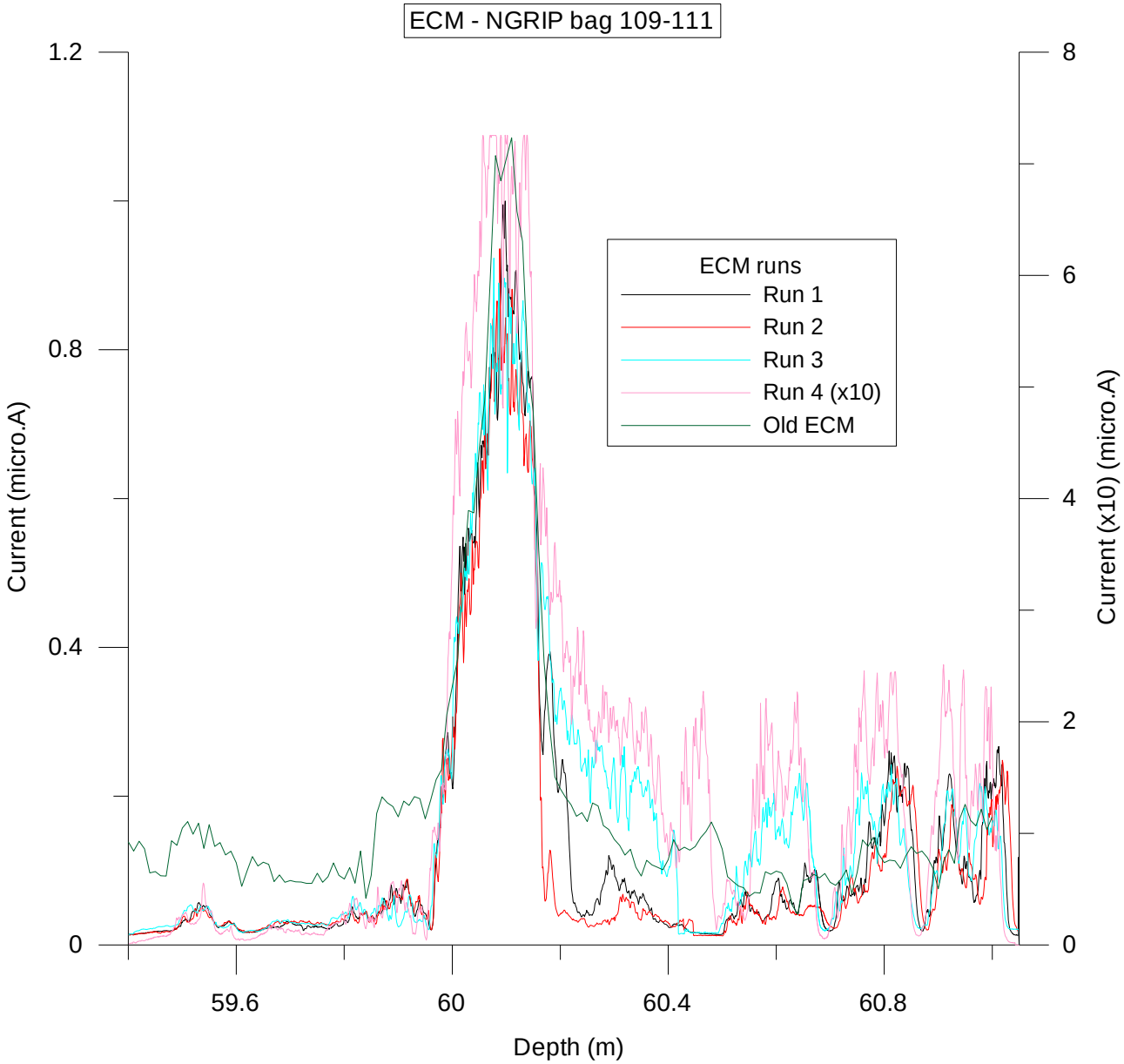

Figure 22 - Four runs shown with one being done with amplification (x10). The air temperature is -16.9°C and the core temperature is -18.0°C. The old ECM is shown in green and follows the x10 y-axis. The deposition depth is 59.975 m.

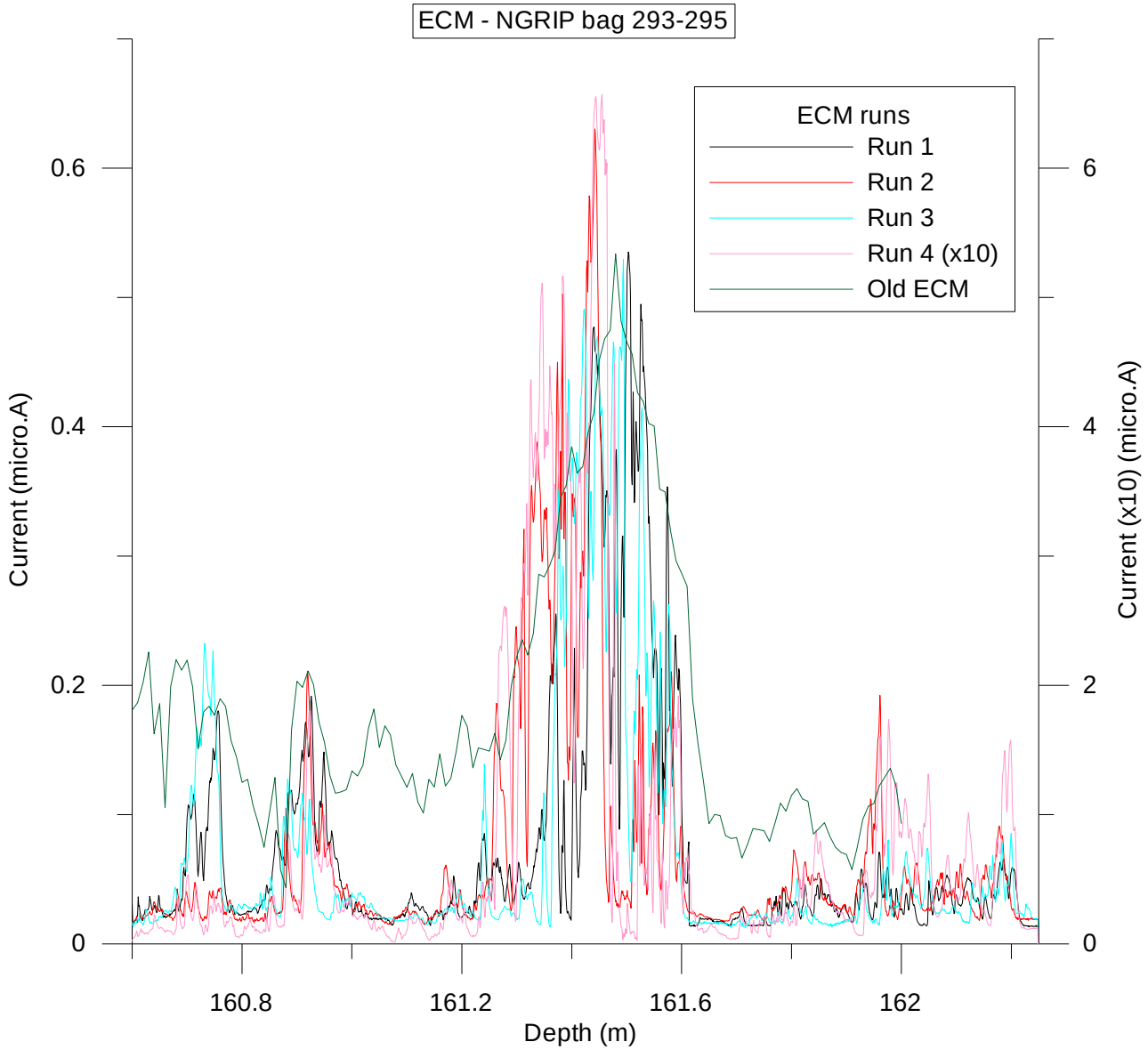

Figure 23 - Four runs with one amplified (x10). The measurements were done with an air temperature of -17.4°C and a core temperature of -17.8°C. The old ECM is shown in green and follows the x10 y-axis on the right. The deposition depth is 161.375 m.

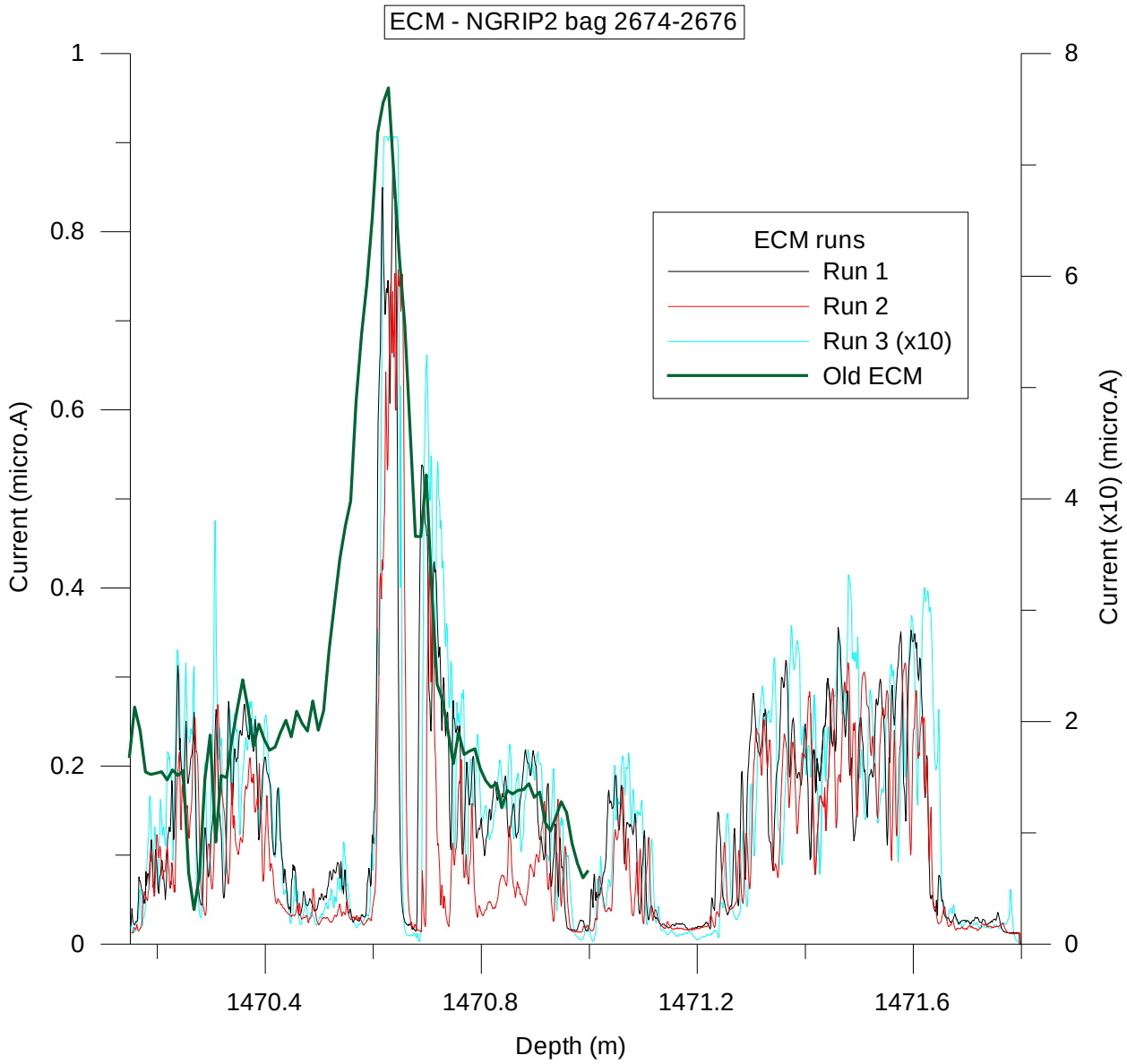

Figure 24 - Three runs were measured with one being amplified. The measurements were done with an air temperature of -18.2°C and a core temperature of -18.6°C. The old ECM is shown in green and follows the x10 y-axis. The deposition depth is around 1470.64 m.

5.1.1.1 ECM on NGRIP

NGRIP 64-66

Figure 20 shows the ECM runs performed on 3 pieces of the NGRIP ice core bag 64-66 with the length; 55 cm 52 cm, 58 cm giving a total of 165 cm and all of the pieces had a diameter of approximately 10 cm. The total depth of this section is 34.65 m to 36.3 m. The air temperature was -18.1°C and the ice was -18.6°C. Bag 64 and 65 both showed a great deal of re-freezing. The 5 runs shows the electrical current measured along the ice and how they differ from each other from measurement to measurement. Remember this is a

high porosity section due to the low density. The figures show a tendency of three peak “sections” at approximately depth of; 34.8 m to 35.1 m, 35.35 m to 35.7 m and the last and a bit more unspecified section 35.75 m to 36.2 m. The maximum value is 1.17 micro.A at 35.81 m depth and of run 3 but not at the correct deposition depth. The maximum value of what appear to be the correct peak depth is from run 2 giving a signal size of 0.175 micro.A at 35.65 m

NGRIP 95-97

Figure 21 - ECM on bag 95-97 is between the depths of 51.7 m to 53.35 m. Measured with an air temperature of -17.8°C and ice core temperature of -18.2°C. The bags 95-97 were of the length; 54.5 cm, 55.5 cm, 55 cm a total of 165 cm, and a core diameter of approximately 10 cm respectfully. There were severe re-freezing and two breaks in bag 97 (see sample description in section 3.7). There are four runs measured with one being amplified times 10, run 4. The deposition of the Tambora eruption is corresponding to a time of 1815 A.D. The maximum value of non amplified runs is 0.47 micro.A (run 1) at a depth of 52.446 m and for the amplified 2.47 micro.A (run 4) at 52.447 m. The peak appears to be at depths of 52.39 m and 52.6 m.

NGRIP 109-111

Figure 22 - Four measurements of the Laki eruption where run 4 is amplified times 10, of ECM on bag 109-111 between the depths of 59.4 m and 61.05 m. The air temperature is -16.9°C and the core temperature is -18.0°C. The 109-111 has a length of 55 cm each, a total of 165 cm, and a core diameter of 6 cm, 6 cm and 10 cm respectively. There were one break in bag 109 and two breaks in bag 111. The deposition depth of the Laki eruption should correspond to the age of the year 1783 A.D. The maximum value if the non-amplified runs is 1.0 micro.A of run 1 at a depth of 60.09 m. The amplified run topped at a value of 7.25 micro.A at the same depth but due to saturation of the instrument at 7.25 micro.A, the true maximum value is unknown. The figure shows a clear peak start around 59.95 which lasts, for run 1 and 2, approx. until 60.2 m. Run 3 and 4 both registers several fluctuations in current measured throughout the last distance.

NGRIP 293-295

Figure 23 - ECM measurements on bag 293-295 from the NGRIP core corresponding to a depth interval between 160.6 m and 162.25 m. The figure shows four runs with run number 4 (pink) as an amplified (times 10) measurement. Each bag was 55 cm, giving 165 cm all together, but the diameter of 293, 294 and 295 was 8.5 cm, 8.5 cm and 6.5 cm respectfully. Bag 293 had one break. The measurements were done with an air temperature of -17.4°C and a core temperature of -17-8°C. The maximum value of the non-amplified run is 0.63 micro.A, run 2, at a depth of 161.442 m. The maximum value for run 4 (the amplified) is 6.5 micro.A at a depth of 161.444 m. The deposition depth of this unknown eruption should correspond to the age of 1257 A.D. There is a clear peak defined between 161.3 m and 161.6 m.

NGRIP 2674-2676

Figure 24 - The final eruption from NGRIP is measured over the bags 2674-2676 corresponding to a depth interval of 1470.15-1471.8 m. Three runs were measured with run 3 being amplified. The measurements were done with an air temperature of -18.2°C and a core temperature of -18.6°C. Each bag is 55cm long giving a total of 165cm and has a diameter of approx. 10cm and there are two breaks in bag 2675. The maximum value of the non-amplified runs is 0.89 micro.A for run 1 and for the amplified, run 3, the maximum value is 7.25 micro.A again, due to saturation of the instrument. The depth measured corresponds to an age around 9305 B.C. The peak starts at 1470.6 m and ends before 1470.8 m.

5.1.2 GRIP ECM measurements

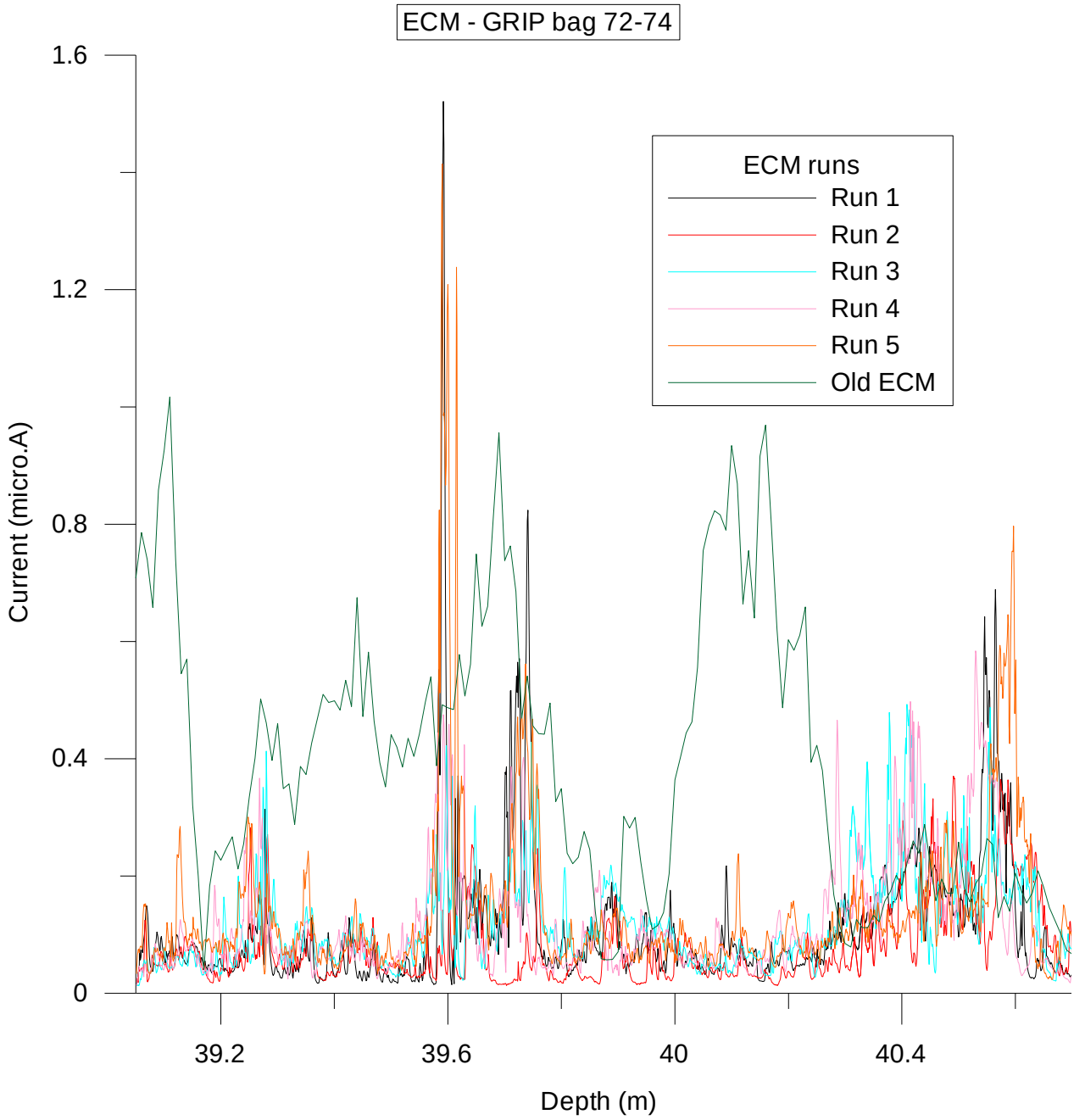

Figure 25 - Five runs were produced. The bags were measured with an air temperature of -17.4°C and a core temperature of -17.8°C. The old ECM is shown in green. The deposition depth is around 39.1 m.

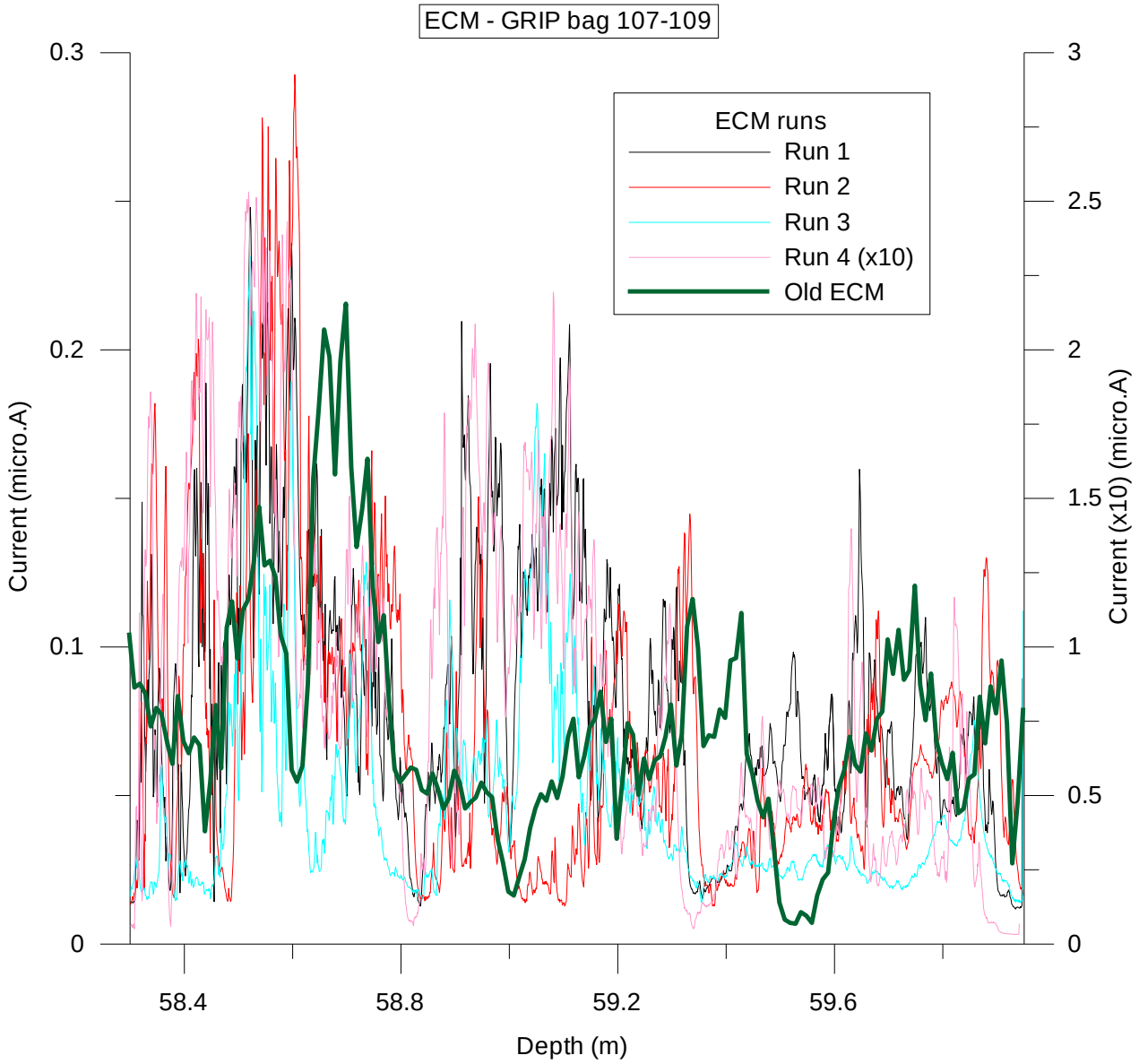

Figure 26 - Four runs are shown above. The measurements were done with an air temperature of -17.4°C and a core temperature of -17.6°C. The old ECM is shown in green and follows uses the x10 y-axis. The deposition depth is around 58.575 m.

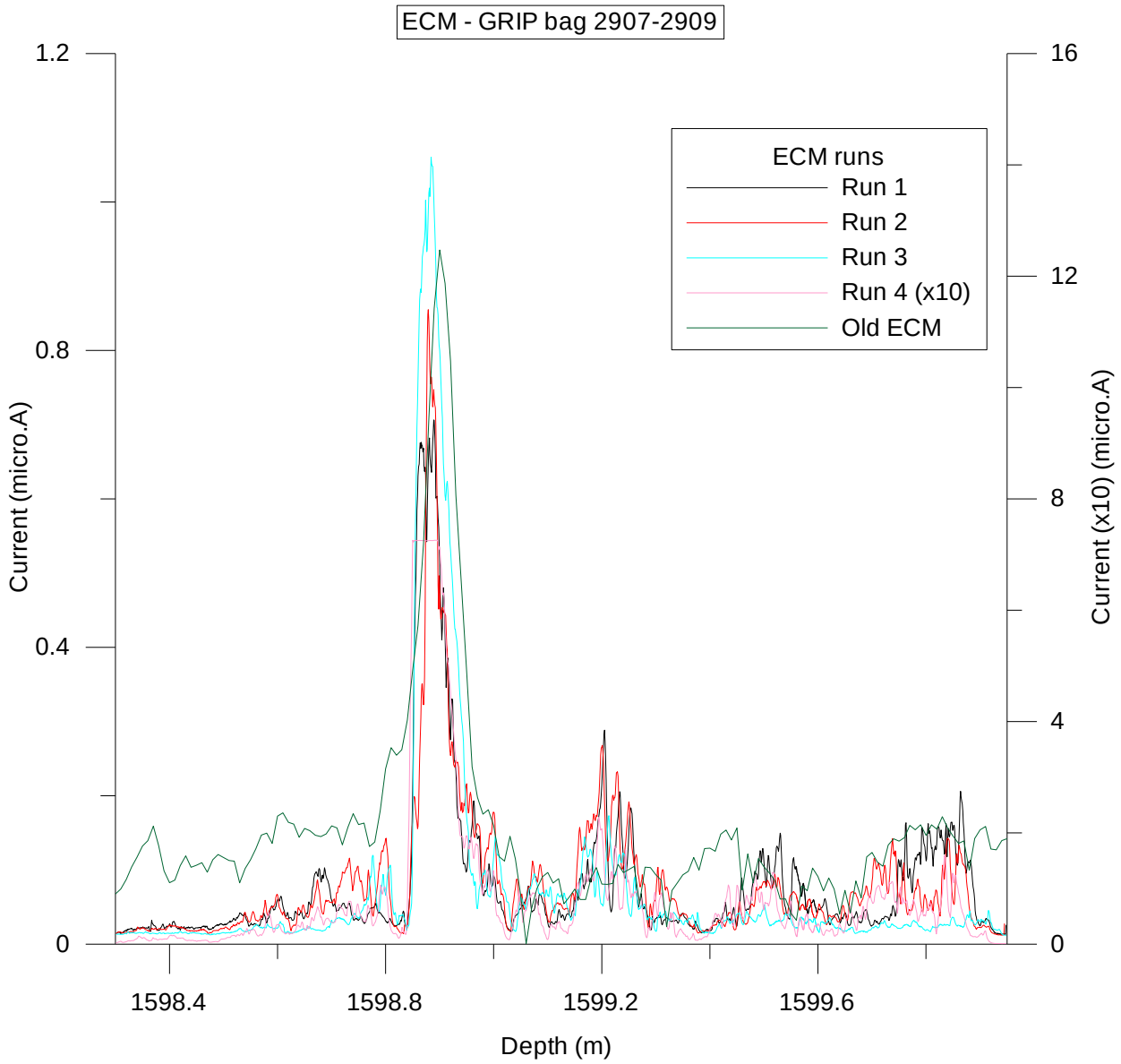

Figure 27 - Four runs with one being amplified were done. The measurements were done with an air temperature of -17.8°C and a core temperature of -18.1°C. The old ECM is shown in green and follows uses the x10 y-axis. The deposition depth is around 1598.86 m

5.1.2.1 ECM on GRIP

GRIP 72-74

Figure 25 - There were performed 5 measurements on bag 72-74 from the GRIP ice core. This section is at the depth 39.05 m to 40.7 m and contains the Krakatoa eruption and therefore corresponds to a time of 1883 A.D. The bags were measured with an air temperature of -17.4°C and a core temperature of -17.8°C. The bags were all 55 cm giving a total of 165 cm and the diameters all approx. 8 cm. They all showed re-freezing. The maximum value is from run 1 with a value of 1.52 micro.A at a depth of 39.59 m. There was

not measured with amplification on due to complications. The main peak has a depth between 39.58 m and 39.62 m with one half size peak shortly after at depths 39.65 m to 39.8 m.

GRIP 107-109

Figure 26 - Shown on this figure are four measurements on bag 107-109 of the GRIP ice core. As shows there are three normal measurements and one with the signal amplification of 10. The depths of these three bags are 58.3 m to 59.95 m showing the Tambora eruption, which occurred in 1815 A.D. The measurements were done with an air temperature of -17.4°C and a core temperature of -17.6°C. The bags are 55 cm in length giving a total of 165 cm and have a diameter of 8 cm. There are signs of Re-freezing on all pieces and two breaks in bag 107 and one in bag 109. The maximum value of the non-amplified runs were of run 2 with a value of 0.29 micro.A at a depth of 58.6 m and for the amplified run the maximum value is 2.5 micro.A at a depth of 58.5 m. The peak is approximately starting at 58.5 m and ends at 58.7 m.

GRIP 2907-2909

Figure 27 - Four measurements done on bag 2907-2909 from the GRIP ice core is shown on this figure. There are three normal runs and one amplified though the amplified measurement reached saturation, as seen earlier, and therefore will not give the true maximum value. The bags are in a depth of 1598.3 m to 1599.95 m. The measurements were done with an air temperature of -17.8°C and a core temperature of -18.1°C. Each bag is 55 cm long and the pieces have diameters of 9 cm, 7.5 cm and 7.5 cm respectfully. There were one break in bag 2907 and melt layers in bag 2908. The maximum value of the non-amplified measurements were of run 3 with a value of 1.06 micro.A at a depth of 1598.88 m and for the amplified run the true maximum value is unknown due to saturation but this saturation of 7.25 micro.A is reached at depth 1598.89 m. The peak is at a depth of 1598.85 m to 1598.95 m.

5.1.3 Dye-3 ECM measurements

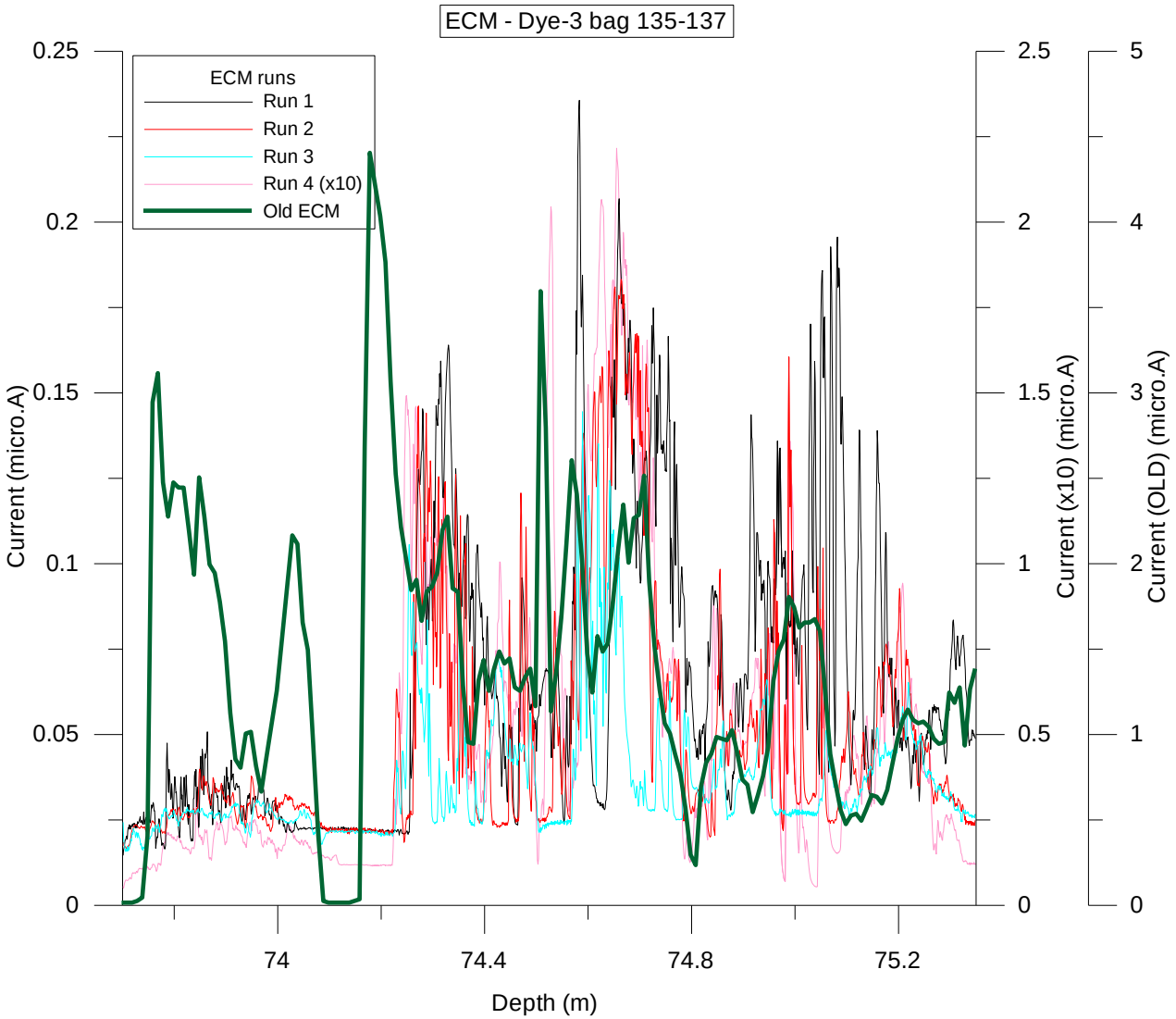

Figure 28 - Four runs are shown above one of with is amplified. These runs were measured with an air temperature of -16.9°C and a core temperature of -18.4°C. The old ECM is shown in green and has its own axis to make the signal form easier to observe. The deposition depth is around 74.158 m.

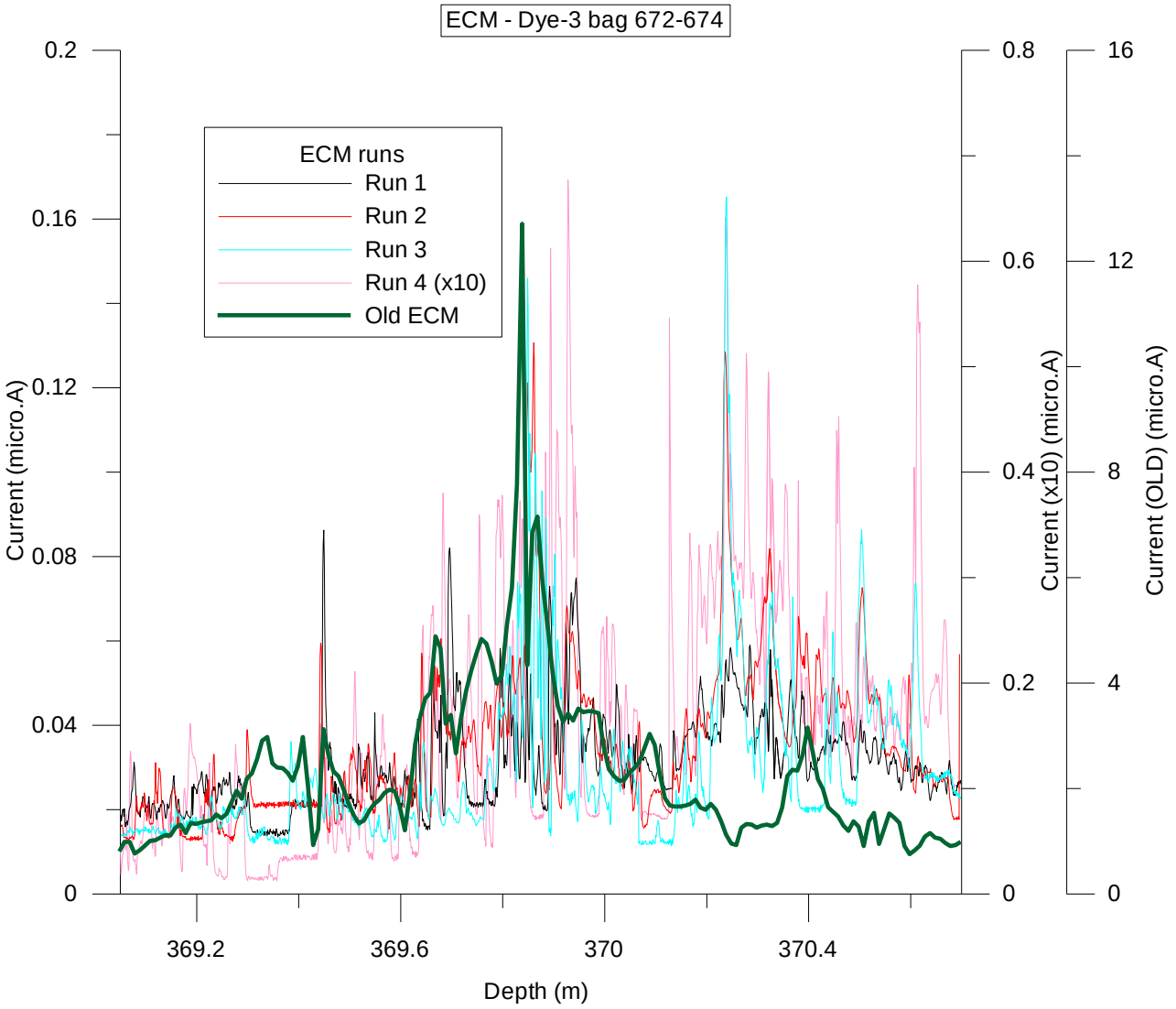

Figure 29 - Four runs were measured, one was amplified. The ice was measured with an air temperature of -17.1°C and a core temperature of -17.5°C. The old ECM is shown in green and has its own axis to make the signal form easier to observe. The deposition depth is around 369.484 m.

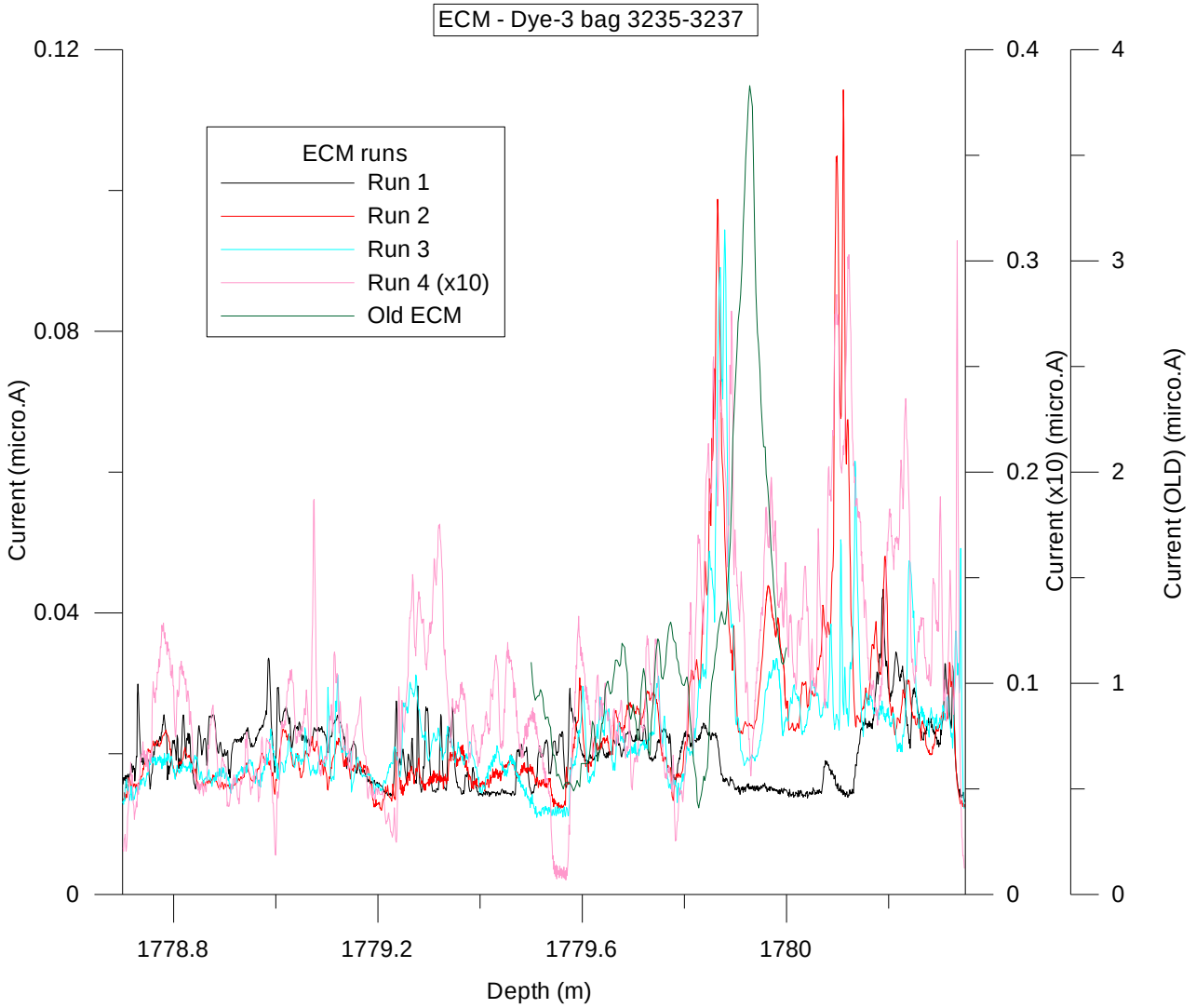

Figure 30 - Four runs with one being amplified are shown above. They were measured with an air temperature of -16.7°C and a core temperature of -17.0°C. The old ECM is shown in green and has its own axis to make the signal form easier to observe. The deposition depth is around 1779.92 m.

5.1.3.1 ECM on Dye-3

Dye-3 135-137

Figure 28 - Measured here are four runs, of witch one is amplified, on the Krakatoa eruption (1883 A.D.) from the Dye-3 ice core. The bags are 135-137 corresponding to a depth of 73.7 m to 75.35 m. These runs were measured with an air temperature of -16.9°C and a core temperature of -18.4°C.The three bags were all reduced in diameter, starting with bag 135, 136 and 137, giving the sizes 8 cm, 8 cm and 7.5 cm. The lengths of the bags are 55 cm, 58.5 cm and 54.5 cm respectfully, giving a total of 168 cm. All three pieces show severe re-freezing also bag 136 had two breaks that were re-frozen and bag 137 had two melt layers. The maximum value 0.21 micro.A is at depth 74.66 m in the non-amplified run 1 and for the amplified run 4, the maximum value is 2.22 micro.A at depth 74.65 m. The peak does not appear sharp but there are

three intervals of higher current. These three intervals are; 74.2 m to 74.5 m, 74.5 m to 74.8 m and last from 74.9 m to 75.2 m.

Dye-3 672-674

Figure 29 - The unknown eruption 1257 A.D. is measured here over four runs. One of the runs is being amplified. The three bags 672-674 give a depth interval of 369.05 m to 370.7 m. The ice was measured with an air temperature of -17.1°C and a core temperature of -17.5°C. The lengths of the bags are 55 cm, 54 cm and 56 cm giving a total of 165 cm. The diameters of the pieces are 8 cm, 7 cm and 7.5 cm. They all show re-freezing and bag 672 has one break as well as some melt layers. The maximum value of current in the non-amplified runs were in run 3 with a value of 0.17 micro.A at a depth of 370.2 m and for the amplified run 4, the maximum value is 0.68 micro.A at a depth of 369.9 m. There are two intervals of possible volcanic activity the first goes from 369.8 m to 370 m and the next from 370.1 m to 370.4 m.

Dye-3 3235-3237

Figure 30 - Bag 3235-3237 from Dye-3 is measured over four runs where one is amplified. The bags are in a depth of 1778.7 m to 1780.35 m. They were measured with an air temperature of -16.7°C and a core temperature of -17.0°C. The length of each bag is 56 cm, 55 cm and 56 cm giving a total of 167 cm and a width of 6.5 cm, 6.5 cm and 7 cm respectfully. All bags had one break and all showed sign of re-freezing. The maximum value was in the non-amplified run 2 with a 0.11 micro.A value at a depth of 1780.1 m and in the amplified run 4 with 0.31 micro.A being the value at depth 1780.3 m. There are two peaks at the intervals, 1779.8 m to 1779.9 m and 1780.1 m to 1780.2 m.

5.2 New and old ECM and IC sulphur figures, averaged over 5 cm

There are no, available, measured sulphate values for all of the Dye-3 ice core and also no values for GRIP bag 72-74 therefore these figures will not be shown.

The ECM runs previously shown from NGRIP, NGRIP2 and GRIP and also the old ECM measurements performed with the old ECM setup have all been averaged over 5 cm too match the IC measurements of sulphate, which primarily is measured as an average of 5 cm. The depth value is the average of the beginning at the mentioned depth moving 5 cm upwards (e.g. 34.8 m is the interval of 34.8 m to 34.85 m). This will be consistent throughout all 5cm-averaged data. The old ECM is shown in the green dotted line and the sulphate in the purple line.

5.2.1 NGRIP

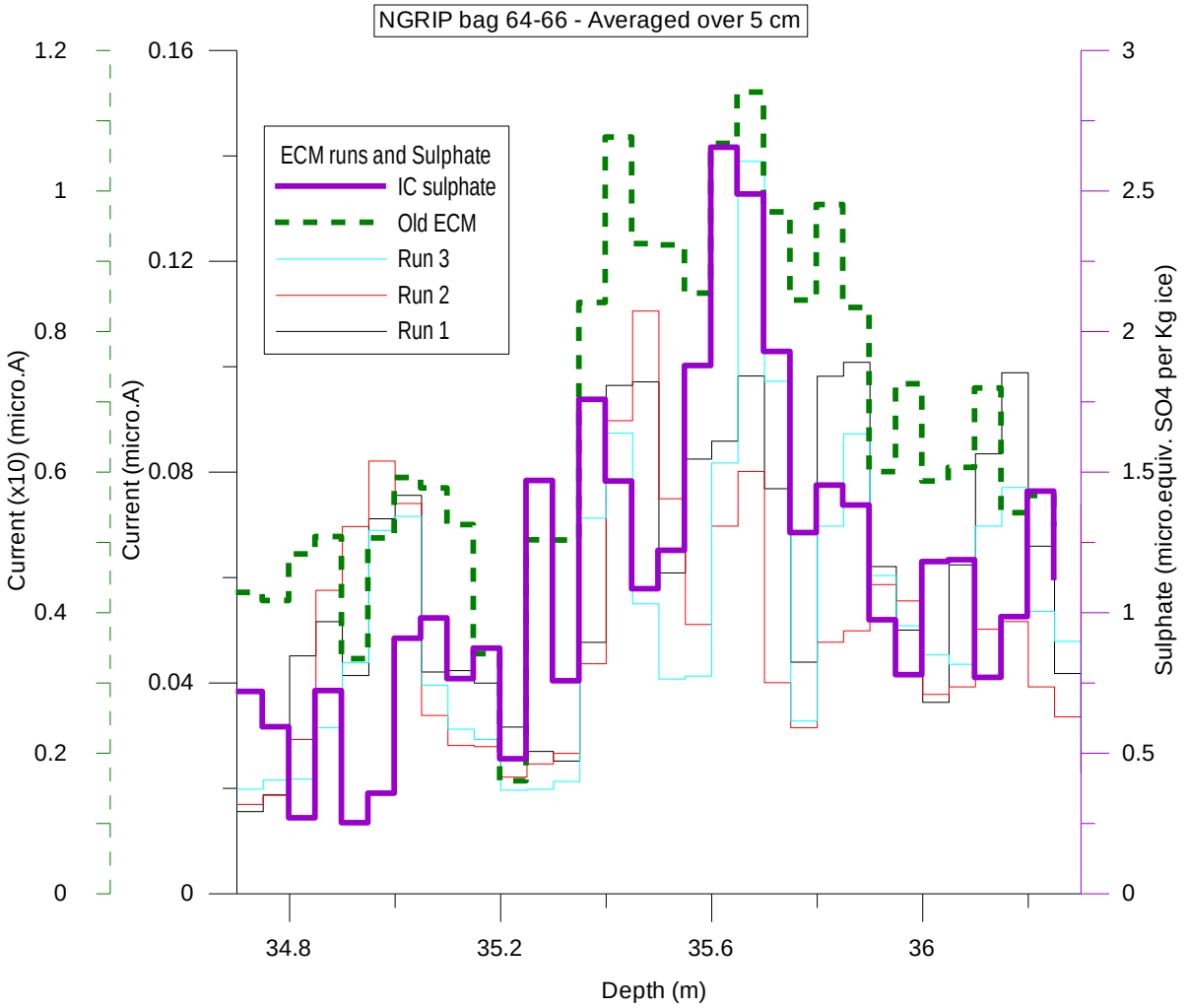

Figure 31 – Show the IC sulphate in purple. The old ECM in dotted green and the new EC measurements in black, red and blue. There is very little resemblance between the new- and old ECM as well as the IC sulphate.

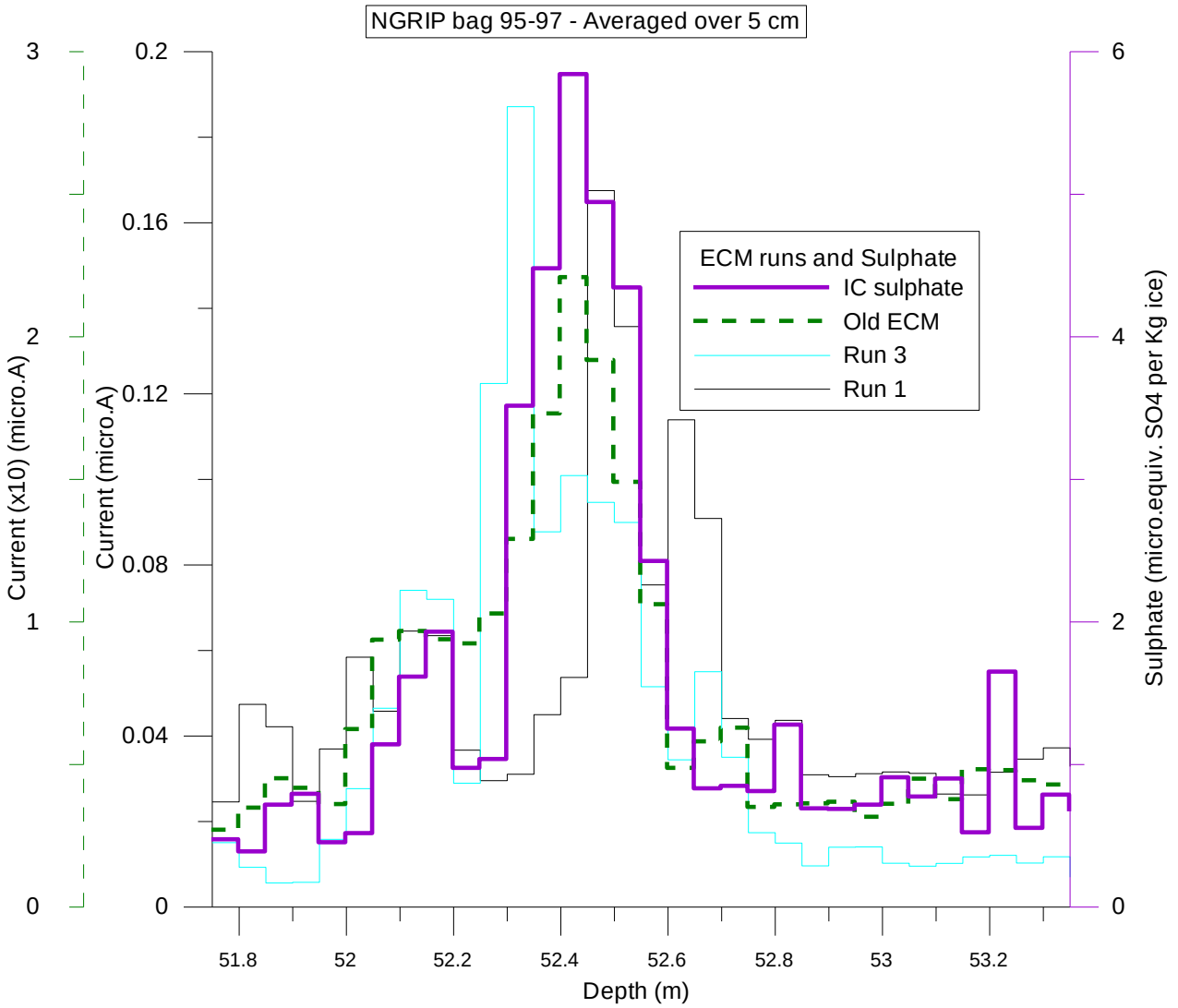

Figure 32 - There is a relatively good agreement between the old ECM and the IC sulphate though run 1 and 3 appears on either side of the peak.

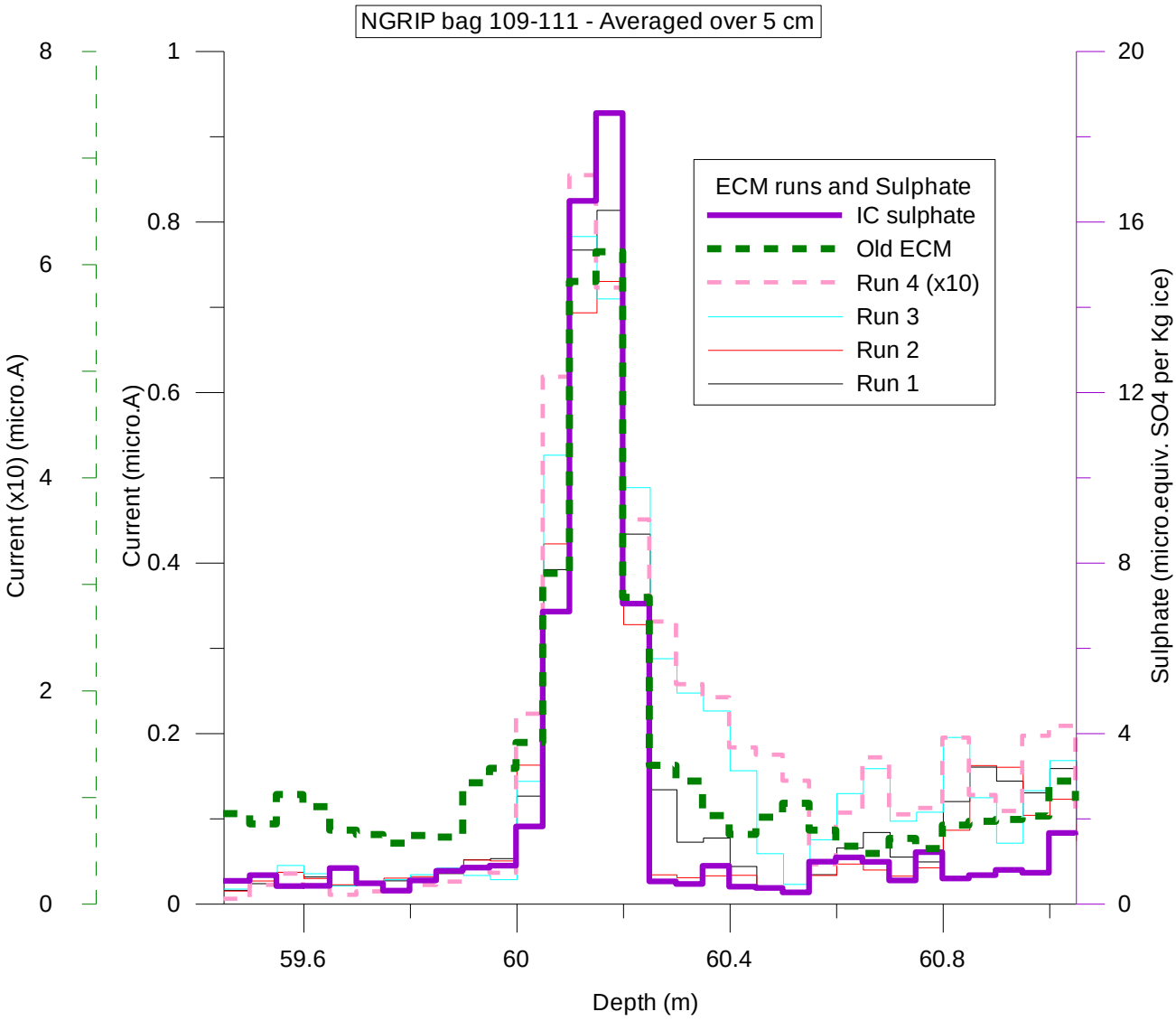

Figure 33 - The agreement between the new EC measurements and the IC sulphate is decent. The old ECM is calibrated data which could explain the high background values. The old ECM and amplified new ECM are following the dotted y-axis called current (x10) (micro.A).

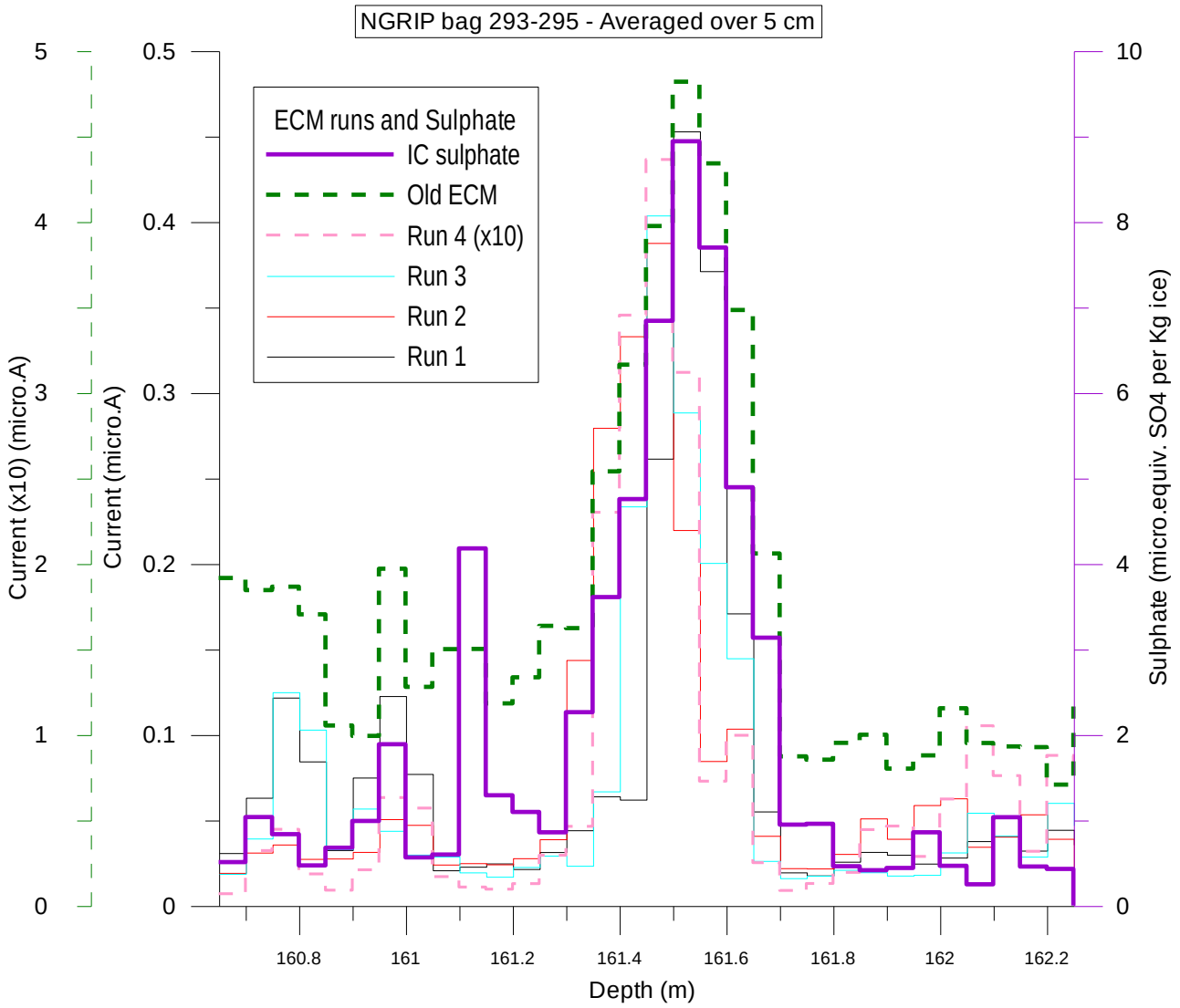

Figure 34 - The IC sulphate peak appear wider than the new ECM otherwise a decent agreement around the peak. The old ECM and amplified new ECM are following the dotted y-axis called current (x10) (micro.A).

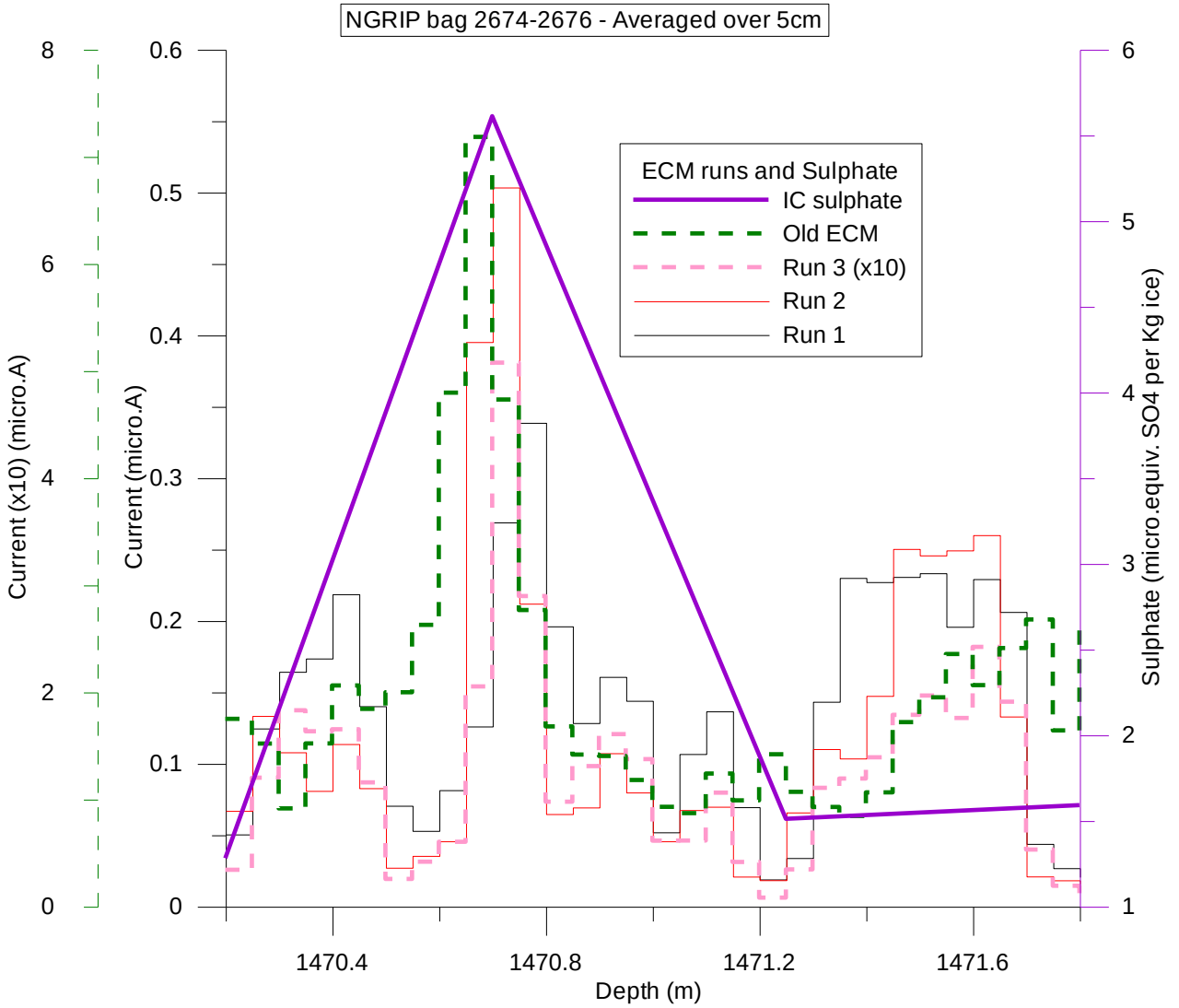

Figure 35 - Only the average of 55 cm of the IC sulphate was available making an evaluation of agreement between sulphate and new/old ECM impossible. The old ECM shows a small offset, which could be accounted for by the X-axis measurement irregularities. The old ECM and amplified new ECM are following the dotted y-axis called current (x10) (micro.A).

5.2.2 GRIP

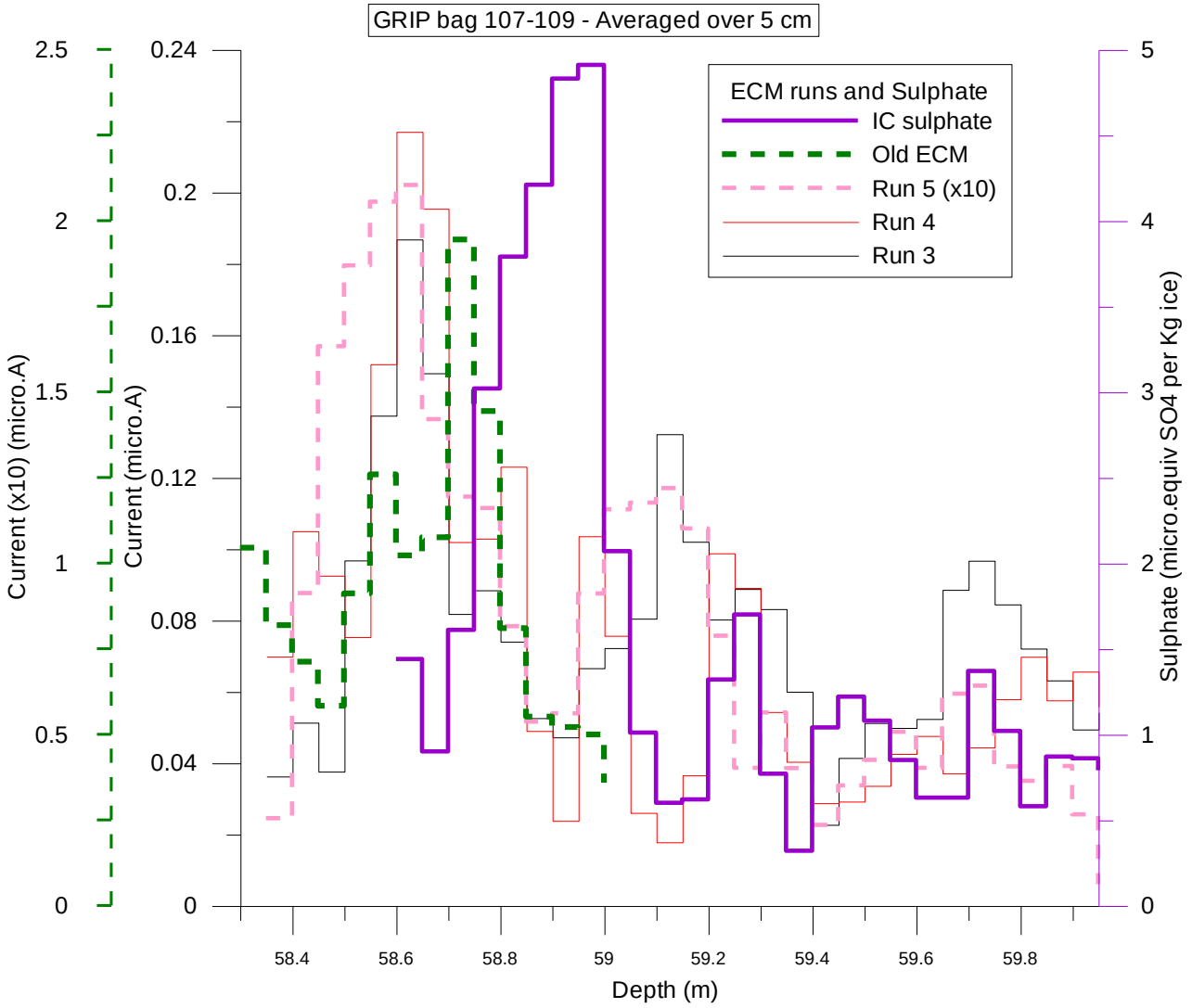

Figure 36 - The old ECM and amplified new ECM are following the dotted y-axis called current (x10) (micro.A). The offset between ECM and sulphate is due to the chemistry measurements being from another core drilled (*Eurocore*) at the same position and therefore still representative. Here approximately 20-30 cm offsets are associated with the depth scale between the two cores. The IC sulphate should fit the ECM when corrected for approx. 25-30 cm offset giving the peak depth of approximately 58.57 m.

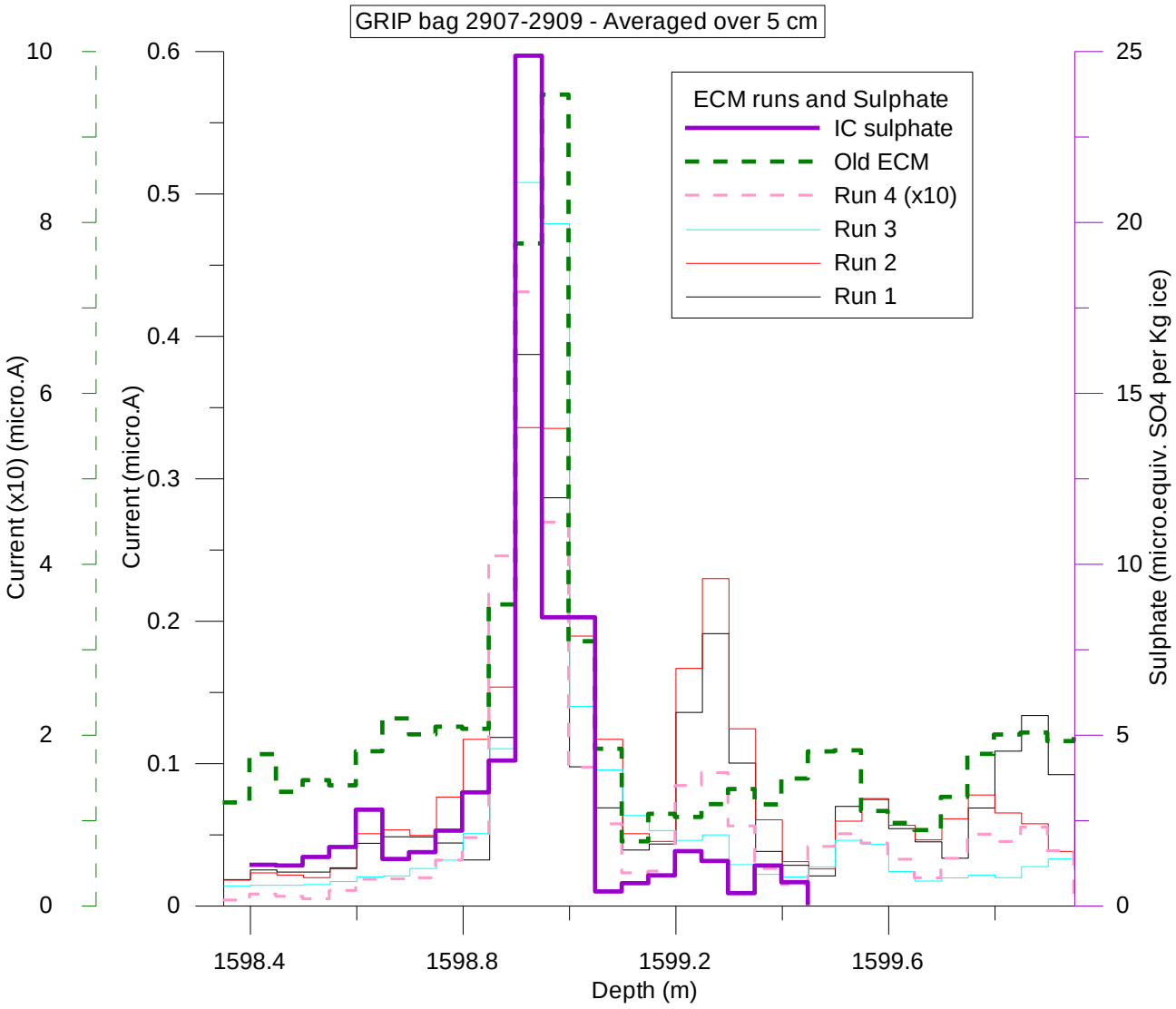

Figure 37 - Good depth agreement between IC sulphate and new ECM. Signal variation is clearly seen. The old ECM and amplified new ECM are following the dotted y-axis called current (x10) (micro.A).

5.3 Temperature experiment

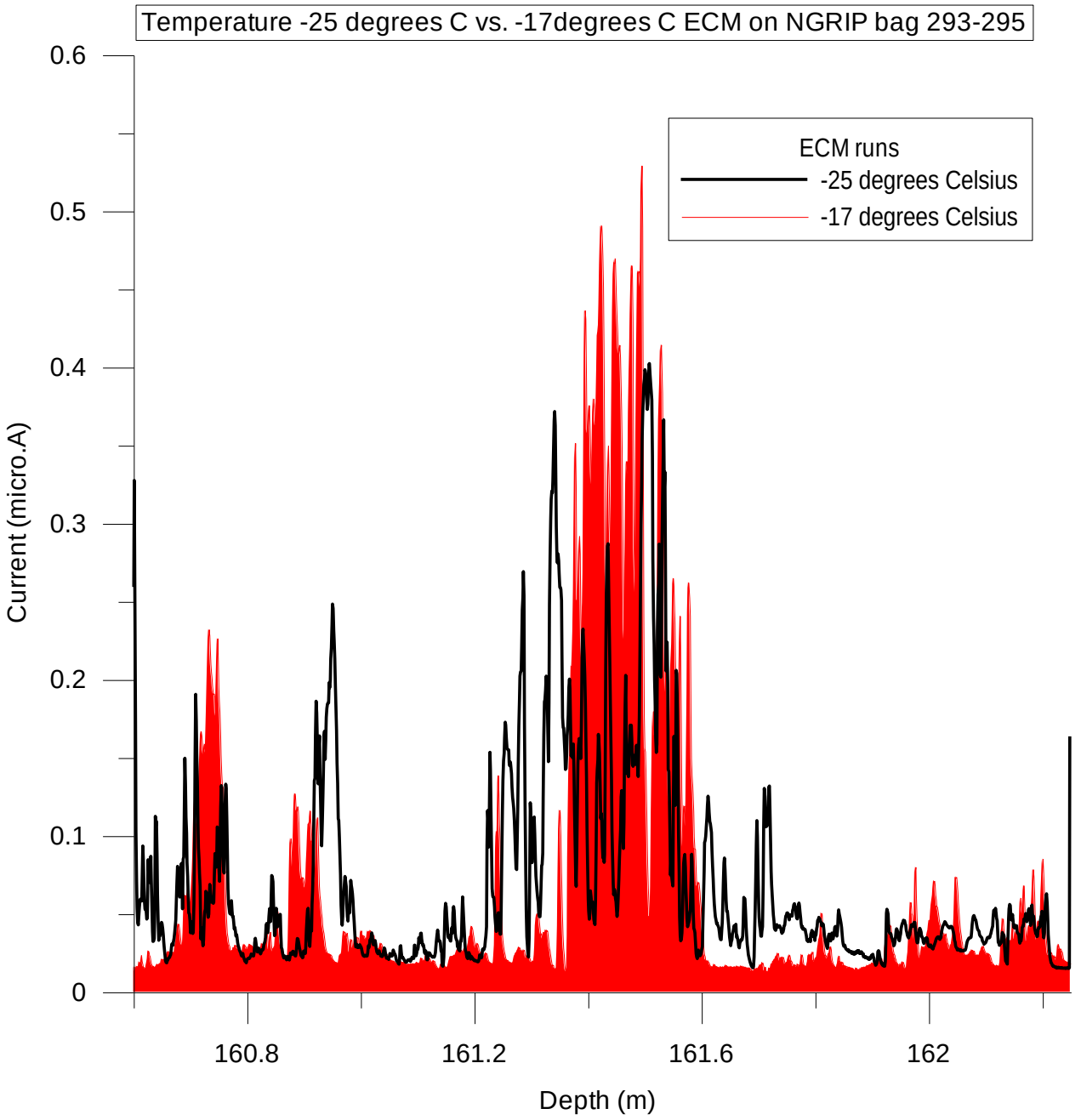

Figure 38 - The air temperature, when measuring the -25.0°C core temperature, was -23°C and the air temperature was -17.4°C when measuring the -17.0°C. It shows a generally lower signal in the -25.0°C measurements though wider compared to the -17.0°C measurement around the peak.

Temperature on bag 293-295 NGRIP	Sulphate per area (Kg SO_4^{2-} /km^2)
1) -17°C	62 ± 8 (n= 3)
2) -25°C	42 ± 4 (n= 3)

Table 5 shows the sulphate per area calculations measured in -17°C and -25°

5.4 Stationary measurements

The stationary measurements were performed with the purpose of evaluating the levels of polarization of the ice when doing measurements. Some data of some of the runs are not plotted throughout the measure time. This is due to negative values, which are discarded. This is most likely the result of the relatively slow response to the start time of the instrument. This does not influence the EC measurements where the depth of interest is usually in the mid bag which isn't measured before several seconds (approximately 10) into the measurement. The descriptions of these results are in the section 6.2.5 of the discussion.

5.4.1 NGRIP 109

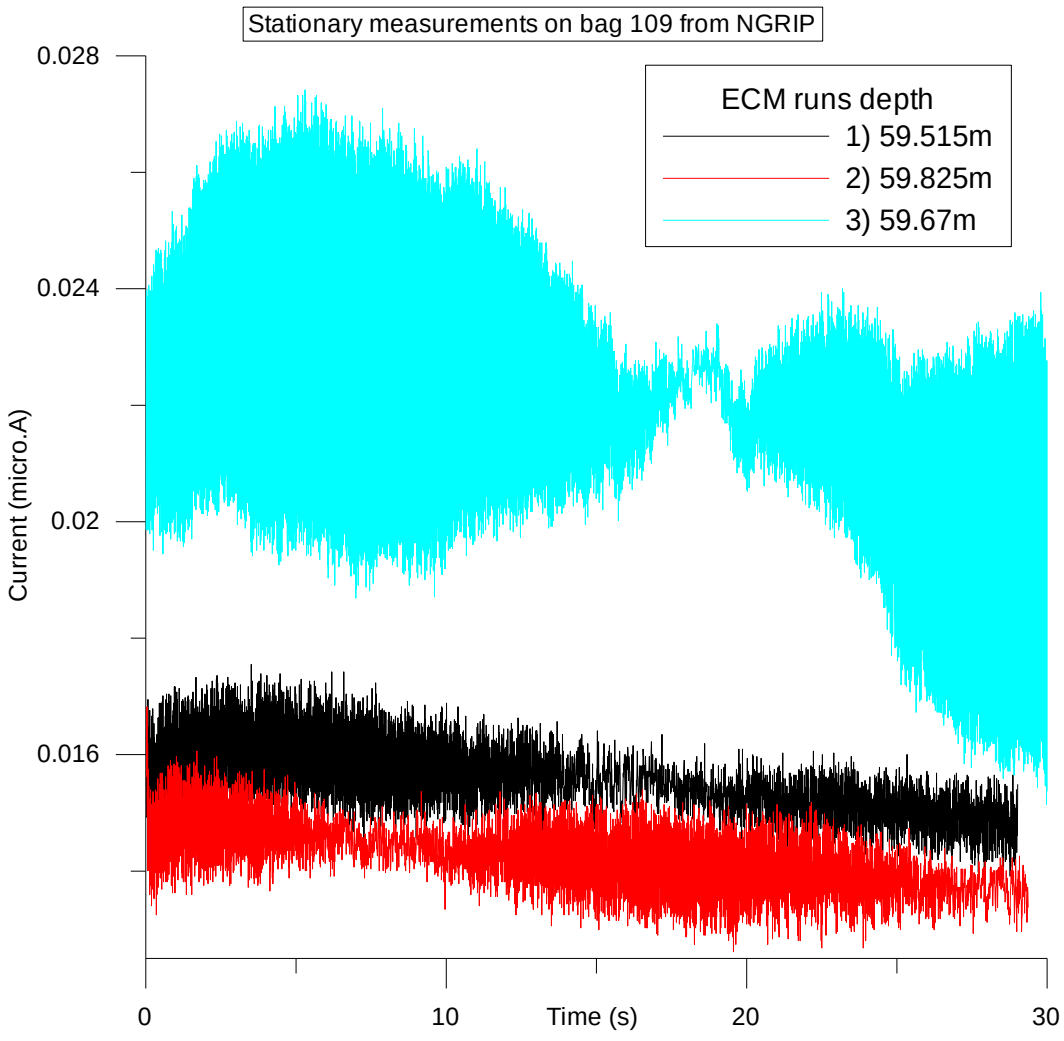

Figure 39 - Run 3 was measured with amplification (times 10) on. The air temperature during measurements was -16.8°C and the core temperature was -17.0°C. See ECM – NGRIP bag 109-111 for depth positioning.

5.4.2 NGRIP 110

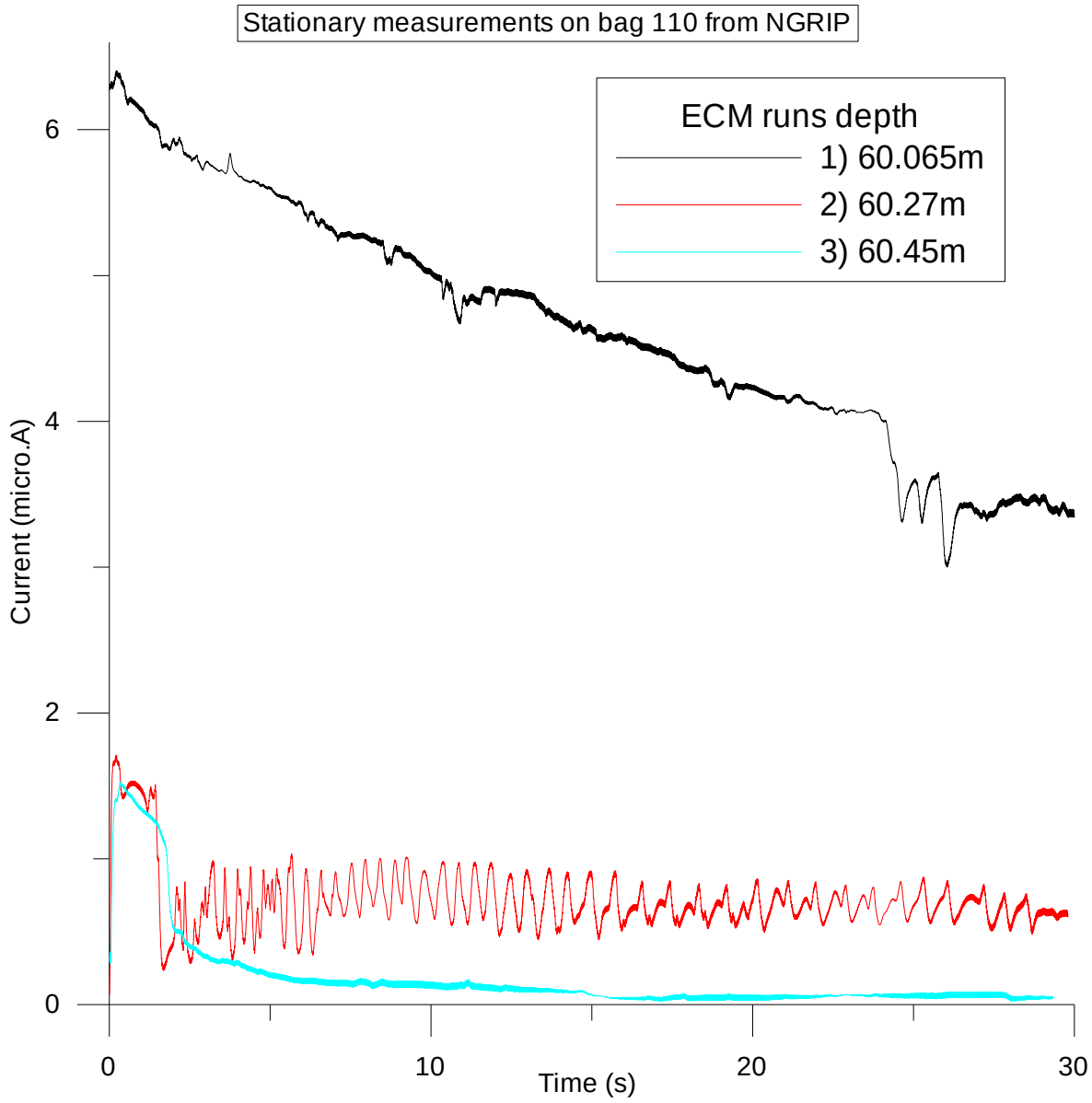

Figure 40 - All three runs were measured with amplification on. The air temperature during measurements was -16.8°C and the core temperature was -17.1°C. See ECM – NGRIP bag 109-111 for depth positioning.

5.4.3. NGRIP 293

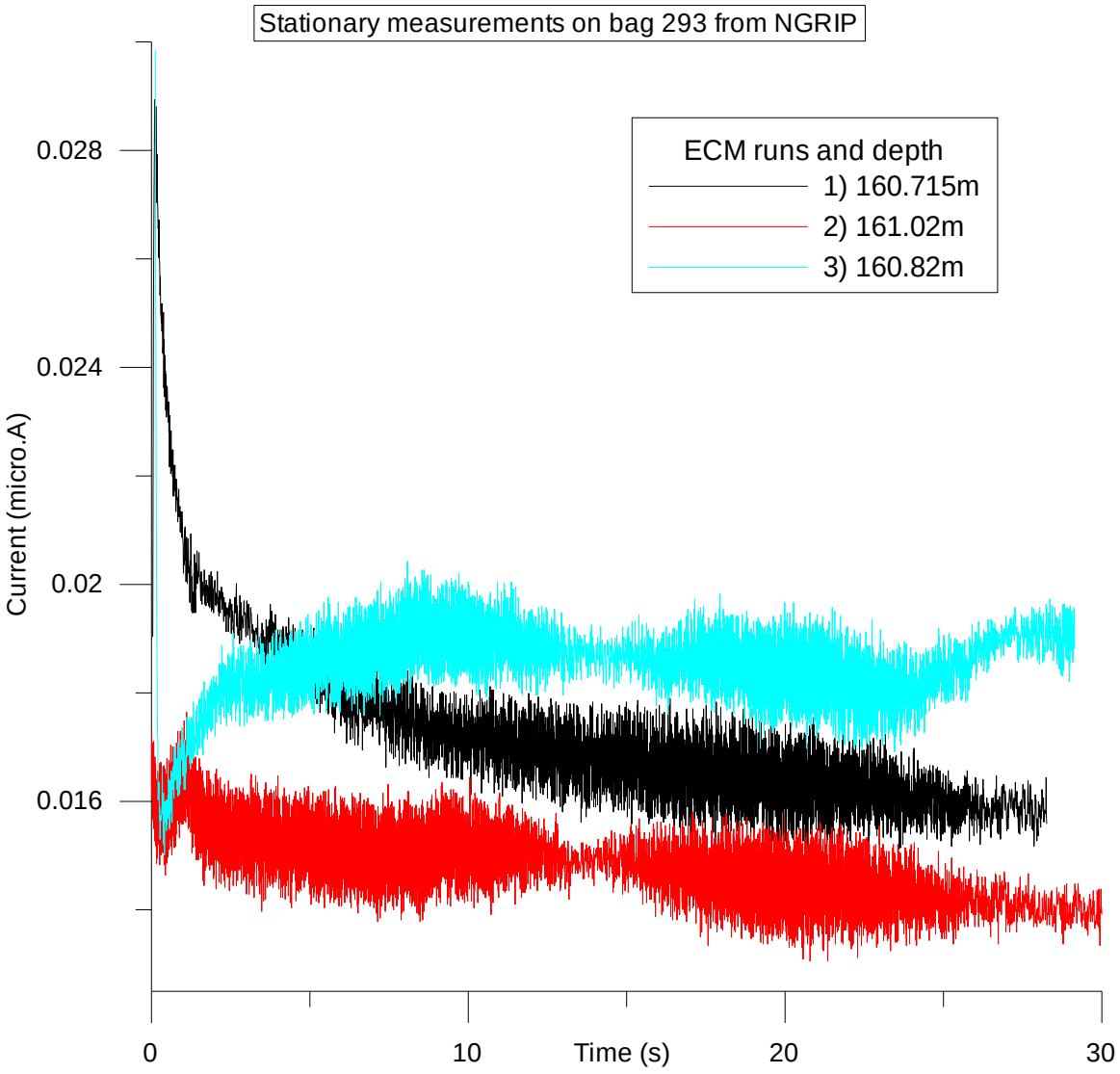

Figure 41 - The air temperature during measurements was -17.5°C and the core temperature was -17.9°C See ECM – NGRIP bag 293-294 for depth positioning.

5.4.4 NGRIP 294

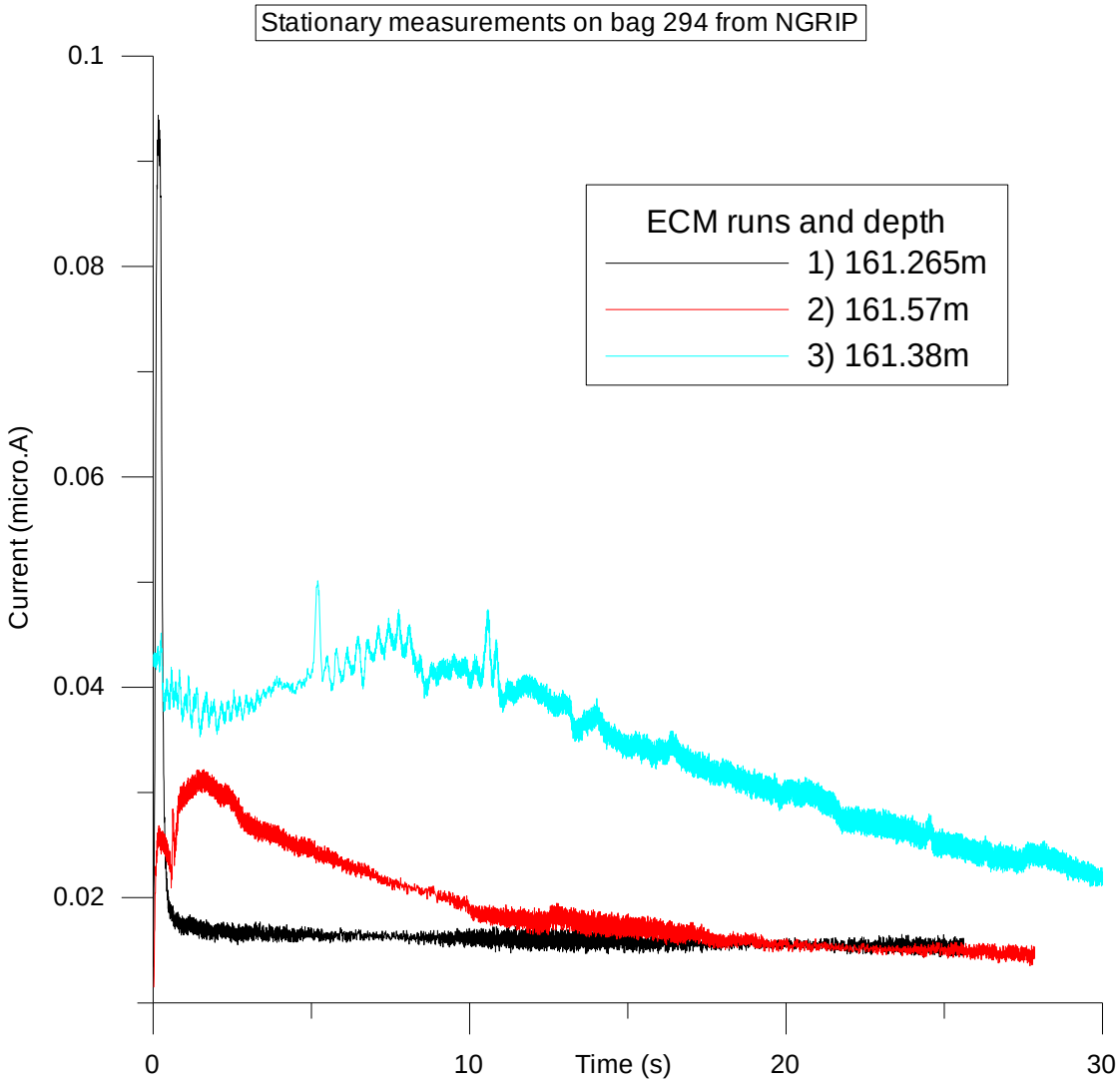

Figure 42 - The air temperature during measurements was -17.5°C and the core temperature was -17.8°C See ECM – NGRIP bag 293-294 for depth positioning.

5.5 The calibration curve

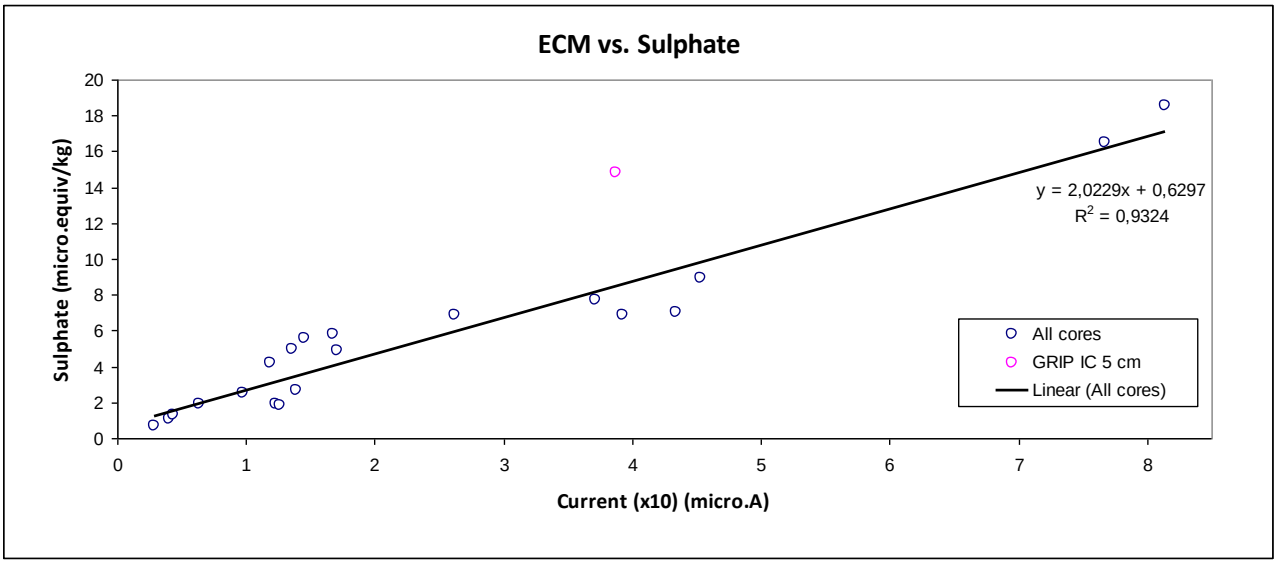

Figure 43 - The calibration is based on the ECM run that was of closest fit to the IC sulphate and not the average of all ECM runs. This is why there are no error bars. The runs having the highest signal, possibly due to the freshly cleaned surface and no polarization from previous measurements are the runs/values used.

5.6 Sulfate deposition in Greenland

Sulphate per Area (Kg SO_4^{2-} /km^2)			
Volcano/ice core	**NGRIP/NGRIP 2** (9305 B.C from NGRIP2)	**GRIP**	**Dye-3**
Krakatoa 1883 A.D.	22 ± 4.1 (n= 3)		
Tambora 1815 A.D.	31 ± 0.5 (n= 2)	45 ± 2.8 (n= 2)	19 ± 3.6 (n= 2)
Laki 1783 A.D.	108 ± 10.7 (n= 3)		
Unknown 1257 A.D.	65 ± 4.9 (n= 3)		17 ± 0.3 (n= 2)
Unknown 9305 B.C.	78 ± 1.1 (n= 2)	89 ± 9 (n= 3)	9 ± 1.8 (n= 2)

Table 6 shows the sulphate per area values for the eruptions in the ice cores.

The peaks have been averaged over the same distance taking the widest peak as the default interval as explained in section 4.1. This could result in an over-estimation but since many of the runs show lower signal size after run 1 the uncertainty should not be significant. Also, should the peak interval be narrower then the only adding of value to the result will be background values. Assuming that this value is negligible in large eruptions this should also not contribute to major uncertainties either.

Background levels have not been removed from any of the results because it was not possible to distinguish well between background and actual peak in the bags with weak signals and for the bags with strong signals the background values are considered negligible. The average value will probably be lower than what correct is.

5.7 Major findings of this thesis

5.7.1 The reproducibility on ECM measurements

Reproducibility is referring to the general likeness between each run. The better the reproducibility the fewer the uncertainties are associated with a) the instrument, b) the measuring procedure or c) the overall core quality.

- The reproducibility is varying from each run and between the cores. One of the most apparent tendencies is that the quality of measurements done on firn is lower than those on ice.

  In case NGRIP 109-111 the deposition depth is still relative shallow but if the peak signal is strong enough then the reproducibility appears better compared to a low peak signal.

  The reader should however be informed that the resolution of each graph is higher with similar signal intervals (a smaller interval) and should be remembered when studying the signals on the graphs.

- It is difficult to say something about the quality of reproducibility of each ice core based on the error bars in table 6 because of the change in number of runs averaged over.

- A general preference was to measure on NGRIP over any of the others even though the reproducibility varied somewhat in this core as well. The preference is based on generally better condition of the ice as well as the possibility of measuring all eruptions.

- In terms of tendencies associated with amplitude, NGRIP; 95-97, 109-111, 2674-2676, GRIP 72-74 and Dye-3 135-137 all have the highest signal in the first measurement (run 1) and then a general decline in amplitude through the rest of the runs.

  NGRIP; 64-66, 293-295, GRIP 107-109, 2907-2909 and Dye-3 3235-3237 all have the highest signal on the second run. Only Dye-3 672-674 has the highest signal on its third run. This equal split in highest signal between run 1 and 2 prevents any description of tendencies.

5.7.2 Temperature experiment

- From the measurements made with different temperatures (figure 38) it appears that higher temperatures equal stronger signal. From figure 38 and table 5 in section 5.3 it is clear that not only is the amplitude is bigger but also the sulphate distribution.

  The -25°C graph showed more fluctuating signal behaviour than the -17°C graph indicating more noise in the signal.

5.7.3 Stationary measurements

The stationary measurements were done to investigate the polarization rate of the ice.

- The three runs from NGRIP bag 109 all show fluctuation, but a general decrease of signal with time is present. During most of the time I measured, the third run spreads over a larger amplitude interval. All three runs show a point in time where the signal appear to narrow its amplitude interval, as a wave, though not at the same time.

- NGRIP bag 110 show three very different responses. The first run is measured right on the eruption (see figure 45 section 6.2.5) and shows a general decrease throughout the time measured. The second and third run both decline to a more stable level after approximately 2 seconds, however showing two very different amplitude intervals.

- NGRIP bag 293 first run decreases immediately and for 5 seconds the signal size changes dramatically. Run 3 show an increase in signal after the first second followed by a signal changing very little. All three runs for bag 293 show the same wave tendency as bag 109.

- In NGRIP bag 294 the first run show an immediately decrease in signal (after 1 second) and then a stable graph after. Run 2 increases in the first 2 seconds and then decreases steadily until reaching 10 seconds followed by a flattening until crossing run 1 around 23 seconds in. Run 3 starts with a decrease until 2 seconds have passed, then increases until 7 seconds have passed and then once more steadily decreasing the rest of the measuring time. For stationary positions relative to signal see figures 45 and 46 in section 6.2.5 further down.

5.7.4 The calibration

The calibration of the new instrument shows that the relationship between conductivity and sulphate is given by $SO_4^{2-} = 2.0229i + 0.6297$.

This linear relationship was found by creating the best fit between the new measured conductivity (*i*) of ice (with impurities from volcanic eruptions) and old IC sulphate SO_4^{2-} measurements at corresponding depths.

5.7.5 Sulphate distribution on Greenland

Table 6 depicts the sulphate distribution pattern of sulphate deposition. From the values calculated it seems that there is a general bigger deposition of sulphate in GRIP compared to NGRIP and Dye-3. This could be related to the meteorological conditions at the deposition time or complications of the ECM data. This is discussed in section 6.2.7.

6. Discussion

The discussion is separated into several paragraphs to make it easier for the reader to follow it. First is a few general points related to the uncertainties on reproducibility. Then interpretations of major findings and the explanations of such are shown. After this the results of this thesis is compared as much as possible to other published results followed by the limitations of this study. Then the generalisability of the results is listed and some unanswered questions asked. Last but not least is given some proposals for future studies on this matter.

6.1 Some general uncertainties related to the signal reproducibility

This section shortly discusses and reminds the reader of some uncertainties involved with the EC measurements. They are general for all measurements and to be kept in mind when reading through the interpretation in section 6.2.

6.1.1 Surface of the ice

If the surface of the ice is not cleaned properly then a reduction in signal is expected due to this previously introduces *aging effect* (Moore *et al.,* 1984). The older the core the more ice need be removed (Taylor *et al.,* 1992). All bags are considered to have been cleaned properly, but uncertainties involved with this should still be taken into consideration when reading through section 6.2. The cutting of the surface also serves the purpose of ensuring as smooth a surface as possible. Obstacles in the ice could affect the signal just like it is seen in some of the measurements where there have been breaks or bag transitions.

6.1.2 Ice thickness

Hammer (1980) recommends that when measuring ice it should have a minimum thickness of 4 cm and width of 2 cm. Some of the ice from Dye-3 (bag 135-137) was not only small in width but also thickness (3 cm). This could possibly have an effect on the signal due to the possibility of "contamination" of the signal from ions not related to H_2SO_4 on the other sides of the core. Sadly is it not clear from any of the measurements presented here whether the thickness is playing a significant role in the strength of the signal.

6.1.3 Voltage

Hammer (ibid.) also argues why the voltage is of importance. He states that the difference in voltage between the electrodes is not critical as long as it is in the range of linearity between voltage and current. 1250 V is within this range it is therefore assumed that the velocity of the measurement is less relevant to the signal size. This is also seen in the stationary measurements where polarization was not appearing immediately after starting the measurement.

6.1.4 Temperature

Different core temperatures show change in signal size. If the temperature of the core is different from the room it is measured in then chances are that temperature might be a contributing uncertainty factor. The reason for this is clearly expressed in the section to come (6.2.4).

6.1.5 Electrodes

The shape of the electrodes is also relevant to the signal and general resolution (Hammer, 1980). A large contact area will results in a high current but low resolution and reproducibility. Hammer (ibid.) used electrodes with a contact area of 1.5 mm^2 which he claimed was "large enough to ensure high current and small enough to give good contact, high resolution and high reproducibility" (ibid.). The electrodes used in these measurements have a contact area of 1 mm^2 which potentially could be too small to get as strong an ECM signal as expected.

6.2 Interpretation of major findings

The major findings presented in section 5.7 are here being interpreted. First discussed are the ECM of the eruptions and some of the similarities in behaviour between the different cores. Then the temperature results are discussed followed by a discussion of the stationary measurements. Last the calibration and the sulphate distribution is discussed. In the following section 6.3, an explanation of what the major discoveries could mean is discussed.

6.2.1 ECM on NGRIP

The reproducibility of measurements done on NGRIP 64-66 (figure 20) does not appear to be good. The amplitudes of the peaks are not similar, but the deposition depth of where they are found is relatively stable. Bag 64-66 is at a depth of 34.65m to 36.3m, which is within the section of firn in the NGRIP core. As previously mentioned, the mobility of ions in the crystal lattice of firn is limited by the high porosity (compared to ice), which make the signal less stable in terms of amplitude. This is possibly why the amplitude varies but not the deposition depth. Bag 65 and 66 both showed signs of refreezing, which mean that some melting has occurred. Melting and refreezing of the firn would naturally increase the density of the affected depth due to compression and thereby enhancing the signal as seen in measurements done on ice. Since the surface of the ice core was cleaned down until what is considered the actual firn of the bag this should not influence the signal significantly. The peak in NGRIP 64-66 is cut off at 35.75m, which is where the transition between bag 65 and 66 is. This could explain the difference in the deposition interval from the old EC measurement by a small offset due to the length of the bag. This change in depth interval could also contribute to the total amount of sulphate per area.

NGRIP 95-97 (figure 21) is also measured in firn (depth 51.7m to 53.35m) which similarly to 64-64 shows a less good reproducibility. The same arguments apply for the bad reproducibility, as listed above (NGRIP 64-66). Bag 97 also showed refreezing but is also considered negligible based on the same arguments as in 64-66.

NGRIP 109-111 (figure 22) shows a much better reproducibility around the peak but after the peak the variation in amplitude from run 1 to 4 is very different. Bags 110 and 111 both have a 4 cm smaller surface to measure on, which mean that the trails of run 1 and 3 are crossing paths. The same goes for run 2 and 4. This could be the reason for the variation in the signal between each run. There is a better resemblance between run 1-2 and run 3-4 which could be explained by the change in temperature. The air temperature was -16.9°C and the ice -18.0°C when the measurements began, hence that the ice temperature was still coming to be in equilibrium with the air. This could mean that run 3 and 4 were measured when the ice had increased in temperature resulting in a higher signal as seen in the temperature experiment.

Run 1 and 3 as well as 2 and 4 are similar in NGRIP 293-295 (figure 23) but do not show a well-defined peak by deposition interval or amplitude. There were no large temperature difference between air and ice which would limit the influence of such on the signal.

Run 1 and 2 from bag 2674-2676 (figure 24) from NGRIP show a good reproducibility around the peak but not so much before and after. The signal of run 2 is generally lower before after the peak. The low signal of run 2 could be due to polarization from run 1. The reason to why that is not the case in run 3 could be that it is an amplified measurement and therefore closer to run 1. There is a dip in the peak around 1470.7 m depth which is most likely due to this being the transition between bag 2674 and 2675.

6.2.2 ECM on GRIP

The five runs measured on bag 72-74 from the GRIP core (figure 25) are not showing a good reproducibility. Being that this section is at depth 39.05 m to 40.7 m and firn, bad reproducibility is expected from the experience of measurements on NGRIP. It is only run 1, 4 and 5 that indicate the peak at depth 39.6 m. However the deposition depth of Krakatoa should be found around depth 39.1 m (CIC database, 2014) so these measurements could possibly be misleading. Should the peak at 39.6 m be the actual deposition depth of Krakatoa then chances are that this is registered incorrectly in the database from which the deposition depth was taken from. In terms of core quality the, all three bags showed sign of refreezing once more assuming that all of this was removed before measuring. The surface of all three bags is only 8 cm wide, which could mean a possible overlap of the different runs leading to a decrease in signal. With five runs measured a decrease in amplitude would be expected with each run but run 5 appears to be the second biggest, after run 1, which would argue against this assumption. The general signal size of the peak is high compared to NGRIP 64-66 but looking at the background values of GRIP 72-74 there is a much better resemblance. The strange signal behaviour as well as the deposition depth both contributes to the questioning of validity in these bags.

Bag 107-109 in the GRIP core (figure 26) is showing a generally bad reproducibility between each run. The depth is from 58.3m to 59.95m, which once more places these bags in the firn of the ice core. This could, as previously shown in the firn measurements of NGRIP, affect the signal of each run. All bags showed signs of refreezing but this, as mentioned before, is assumed not to affect results when cleaning of the surface is performed. GRIP 107-109 and NGRIP 109-111 both show the Tambora eruption and in both cases the

deposition depth as well as the general amplitude of the signal varies much between each run. The signal size is four times bigger in NGRIP than GRIP.

Bag 2907-2909 from GRIP (figure 27) gives a well-defined deposition interval but shows opposite behaviour, in terms of increase/decrease in signal from run 1 to 3. It appears that run 3 (excluding the amplified measurement) has the highest signal and run 1 the lowest. The surface width is 7.5 cm for bag 2908 and 2909 which could result in crossing of the trails and therefore a lower signal. This does not change the rather increase in increasing signal compared to decrease in signal with each run. The size of the amplitude at the peak is a little higher (0.2 micro.A) than in NGRIP.

6.2.3 ECM on Dye-3

Dye-3 bag 135-137 (figure 28) shows a bad reproducibility but is also a measurement on firn as the previous Krakatoa eruptions in NGRIP and GRIP. The deposition depth is supposedly around 74.2 m (CIC database, 2014), but as seen on the graph the signal is not even present before 74.25 m which is where bag 136 starts. The variation in signal from run 1 to 4 could be a result of changing temperature since the temperatures of the air was -16.9°C and the ice -18.4°C at the start of the measurements. How big the change in temperature was between run 1 and 4 is unknown but run 3 appears to be much lower in signal which would be different if an increase in temperature occurred, compared to earlier runs. On the other hand a polarization effect from the previous measurements, and perhaps overlapping of measuring trails due to the only 8 cm width of bag 136-137, would result in a lower signal, which is what is actually seen. There is a melt layer present at depth 74.51 m, which could explain the peak in run 4. Compared to NGRIP the signal size is low and less defined in depth as for GRIP the signal size is similar as equally undefined in peak depth interval.

Bag 672-674 of Dye-3 (figure 29) is not showing good reproducibility of the signal between each run and the signal is generally low compared to the 1257 eruption in NGRIP (bag 293-295). All three bags showed signs of refreezing and the width of the surface is between 7 cm and 8 cm, which could mean crossing of measuring trails and a decrease in signal. Temperature difference between air and ice should not be of any significance when considering a difference of only 0.4°C which several of the measurements have.

Dye-3 Bag 3235-3237 (figure 30) also shows a poor reproducibility between each run. Run 1 show no peak at all but a decrease in signal across the peak area, which would indicate that something is completely wrong with those measurements. Run 2, 3 and 4 show a peak around 1779.81 m and run 2 and 4 another peak of bigger signal around 1780.1 m depth. This however, is right after a break at depth 1779.9 m, which could influence the signal though usually in the opposite direction (meaning lowering of signal). The deposition depth should be around 1779.9 m, which would backup the first peak depth mentioned. The general width of the surface is 6.5 cm, which would definitely result in overlapping of trails and therefore higher risk of seeing a polarization effect on the signal with each run. The signal of run 3 is generally lower

than run 2 but not significantly around the peak. Compared to NGRIP and GRIP the signal size is small overall in Dye-3. This could be a result of the less good core quality.

6.2.4 Temperature experiment

The temperature experiment on NGRIP 293-295 (figure 38) shows the temperature dependence of the signal size. There is approximately a 20 Kg sulphate/km^2 difference in the deposition calculations between -17°C and -25°C measurements (table 5). The ECM signal at -17°C is higher and therefore the sulphate deposition is higher as well. Muto and Shimizu, 2013, explains that the defects in the ice lattice referred to as L- (no protons on the O-O line) and D-defects (two protons on one O-O line) (see figure 44 below) makes it possible for the protons to "jump" to proton vacancies in the crystal structure which creates the conductivity. The jumping is increased with increasing temperature (Muto and Shimizu, 2013).

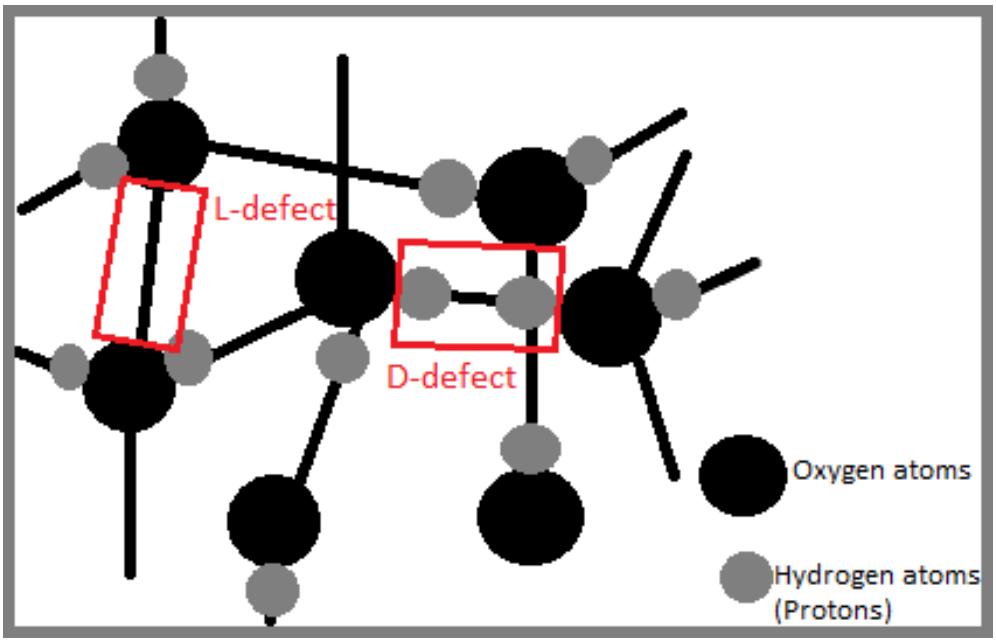

Figure 44 shows L- and D-defects in the crystal lattice.

The temperature measurements on NGRIP 293-295 clearly show this better signal with higher temperatures. The likeness of the average values of the NGRIP 293-295 runs, that were used to calculate the amount of sulphate per area gave a value of 65±4.9 (n=3), compared to the value of the temperature experiment measurements at -17°C, 62±8 (n=3) the likeliness is very high and therefore the signal difference between the -17°C and -25°C measurements is assumed to be due to temperature

6.2.5 Stationary measurements

Bag 109 (figure 39)

Looking at the results from the stationary measurements done on bag 109 (NGRIP) run 1, 2 and 3 probably show the noise signal caused by the instrument. Run 3 show a wider amplitude interval than the other two, which could be related to the amplification of the signal compared to run 1 and 2. This could mean that the noise, and not just the signal, is generally higher when the x10 amplification is on during a measurement.

Bag 110 (figure 40)

The three runs of bag 110 were all performed with the x10 amplification. Run 1 was measured in the middle of the eruption, which explains the high initial value. Since the current signal does not go to zero after 30 seconds it shows that the chance of polarization in the ice, at this peak, is negligible (at least when the amplification is on). Run 2 and 3 are measured with amplification as well but show a different pattern. Focusing on the first two seconds of both runs, they show a decrease in signal but only run 3 seems to be getting closer to zero within the 30 seconds. The initial values of the measurements are very close to each other which would indicate a similar conductivity at the chosen measure points however after the first 2 seconds the change in signal/amplitude from one another becomes clear. This could be because of the signal of run 3 is affected by polarization from the previous runs and therefore shows less fluctuation. This however does not explain the signal from run 2 but this could be a result of run 2 being measured right before a small peak (see figure 45 below). It should be noted that the signal of the graph does not respond to the stationary measurements but is simply put in to show positions of measurements relative to the peak, which would mean more protons (from H_2SO_4) present close by to be influenced by the electrical field created.

Bag 293 (figure 41)

Run 1 from bag 293 (NGRIP) shown is a quick decline in signal immediately after the measurement was started. The decline in signal is expected what is not however, is the behaviour of run 3 that shows the same immediate decline as run 1, but then directly after that increases until approximately 2 seconds into the measurement. The conditions are somewhat similar to run 2 in bag 110 and so is the signal, which could imply that the position is dominating the signal response form (see figure 46 below). The signal from run 2 slowly decline over the 30 seconds with the same slope, which would indicate that polarization of the ice, even with extremely small amounts of acid present, takes longer than 30 seconds. The behaviour of run 3 (and run 2 in bag 110) could be explained by the appearance of nearby protons available on either side of the measuring point chosen.

Bag 294 (figure 42)

Bag 294 once more shows an immediate decline in signal and then it stabilizes after 0.5 seconds, in run 1. Run 2 shows a high initial signal (most likely due to the positioning of the electrodes which could be placed within peaks see figure 46 below). It should be noted that the signal of the graph does not correspond to the stationary measurements but is simply put in to show positions of measurements relative to the peak. Once more the strange behaviour of a dip and then an increase in signal is seen in both runs. Again, this could possibly be explained by the appearance of nearby protons available on either side of the measuring point chosen.

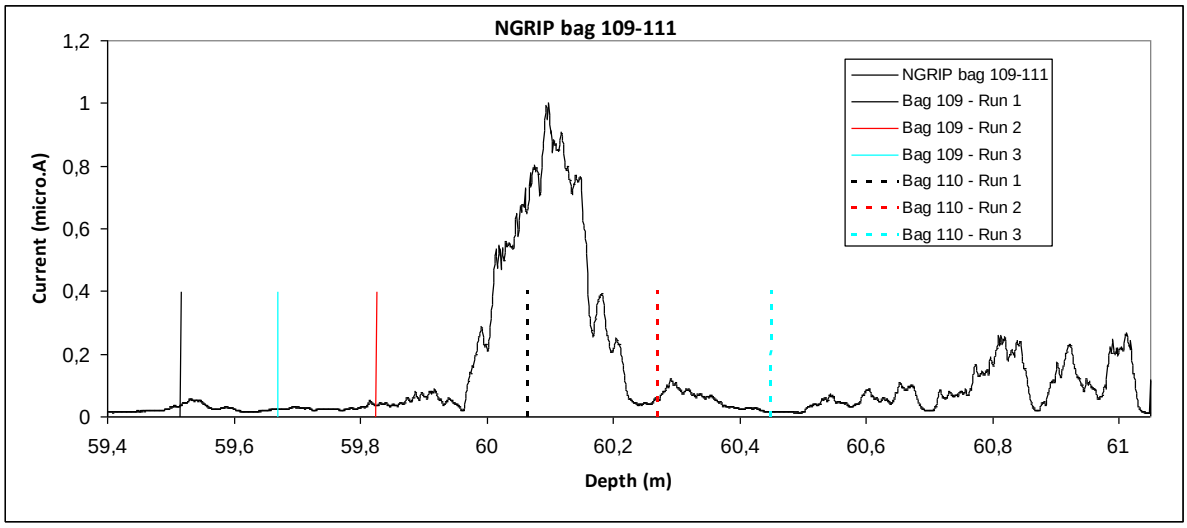

Figure 45 - shows an ECM figure measured on NGRIP 109-111. Vertical lines across bag 109 and 110 indicate the stationary measurement positions. It should be noted that the size of the vertical markers on the figure do not correspond to the stationary measurements signal size. This goes for figure 46 below as well.

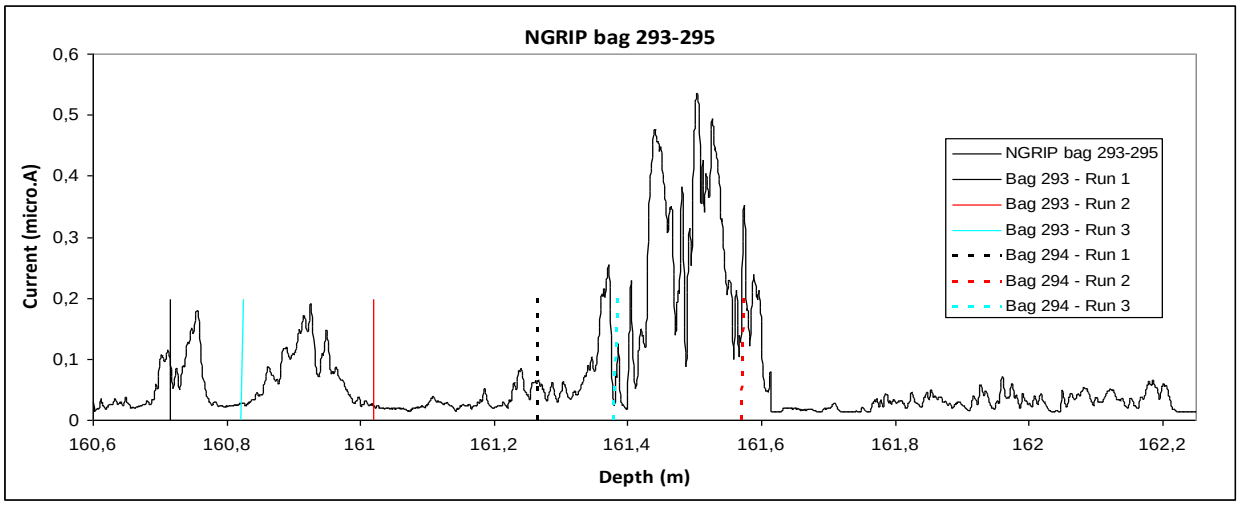

Figure 46 - shows another ECM figure of bag 293-295 of NGRIP. Once more the vertical lines shows the stationary measurements position.

6.2.6 The Calibration

The fact that all the calibration points are not all on the fitted a line (see figure 43) could have several causes, these things are listed below.

6.2.6.1 Some uncertainties involved with the ECM and IC sulphate

The instrument used could have some uncertainties related to it even though some of those have been minimized through the improvements listed in section 3.1. The amplification option (x10) should enhance the signal by a factor of ten. What is seen on figure 47 below is the amplified and non-amplified value of certain top values from the different ECM runs. Ideally the amplification of the signal versus the non-amplified would result in a linear relationship but figure 47 shows some deviation from that. It should be mentioned that the instrument has a saturation effect around 7.26 micro.A, which is why there is a flattening of the values above that.

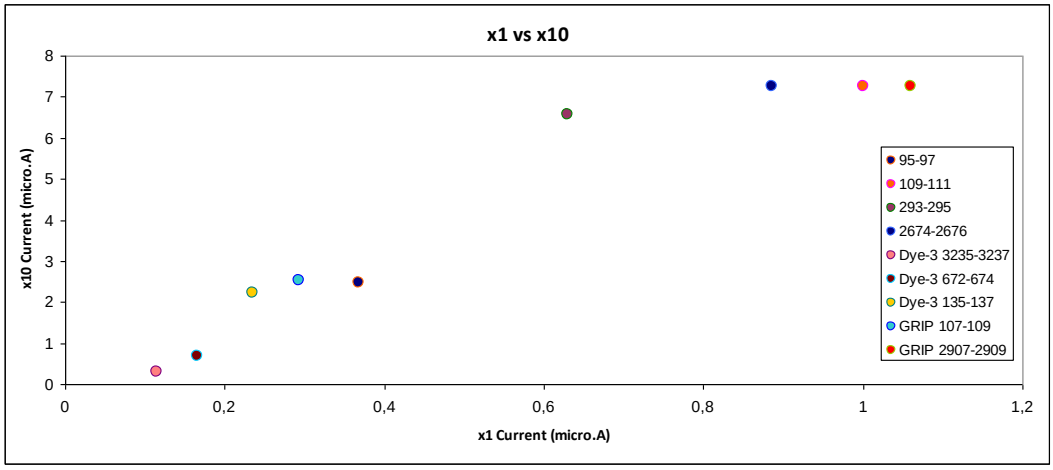

Figure 47 shows the relationship between the amplified measurements and the non-amplified. The values are chosen from the amplified and the non-amplified peak value at the same depth.

From the table 6 it is clear that the signal changes to some extent between each run made. This, however, is not the case in the calibration where only the measurements of the first run are used to produce the plot, in order to eliminate the possibility of polarization.

What could influence the individual measurements are temperature as well as the density (pressure), which is described earlier in section 2.3 and 2.4. Remembering that very few bags were measured at a stable temperature (between air and bag) and that there was a general temperature variation between the different eruptions/ice cores measured, this might very well cause some uncertainties in the ECM values used.

Being that the IC sulphate was given in 5 cm interval values, the same was done to the ECM values. This affects the signal size making it either bigger or smaller than initially measured at the given point which creates some uncertainty in the final sulphate value.

Focusing on the data points with low current values it would be expected that with low conductivity there would also be only a small amount of sulphate present. This is not the general case with the firn measurements (NGRIP 64-66 and 95-97) (see figure 48 below). Relative to measurements with higher conductivity (2-5 micro.A) the sulphate values of the low conductivity (0-2 micro.A) seems high. Because of this it appears that the lack of stability of ECM on firn is changing the actual function of the calibration. The calibration could be made without the firn measurements which might change the calibration function.

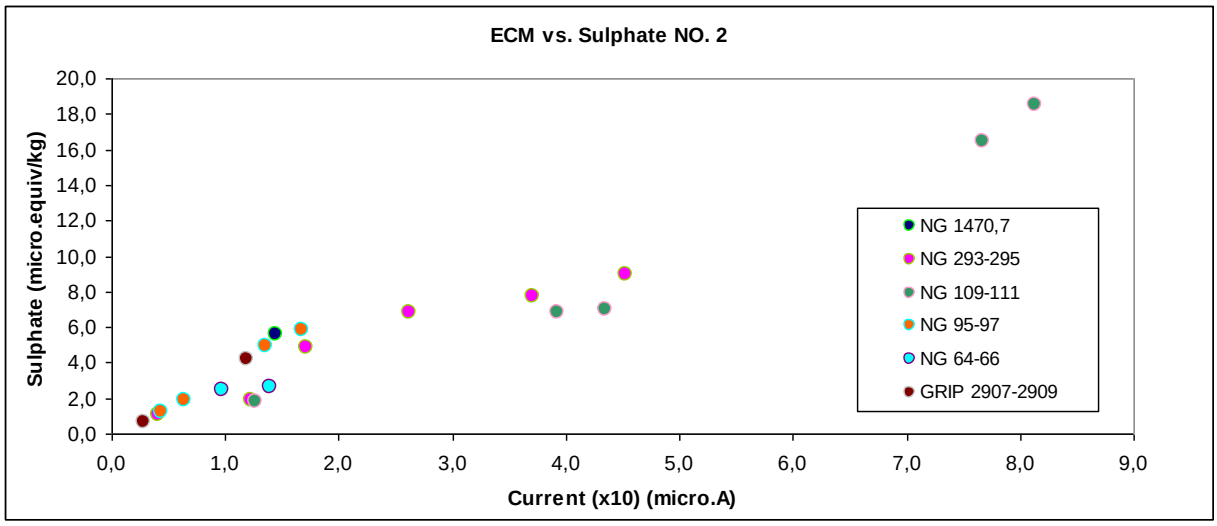

Figure 48 - shows the different points from bags and cores used to produce the calibration equation used for the calculations of sulphate deposition.

6.2.6.2 Conductivity is also caused by H^+ from other impurities than H_2SO_4

It is assumed that the protons come only from H_2SO_4 but if that was the case then there would be no signal measured on either side of the actual eruption deposition. Seeing that a signal is still present outside the deposition depth (background values) this assumption is incorrect, but what is then assumed is that the amount of present H^+ from other impurities is not significant in relation to the signal of an eruption. The amount of signal from other impurities than H_2SO_4 is unknown but could be calculated by subtracting the estimated background values.

6.2.6.3 Insufficient amount of measurements

Measurements with higher EC values could have changed the fit from a linear to a power-law relationship. Hammer shows current values going all the way up to 40 micro.A (figure 49 below), which gives a wider range and therefore possibly also the change in relationship from linear to power-law or generally just non-

linear. It is the Laki eruption from Cretê and Dye-3 that have the high EC response in figure 49. Laki was not possible to measure due to an insufficient amount of ice left. Even though some of the strongest eruptions, in signal, have been used for the calibration the current does not reach any higher than 7.26 micro.A due to the saturation, and this says more about the instrument than the actual size of the signal from the eruption. Though this was one could expect that the instrument should react the same way no matter the saturation level.

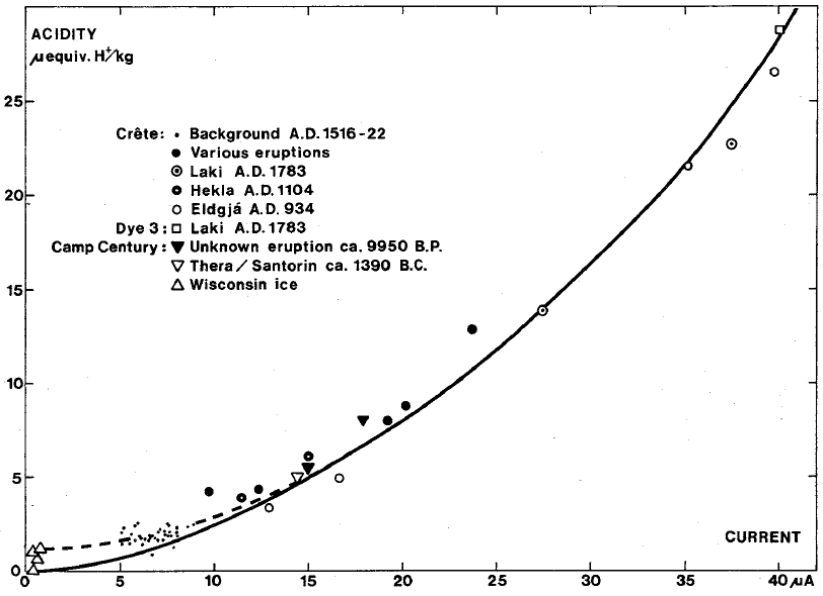

Figure 49 - Hammer 1980's calibration that produced equation 1. The figure shows the power-law relationship between acidity and conductivity.

6.2.7 Sulphate deposition and distribution

Precipitation, temperature and therefore accumulation is higher in the southern part of Greenland, relative to the north. The table 5 showed that these meteorological conditions at the deposition time, for each event, favours a central Greenland (GRIP) to northern Greenland (NGRIP) to southern Greenland (Dye-3) deposition route. The table values from Dye-3 are generally low compared to the other two ice cores, but it is also the oldest core, which means that it has been stored for the longest time. This means that the ECM signals could be affected by the *Aging effect*, which has been mentioned before. This aging effect means that the core conditions are affected by the storing time. They sulphate deposition values were generally lower in Dye-3 compared to GRIP and NGRIP. All Dye-3 bags showed signs of refreezing (meaning exposure to changing temperatures and through that a possible influence on the sulphate content in the ice). The surface width was in all three measuring cases also smaller than GRIP and NGRIP resulting in overlapping of measuring trails. For GRIP the sulphate deposition shows higher values than in NGRIP, which strongly reduces the argument of any aging effect influencing these results.

The interpretation of the major findings will in the next section be given an explanation if possible.

6.3 Explanation of what the major findings could mean

6.3.1 Reproducibility

The low density probably explains the big variation in ECM signal in firn measurements. This would mean that ECM on firn, to some extent, is unreliable.

The core quality could be a dominating factor in terms of influence on signal size especially in the firn because of the already low signal. If the cleaning of the surface was not done properly, specifically for the older Dye-3 core, then the generally lower (compared to other published values see table 7 section 6.4) signal of Dye-3 could be explained by this. This means that cores of lesser quality, due to storing and cut off making the core width smaller, could result in underestimations of the general sulphate deposition. As mentioned in section 5.7.1 then the preference of measuring on NGRIP is based on the generally better core quality.

6.3.2 Temperature

The temperature measurements show the importance of stable temperatures during measurements. Whether the ECM signal of the measurements presented in section 5.1.1-5.1.3 are influenced by the temperature difference between air and core is unknown but the measurements where there is more than 1°C difference is mentioned and should be taken to consideration in case of significance.

6.3.3 Stationary measurements

The stationary measurement of bag 110 run 1 show that total polarization within a peak is not happening immediately but rather over a longer period of time than the 30 seconds. They also show that a decrease in signal occurs between each successive measurement, which could explain the lowering of signal from run 1 throughout the rest of the normal ECM runs, not the stationary measurements.

6.3.4 The calibration

The different relationship between acidity and current than previously shown by Hammer in equation 1, could be explained by the different acidity measuring methods. The relationship is clearly different which could be due to; the setup and the changes done to is, measuring procedure or a difference in the use of SO_4^{2-} to H^+. Being that the measuring procedure was the same as Hammers and the setup changes seem to remove certain uncertainties related to pressure and pulling rate it leaves the relationship between SO_4^{2-} and H^+ to be the reason for the new linear relationship.

6.3.5 Sulphate distribution

There appears to be a decrease in sulphate deposition from GRIP to NGRIP and from NGRIP to Dye-3 based on the sulphate per area calculations in table 6. This could indicate that there is no north to south gradient

in deposition tendencies but a more complicated meteorological behaviour than previously thought. The sulphate deposition in Dye-3 is to be thought of with caution since the values are considered low compared to previous published values (see table 7 section 6.4.3). Also remembering that precipitation and accumulation rates are higher in the southern Greenland then the amount of deposition could be questioning. This is not definite since the wind patterns could be favouring central to north Greenland during the time of deposition but is advised to be taken to consideration.

6.4 Comparing the results to published literature

6.4.1 New ECM compared to old ECM and sulphate

Comparing the ECM measurements from the old setup (CIC database, 2014) to the new, there is a general good agreement in shape between the bags. With the exception of GRIP 72-74 and Dye-3 135-137, where the peaks in the new ECM are located differently from the old. In GRIP this could be explained by the offset in depth/bag notation. This is of no importance to the calibration produced since these measurements are not included. The old EC is already calibrated which could explain the generally higher "background" values. Compared to the new EC the deposition depths of the old ECM appear to be less well defined which could result in a higher estimation of the amount of sulphate deposited. The current is generally measured with the x10 amplification, which with the new instrument was shown in the stationary measurements to show more noise with the new instrument. Since one of the aims with a new setup was to increase signal to noise it is assumed that measurements done on the old instrument is more influenced by noise. Because of the calibration of the old ECM the noise level between new and old cannot be compared. However the improvements of the setup are mentioned in the method section. Any offsets of 1-2cm between the old ECM and new depth axis could be due to the pulling system of the electrodes, see method section again paragraph 3.1.

The IC sulphate values in NGRIP 64-66 indicate the deposition depth and amount of sulphate much better than both the old and new EC measurements. This is probably a result of density being a factor influencing ECM but not the IC method. IC of NGRIP 95-97, 109-111 and 293-295 and GRIP 107-109 and 2907-2909 all show a relatively good correlation between deposition depth as well as shape of the peak to the new ECM. A quick reminder that this is with the correction of depth offset of 20 cm in the IC measurements on GRIP 107-109. The offset of 20 cm is explained by the general depth offset of the *Eurocore*, from which the IC measurements comes, to the GRIP core onto which ECM is measured. NGRIP 2674-2676 only had sulphate values in 55 cm averages hence the appearance of the sulphate curve in figure 35. The difference in factors from IC sulphate to new ECM is mostly approximately 20 except from figure 35 (NG 2674-2676) where there is approximately a factor 10 between them.

6.4.2 Calibration

The calibration produced (equation 5) is specific for the setup introduced in this thesis and because of this is not completely comparable to other calibrations. On the other hand, what could be discussed is the difference in relationship between conductivity and H^+ or conductivity and SO_4^{2-}. Hammers calibration

(equation 1) showed a power-law relationship of acidity (H^+) to current. This was produced by measured pH of melted ice, which was corrected for CO_2-induced ions (Hammer, 1980). The calibration produced in this thesis is based on SO_4^{2-} instead of H^+. This could be why the calibration shows the linear relationship between (SO_4^{2-}) and current compared to Hammers non-linear relationship. H^+ and SO_4^{2-} should be closely related, if the assumption is correct that H^+ comes only from H_2SO_4.

Moore *et al.,* 1984 finds a different fit in data from Site G (Greenland) and Dolleman Island (Antarctica) and therefore also a different function for calibration they argue that the calibration relationship varies with ice core sites (Moore *et al.,* 1984). The produced sulphate deposition values are compared to other published values in the section below.

6.4.3 Sulphate per area

As mentioned in the section above, several calibrations of ECM and H^+ have been produced since the first done by Hammer in 1980. The values shown in table 7 come from different publications where there have been different measuring procedures of the acid concentration. The procedures are all listed in table 7 below.

Ice core	Eruption	Size/value	Unit	Deposition time (year)	Procedure used/Reference
NGRIP	Krakatoa	15.4 ± 2.7	Kg SO_4^{2-} /km^{2}ice	2.7	1
	Krakatoa (new)	22 ± 4.1	Kg SO_4^{2-} /km^{2}ice	-	0
	Tambora	40.3 ± 1.8	Kg SO_4^{2-} /km^{2}ice	1.8	1
	Tambora (new)	31 ± 0.5	Kg SO_4^{2-} /km^{2}ice	-	0
	Laki (new)	108 ± 10.7	Kg SO_4^{2-} /km^{2}ice	-	0
	Unknown, 1257	98.6 ± 2.2	Kg SO_4^{2-} /km^{2}ice	2.7	1
	Unknown, 1257 (new)	65 ± 4.9	Kg SO_4^{2-} /km^{2}ice	-	0
	Unknown, 9305 (new)	78 ± 1.1	Kg SO_4^{2-} /km^{2}ice	-	0
GRIP	Tambora	13	Kg(H_2SO_4)/km^{2}ice	1.1	2
	Tambora (new)	45 ± 2.8	Kg SO_4^{2-} /km^{2}ice	-	0
	Laki	70	Kg(H_2SO_4)/km^{2}ice	1.6	2
	Unknown, 1257	161	Kg(H_2SO_4)/km^{2}ice	3.0	2
	Unknown, 9305 (new)	89 ± 9	Kg SO_4^{2-} /km^{2}ice	-	0
Dye-3	Tambora	37	Kg(H_2SO_4)/km^{2}ice	0.9	2
	Tambora	54	Kg SO_4^{2-} /km^{2}ice	-	3
	Tambora (new)	19 ± 3.6	Kg SO_4^{2-} /km^{2}ice	-	0
	Laki	101	Kg(H_2SO_4)/km^{2}ice	1.6	2
	Laki	173	Kg SO_4^{2-} /km^{2}ice	-	3
	Unknown, 1257	88	Kg(H_2SO_4)/km^{2}ice	2.2	2
	Unknown, 1257 (new)	17 ± 0.3	Kg SO_4^{2-} /km^{2}ice	-	0
	Unknown, 9305 (new)	9 ± 1.8	Kg SO_4^{2-} /km^{2}ice	-	0
NEEM	Krakatoa	18.5 ± 3.6	Kg SO_4^{2-} /km^{2}ice	2.7	4
	Tambora	39 ± 2.4	Kg SO_4^{2-} /km^{2}ice	2.0	4
	Laki	178.6 ± 4.3	Kg SO_4^{2-} /km^{2}ice	1.7	4
	Laki	11.1 ± 2.5	Kg SO_4^{2-} /km^{2}ice	0.9	5
	Unknown, 1257	82.1 ± 2.2	Kg SO_4^{2-} /km^{2}ice	2.4	4
Cretê	Tambora	53	Kg SO_4^{2-} /km^{2}ice	-	3
	Laki	138	Kg SO_4^{2-} /km^{2}ice	-	3

Table 7 – sulphate deposition values are shown here. The different methods used to obtain the value are stated below.

The different procedures (*) for finding the values in table 7 are mentioned below

0) Values are produced in this thesis.

1) All values are calculated from IC measurements over 5 cm intervals. Sea salts have been removed from these values. (Plummer *et al.,* 2012)

2) All values are made by the use of Hammer's 1980 calibration ($H^+ = 0.045i^{1.73}$ micro.equiv.kg^{-1} at T= -15°C) (Hammer, 1980). The value is the mass of both H^+ and SO_4^{2-} which is different from the values presented in this thesis but since the difference in mass is only 2 au (the weight of H_2SO_4 is 98 au and SO_4^{2-} is 96 au) it is considered negligible and therefore still comparable to the values measured in this thesis (Clausen *et al.,* 1997).

3) The values are based on the Hammer 1980 calibration where the acid measurements are done on pH. The deposition time was not easily found and is therefore not included (Clausen and Hammer, 1988).

4) These values are all direct measurements of IC (continuous IC measurements). All measurements have been corrected for sea salts. (Sigl *el al.,* 2013)

5) The values from this paper are found by the use of Hammers 1980 calibration equation. (Skjoldborg *et al.,* 2013)

Comparing the new deposition values from NGRIP to the other values shown above in table 7, it shows that for Krakatoa the new calibration makes the deposited sulphate value higher by approximately 7 Kg SO_4^{2-}/km^{2}ice.

In Tambora and 1257 the values of the new calibration are lower than the ones published by Plummer *et al.,* 2012. The published values are all IC measurements on sulphate and not produced by ECM. Remembering the bad reproducibility of the runs from Krakatoa there is a chance of overestimation, of the values which could explain the higher value in the new calculations compared to the ones produced by Plummer *et al.,* 2012.

For GRIP the new value of the Tambora eruption (table 7) is much higher than the value published and seen in table 7 as well. The Tambora eruption is measured on firn, which in light of the large uncertainties for the firn measurements, could result in an overestimation of the new value compared to the published. Based on the fact that the old published value is calculated from H_2SO_4 where the new value presented in this thesis is only based on SO_4^{2-} the value is expected to be slightly higher (if the same calibration was used). Because of this difference in calibration and no other data presented here, on this core, it is difficult compare the results.

The new values produced from the Dye-3 core are lower than any previously published but since Moore *et al.,* 1984 measured the ECM signal in 1992 and Clausen and Hammer in 1988 there is a chance of a general lowering of the ECM signal (and thereby sulphate deposition value) due to the previously mentioned *aging effect*. Comparing the two previously published values then they show a 17 KgSO_4^{2-}/km^{2}ice difference with the 37 Kg(H_2SO_4)/km^{2}ice measured earlier (1980) than the 54 KgSO_4^{2-}/km^{2}ice published by Clausen and

Hammer, 1988. This is arguing against the possible *aging effect* explanation. For the 1257 A.D. eruption in Dye-3 the published value 88 Kg(H_2 SO_4^{2-})/km^{2}ice is also much higher compared to the new ~17 KgSO_4^{2-}/km^{2}ice value.

Comparing deposition times for a specific eruption shows some variation between the different published values, which could influence the calculations of the sulphate deposited. Because none of the newly produced values in this thesis are shown by time but instead by depth, it is difficult to argue whether this is a dominating factor or not.

Skjoldborg *et al.,* 2013 calculated a value of approximately 11.1 KgSO_4^{2-}/km^{2}ice for the Laki eruption in the NEEM ice core based on ECM and the calibration produced by Hammer in 1980 (equation 1) which they compared to the value from Sigl *el al.,* 2013, approximately 178.6 KgSO_4^{2-}/km^{2}ice (also found by ECM) of the same eruption. What appears to be the only difference is the deposition interval (time), which was 0.89 and 1.7 years respectively for the stated values. This would argue that the time interval could be of somewhat importance. Other factors could influence these results such as the general quality of the ECM signals produced by both parts.

6.5 The limitations of this study

6.5.1 Too few measurements on ice

As mentioned in the purpose section the original intention was to measure five eruptions in NGRIP, GRIP and Dye-3. This was not possible due to an insufficient amount of ice left (in GRIP and Dye-3) in many of the sections containing the chosen eruptions. Six bags with eruptions were measured in GRIP and Dye-3, three with ice density and three of firn density. The bags with firn densities are as discussed previously, showing less stability in the reproducibility of signals which could influence the calibration and therefore the calculations of sulphate per area.

6.5.2 Bad ice core quality

The overall quality of the Dye-3 ice core also makes it difficult to evaluate the actual signal size. This is seen when comparing to previously published sulphate per area values where a general low amount is found using the new EC measurements and calibration.

6.5.3 Temperature dependence

The temperature experiment could have been extended so that temperatures even lower than -25°C would have been measured, with the purpose to see at what temperatures the signal ceases to exist. This could be of use when performing ECM directly after drilling the ice core, where temperatures can be lower than the approximately -17°C which the calibration is based upon.

6.5.4 Comparison of calibration

Because the calibration is based on SO_4^{2-} and not H^+ it is not possible to compare the calibration with most other published calibration curves. Therefore it is difficult to see which parameter that influences what. Generally speaking it is difficult to say much about whether it is the instrument, core quality or the difference in use of SO_4^{2-} instead of H^+ to produce the calibration that changes the relationship.

6.6 The generalisability of the results

It is important to remember that the calibration produced is specific for this setup and can therefore not be used for measurements not done on this ECM system.

It is also advised to remember that the calculation of sulphate deposition is made using a calibration formula that is based on SO_4^{2-} which could give a different value than when using calibrations based on H^+, as mentioned in the section 6.5.4 above.

Another thing is that it is implied by Moore *et al.,* 1984 that the calibration changes somewhat with the core site, which means that the calibration possibly only applies to regions close to NGRIP due to that being the main contributor to the production of the calibration.

6.7 A couple of unanswered questions

- How is the exact temperature dependence with this setup? Is 0.5°C enough to change a signal significantly?
- What is the difference between using H^+ and SO_4^{2-} for the calibration?

6.8 Proposals for further research on the subject

- Because the calibration is mainly based on the measurements done on NGRIP it could mean that it also mainly applies to measurements done in that region. Therefore a suggestion would be to measure on newer cores from different regions of Greenland to see if the calibration changes with site and if so then make a study of the changes. This could give an idea of the actual difference in calibration relationship between different sites in e.g. Greenland**.**

- It could also be a good idea to make a calibration that is not based on firn measurements to remove the uncertainties associated with them.

- In respond to the two questions asked in the section 6.7 above then testing the temperature dependence of the measurements could give a reduction in uncertainties involved with the instrument. This is based on the lack of knowledge on which uncertainties that are associated with the instrument, core quality or SO_4^{2-} versus H^+ relationship. Therefore temperature experiments could help clarify some unanswered questions.

- The same argument goes for an investigation of the role of the difference between SO_4^{2-} and H^+. Here a calibration based on H^+ and the same ECM values used for the SO_4^{2-} calibration could enlighten the difference in the two methods and clarify if the linear relationship is due to any of the same parameters as listed above.

6.9 General considerations on ECM

Some not mentioned considerations on ECM are listed below with the purpose that the future users of the ECM system are being reminded of some tendencies seen by other publicized data.

These are not necessarily shown in any results presented here but are stated by some of the used publications.

Zhiwen *el al.,* 2009 states that a significant decrease in conductivity due to the high concentration of alkaline dust is seen in measurements done on ice from cold periods (glacial periods) throughout time. This should be remembered if an interpretation is done on ice from such a period. Should sufficient ECM data be available on several inter glacial and glacial stages then perhaps it could be possible to detect a pattern which could be used for synchronization of different climate archives.

Another statement, from Neftel et al. is that a higher signal is expected in ice with a lot of melt layers. This is mentioned in this thesis earlier but is considered an important thing and is therefore mentioned again here.

Hammer 1980 also says that a higher conductivity signal is expected in summer than in winter precipitation because “in summer the release of H_2S and the intensity of light available for its oxidation is higher in winter, while at the same time the wash-out of H_2SO_4 from moist air masses prior to their arrival in Greenland is lowest in summer” (Hammer, 1980, p. 365).

7. Conclusion

The objectives of this thesis was to produce a new calibration of the improved ECM setup at Centre for Ice and Climate as well as to find the distribution of sulphate in the ice cores sites across Greenland.

The improvements to the instrument enable several users to measure with fewer uncertainties associated with the pressure applied and the measuring rate. The overall reproducibility in response to the improvements is difficult to conclude anything on since so many of the measurements were done on firn which proved to be less stable due to the low density.

Compared to the old setup the new ECM signals appear better defined in terms of the deposition depth, which results in a more precise estimation of sulphate distribution.

The ECM signal seems to be highly dependant of the core quality, which makes measurements performed on old cores less reliable, such as Dye-3. The measurement showed to be temperature dependant though how much the maximum temperature differs between each run is unknown but is advised to be further investigated.

The new calibration shows a linear relationship between SO_4^{2-} and current which is different from any previously published calibration curves. The reason for that is not certain but is either due to insufficient amount of data, the *improvements* done to the old setup or the difference in the use of SO_4^{2-} instead of H^+.

From the sulphate distribution shown in table 7, the highest sulphate deposition is in the GRIP core followed by NGRIP and last Dye-3. Based on table 6 values this would indicate that the meteorological conditions at the deposition time favoured central Greenland, deposited most of the sulphate there and least southern Greenland. However the uncertainties associated with the Dye-3 core quality makes this prediction less agreeable.

8. References

(2014), CIC database, http://www.iceandclimate.nbi.ku.dk/data/

(2014a), http://www.gfy.ku.dk/~www-glac/ngrip/index.html)

(2014b), http://www.iceandclimate.nbi.ku.dk/research/drill_analysing/cutting_and_analysing_ice_cores

(2014c), CIC publications, http://www.iceandclimate.nbi.ku.dk/publications/

- Bales, R. C., J. R. McConnell, E. Mosley-Thompson and B. Csatho, Accumulation over Greenland ice sheet from historical and recent records, *Journal of Geophysical Research, 106,* 33,813-33,825, 2001

- Bigler, M., A. Svensson, E. Kettner, P. Vallelonga, M. E. Nielsen and J. P. Steffensen, Optimization of High-Resolution Continuous Flow Analysis for Transient Climate Signals in Ice Cores, Environmental Science and Technology, 45, 4483-4489, 2011

- Clausen, H. B. and C. U. Hammer, The Laki and Tambora eruptions as revealed in Greenland ice cores from 11 locations, *Annals of Glaciology, 10*, 16-22, 1988

- Clausen, H. B., C. U. Hammer, C. S. Hvidberg, D. Dahl-Jensen and J. P. Steffensen, A comparison of the volcanic records over the past 4000 years from the Greenland Ice Core Project and Dye-3 Greenland ice cores, *Journal of Geophysical Research, 102*, 26,707-26, 723, 1997

- Cuffey, K. M. and W. S. B. Paterson, The Physics of Glaciers, *Elsevier, Fourth edition,* 1-683, 2010

-Dansgaard, W., Stable isotopes in precipitation, *Phys. Lab. Report*, 1-33, 1964

-Dansgaard, W., Frozen Annals, *Narayana Press*, 9-120, 2004

- Fiacco, R. J. JR., T. Thordarson, M. S. Germani, S. Self, J. M. Palais, S. Whitlow and P. M. Grooters, Atmospheric Aerosol Loading and Transport Due to the 1783-84 Laki Eruption in Iceland, Interpreted from Ash Paticles and Acidity in the GISP2 ice core, *Quaternary Research, 42*, 231-249, 1994

- Hammer, C. U., H. B. Clausen, and W. Dansgaard, Greenland ice sheet evidence of post-glacial volcanism and its climatic impact, *Nature, 288*, 230-235, 1980

- Hammer, C. U., Acidity of polar ice cores in relation to absolute dating, past volcanism, and radio-echoes, *Journal of Glaciology, 25*, 359-372, 1980

- Heinmets, F. and R. Blum, Conductivity Measurements on Pure Ice, Colloqium on the Physics of Ice Crystals (Erlenbach, Switzerland, 1962), 1962

- Herron, M. M. and C. C. Langway, Jr, Firn densification: An empirical model, *Journal of Glaciology, 25*, 373-385, 1980

- Hvidberg, C. S., A. Svensson, and S. L. Buchardt, Dynamics of the Greenland Ice Sheet, *Encyclopedia of Quaternaty Science, 2,* 439-447, 2013

- Kinnison, D. E., H. S. Johnston, D. J. Wuebbles, Model study of atmospheric transport using carbon 14 and strontium 90 as tracers, *Journal of Geophysical Research, 99*, 20,647-20,664, 1994

- Lavigne, F., J. P. Degeai, J. C. Komorowski, S. Guillet, V. Robert, P. Lahitte, C. Oppenheimer, M. Stoffel, C. M. Vidal, Surono, I. Pratomo, P. Wassmer, I. Hajdas, D. S. Hadmoko and E. De Belizal, Source of the great A.D. 1257 mystery eruption unveiled, Samalas volcano, Rinjani Volcanic Complex, Indonesia, *PNAS Early Edition*, 1-6, 2013

- Lazrus, A. L. and R. J. Ferek, Acidic sulphate particles in the winter Arctic atmosphere, *Geophysical Research Letters, 11*, 417-419, 1984

- Moore, J. C., E. W. Wolff, H. B. Clausen and C. U. Hammer, The Chemical Basis for the Electrical Stratigraphy of Ice, *Journal of Geophysical Research, 97*, 1887-1896, 1992

- Muto, Y., Y. Muramoto and N. Shimizu, Dielectric Constant and Depolarization Current of Ice, IEEE International Conference on Solid Dielectrics, 537-540, 2013

- Neftel, A., M. Andrée, J. Schwander and B. Stauffer, Measurements of a kind of DC-conductivity on cores from Dye-3, *Geophysical Monograph Series, Greenland Ice Core: Geophysics, Geochemistry, and the Environment, 33*, 32-38, ?

- Plummer, C. T., M. A. J. Curran, T. D. van Ommen, S. O. rasmussen, A. D. Moy, T. R. Vanee, H. B. Clausen, B. M. Vinther and P. A. Mayewski, An independently dated 2000-yr volcanic record from Law Dome, East Antarctica, including a new perspective on the dating of the 1450s CE eruption of Kuwae, Vanuatu, *Climate of the Past, 8*, 1929-1940, 2012

- Rampino, M. R. and S. Self, Histroic Eruptions of Tambore (1815), Krakatau (1883), and Agung (1963), Their Stratospheric Aerosols, and Climatic Impact, *Quaternary Research 18,* 127-143, 1982

- Robock, A., Volcanic Eruptions and Climate, Review of Geophysics, 28, 191-219, 2000

- Schytt, V., Lateral drainage channels along the northern side of the Moltke glacier, North-West Greenland, *Geografiska Annaler 38A,* 64-77, 1956

- Schwander, J., A. Neftel, H. Oeschger and B. Stauffer, Measurement of Direct Current Conductivity on Ice Samples for Climatological Applications, *J. Phys. Chem., 87*, 4157-4160, 1983

- Self, S., M. R. Rampino, M. S. Newton and J. A. Wolff, Volcanological study of the great Tambora eruption of 1815, *Geology, 12*, 659-663, 1984

- Sigl, M., J. R. McDonnell, L. Layman, O. Maselli, K. McGwire, D. Pasteris, D. Dahl-Jensen, J. P. Steffensen, B. Vinther, R. Edwards, R. Mulvaney and S. Kipfsthul, A new bipolar ice record of volcanism from WAIS Divide and NEEM and implications for climate forcing of the last 2000 years, *Journal of Geophysical Research: Atmospheres, 118*, 1151-1169, 2013

- Skjoldborg, K. L., I. C.G. Cortzen, K. K. Mortensen og J. M. R. A. Thomsen, Estimering af størrelsen og varigheden af vulkanudbruddet fra Laki (år 1783 e.v.t.) baseret på en grønlansk iskerne, Experimental Physics, Niels Bohr Institute, 2013

- Thordarson, T. and S. Self, Atmospheric and environmental effects of the 1783-1784 Laki eruption: A review and reassessment, *Journal of Geophysical Research, 108*, 1-29, 2003

- Taylor, K., R. Alley, J. Fiacco, P. Grootes, G. Lamorey, P. Mayewski and M. J. Spencer, Ice-core dating and chemistry by direct-current electrical conductivity, *Journal of Glaciology, 38*, 325-332, 1992

- Uchida, T., P. Duval, V. Y. Lipenkov, T. Hondoh, S. Mae and H. Shoji, Brittle Zone and Air-hydrate formation in Polar Ice Sheet, *Mem. National Institute of Polar Research, 49*, 298-305, 1994

- Vinther, B. M., H. B. Clausen, S. J. Johnsen, S. O. Rasmussen, K. K. Andersen, S. L. Buchardt, D. Dahl-Jensen, I. K. Seierstad, M. –L. Siggard-Andersen, J. P. Steffensen, A. Svensson, J. Olsen and J. Heinemeier, A synchronized dating of three Greenland ice cores throughout the Holocene, Journal of Geophysical Research, 11, 1-11, 2006

- Wolff, E. W., W. D. Miners, J. C. Moore and J. G. Paren, Factors Controlling the Electrical Conductivity of Ice from the Polar Regions – A Summary, *J. Phys. Chem., 101*, 6090-6094, 1996

- Wolff, E. W., J. C. Moore, H. B. Clausen and C. U Hammer, Climatic implications of background acidity and other chemistry derived from electrical studies of the Greenland Ice Project ice core, *Journal of Geophysical Research, 102*, 26,325-26332, 1997

- Yokoyama, A Geophysical Interpretation of the 1883 Krakatau Eruption, *Journal of Volcanology and Geothermal Research, 9*, 359-378, 1980

- Zhiwen, D., Z. Mingjun, L. Zhongqin, W. Feiteng and W. Wenbin, The pH value and electrical conductivity of atmospheric environment from ice cores in the Tianshan Mountains, *Journal of Geographical Science, 19*, 416-426, 2009